DEPARTMENT OF PHYSICS, UNIVERSITY OF JYVÄSKYLÄ
RESEARCH REPORT No. 1/1990

NEW FEATURES IN SYSTEMATICS OF LOW-SPIN STATES IN EVEN $^{106-120}$Cd

BY
JAANA KUMPULAINEN

Academic Dissertation
for the Degree of
Doctor of Philosophy

Jyväskylä, Finland
May 1990

URN:ISBN:978-951-39-9887-5
ISBN 978-951-39-9887-5 (PDF)
ISSN 0075-465X

Jyväskylän yliopisto, 2023

ISBN 951-680-299-0
ISSN 0075-465X

DEPARTMENT OF PHYSICS, UNIVERSITY OF JYVÄSKYLÄ
RESEARCH REPORT No. 1/1990

NEW FEATURES IN SYSTEMATICS OF LOW–SPIN STATES IN EVEN $^{106-120}$Cd

BY
JAANA KUMPULAINEN

Academic Dissertation
for the Degree of
Doctor of Philosophy

To be presented, by permission of the
Faculty of Mathematics and Natural Sciences
of the University of Jyväskylä,
for public examination in Auditorium S-212 of the
University of Jyväskylä on May 26, 1990,
at 12 o'clock noon

Jyväskylä, Finland
May 1990

Acknowledgements

To my supervisors Professor Juhani Kantele and Docent Rauno Julin I wish to express my sincere thanks for the guidance throughout this work. Rauno always had time to my questions, and he inspired me with his never failing enthusiasm for physics and nuclear physics experiments.

Also the other "Ø-group" members, Docent Arto Passoja, Dr. Wladyslaw H. Trzaska, Matti Luontama, Esa Verho and Jukka Väärämäki, did a great work in the lonely, sometimes nervy, nights when performing the experiments and data analysis. Thanks for them. My thanks go also to Hannu Leinonen and Teuvo Poikolainen, who forged the cyclotron beam out and made our measurements possible.

Associate Professor Jorma Hattula introduced me into the field of nuclear physics. His interest in my studies has been of great value, as well as, the free spirit of the whole Department.

With Professor John L. Wood and Dr. Henryk Mach I had many stimulating discussions during their visits to our department. Dr. Henryk Mach and Professor Steven W. Yates gave valuable criticism on the text and revised the language of the manuscript.

To my mother, Vieno, I wish to express my warmest thanks for her continuous encouragement throughout all my studies. I am grateful to my mother-in-law, Toini, for her help in everyday life. Dear Seppo solved all my typographic problems with patience, and offered a wealth of understanding and support all the way of this work.

The Emil Aaltonen Foundation supported my work with research grants, which is gratefully acknowledged.

Jyväskylä, April 1990

Jaana Kumpulainen

NEW FEATURES IN SYSTEMATICS OF LOW-SPIN STATES IN EVEN $^{106\text{-}120}$Cd

Abstract

Low-lying low-spin collective states in even ^{106,108,110,112,116}Cd were investigated by means of in-beam and off-beam γ-ray and conversion-electron spectroscopy. New spin assignments and decay branching ratios for the levels in ^{106}Cd, ^{108}Cd, ^{110}Cd and ^{112}Cd were obtained. The present results essentially complement the level systematics from ^{106}Cd to ^{120}Cd. From the new data, it is inferred that two sets of low-lying 0+ states having different excitation characteristics cross between ^{114}Cd and ^{116}Cd. No such crossing is observed on the neutron-deficient side. One of these sets appears to have features of both intruder and two-quadrupole-phonon states.

Contents

1. Introduction....1

2. Experimental methods and data analysis....6

2.1. Inelastic proton scattering....8

2.1.1. Gamma-ray spectroscopy....8

2.1.2. Electron spectroscopy....12

2.2. (p,2n) reaction....15

2.2.1. Gamma-gamma coincidence measurements....15

2.2.2. Angular-distribution measurements....20

2.2.3. Excitation-function measurements....24

2.3. (α,2n) reaction....27

2.4. Decay measurements....27

3. Experimental results....34

3.1. The nucleus ^{106}Cd....35

3.2. The nucleus ^{108}Cd....42

3.3. The nucleus ^{110}Cd....48

3.4. The nucleus ^{112}Cd....53

3.5. The nucleus ^{116}Cd....59

4. Level systematics....63

4.1. The quintuplet of states: (0_2^+, 2_2^+, 4_1^+, 0_3^+, 2_3^+)....63

4.1.1. The 0_A^+ state....68

4.1.2. The 0_B^+ state....70

4.1.3. The 2_3^+ state....71

4.2. Other states....71

5. Discussion 77
5.1. Vibrational features in Cd isotopes 77
5.1.1. Quadrupole vibrations 77
5.1.2. Octupole vibrations 79
5.2. Rotational features in Cd isotopes 80
5.3. Intruder states in Cd isotopes 82
5.4. The role of mixing 88
5.5. Conclusions 89
6. Summary 91
References 92

1. Introduction

In the even-mass Pd, Cd, Sn and Te nuclei, close to the magic proton number Z = 50, the low-lying positive-parity states are commonly described by the spherical quadrupole vibrator model. This model predicts equally spaced sets of energy levels with the same vibrational quantum number n for harmonic vibrations. The spin of the first excited state is 2^+, while at twice the energy of this state there is a degenerate triplet of states having spins 0^+, 2^+ and 4^+ (the two-phonon states). At three times the energy of the 2_1^+ state there is a quintuplet of states with spins 0^+, 2^+, 3^+, 4^+, 6^+ (the three-phonon states). Electric quadrupole transitions (E2) are only allowed between the states differing by one phonon ($\Delta n = \pm 1$) and electric monopole transitions (E0) between the states with the same spin within the same multiplet ($\Delta n = 0$) or differing by two phonons ($\Delta n = \pm 2$). Many features of the Pd, Cd, Sn and Te nuclei agree quite well with this simple model, although already at the energy region of the three-phonon states the particle-like excitations are possible and the identification of the phonon states is difficult.

The observed energy splitting of the states in the phonon multiplets can be accounted for by anharmonic effects in the model. The non-zero quadrupole moment of the 2_1^+ state in ^{114}Cd, measured by de Boer et al. [Boe65], can be explained by the anharmonic vibrator. However, detailed studies have revealed serious discrepancies which cannot be explained even by anharmonicity effects.

In the ^{112}Cd and ^{114}Cd isotopes the simple vibrator picture is strongly disturbed already at the two-phonon energy region: In addition to the two-phonon triplet of states, these nuclei contain extra 0^+ and 2^+ states forming a quintuplet of states at that energy region (0_2^+, 2_2^+, 4_1^+, 0_3^+, 2_2^+). The extra states have been a long-standing challenge to the models of nuclear structure.

Several authors have proposed that deformed states coexist with spherical quadrupole vibrational excitations in these Cd isotopes [Gne71, Ber73, Mey77,

Paa79]. However, these explanations were only qualitative, partly due to the lack of experimental data at that time.

During the past few years it has generally been assumed that intruder configurations involving two-proton main shell excitations are present in odd-mass In (Z = 49) and Sb (Z = 51) nuclei and also in even-mass Sn (Z = 50) nuclei [Hey83]. These excitations provide an explanation for the observed rotational-like bands at low energies in these nuclei. The existence of the intruder states is established also in heavy nuclei around Z = 82: in the odd-mass Au, Tl and Bi, and the even-mass Hg, Pb and Pt nuclei [Hey83, Hey87]. There are several distinctive features of these states:

(i) Considerable deformation as a result of the proton-neutron interaction among the increased number of valence particles outside a closed shell. This implies that the proton intruder states should be lowest in energy in the middle of the neutron shell, increasing rapidly in energy when moving away from the midshell.

(ii) A rotational band built on the intruder state. The rotational bands e.g. in the even $^{112\text{-}118}$Sn isotopes have been established on the basis of the level spacings and the enhanced intraband transitions as compared with the interband transitions [Bro79, Har88, Har89].

(iii) Increased excitation cross section in specific few-nucleon transfer reactions. In the Sn isotopes the intruder 0^+ band-head is strongly populated in the (^{3}He,n) two-proton transfer-reaction [Fie77].

The finding of the intruder states in Cd isotopes is critical to the whole concept of intruder states. In the even-even Cd isotopes the intruder configurations are expected to be the two-particle four-hole (2p-4h) excitations across the Z = 50 closed shell (Fig. 1.1). Strong population of low-lying 0^+ states of even-mass Cd nuclei in the (^{3}He,n) two-proton transfer-reaction [Fie77] is regarded as a clear evidence of an intruding two-proton component of those states. In ^{110}Cd the observed rotational band is build on top of the first excited 0^+ state [Mey77]. Fast E0 transitions between excited 0^+ states in the even Sn isotopes [Bäc81, Kan79] are explained as being due to a mixing of

different shapes of those 0^+ states. In ^{112,114}Cd the E0 transitions between the 0_3^+ and 0_2^+ levels are weak indicating that the mixing is not strong, or the deformation associated with these states is weak [Jul80].

The most detailed description of collective properties of even-mass Cd isotopes has been based on the idea of mixing of intruder and vibrational phonon states. The particle-core coupling model and the interacting boson model (IBM) have been applied in several works [Sch82, Sam82, Hey82, Mhe84, Apr84, Kus87, ODo88]. The mixed-symmetry states of IBM have been studied by Lipas et al. [Lip86].

Heyde and Aprahamian et al. [Apr84] have introduced a schematic model in the IBM formalism to describe the behaviour of intruder and vibrational states in Cd isotopes. In this scheme the "normal" or vibrational states in Cd isotopes are formed in

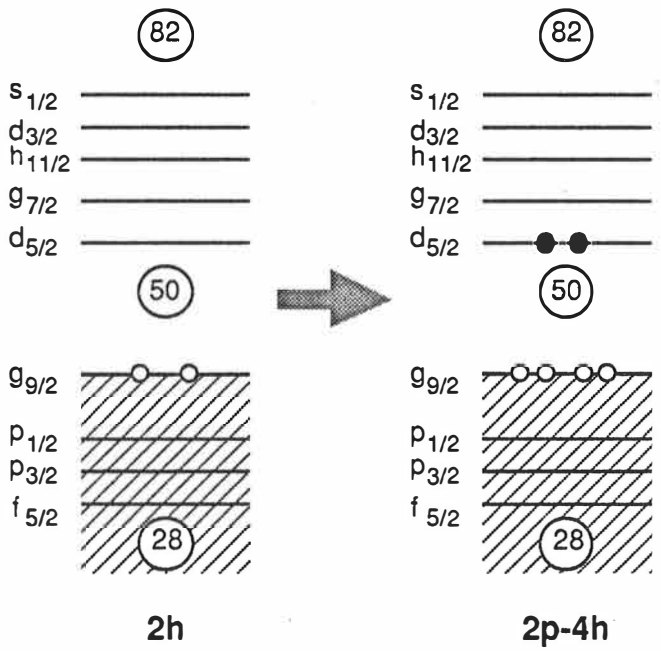

Fig. 1.1: A schematic representation of the normal proton configuration (left) and the intruder proton 2p-4h configuration (right) of the even-mass Cd isotopes (Z = 50 - 2). The proton pair from the $g_{9/2}$ orbital is excited across the closed-shell gap forming the two-particle four-hole configuration.

a system consisting of a one proton boson and several neutron bosons (maximum 8, for ^{114}Cd). The 2p-4h intruder or rotational states corresponding to the excitation of a proton pair to the next shell results in a system which can be approximated by three proton bosons instead of one. The two systems mix. The quadrupole-quadrupole interaction between proton and neutron bosons is approximately proportional to the product of the number of proton and neutron bosons. This leads in the mixed system to the "V" shaped systematic behaviour for the intruder states; they are decreasing in excitation energy when approaching the neutron midshell and rising thereafter. The mixing of the intruder states with the normal states is therefore believed to increase towards the neutron midshell.

The ^{118}Cd and ^{120}Cd isotopes have been studied in the view of this schematic model [Apr84, Apr85, Apr87]. As a consequence of raising of the energy of the 0^+ intruder state, ^{118}Cd was expected to be marginally affected by mixing of the vibrational and intruder states. Indeed, based on the energy spacings and the general de-excitation patterns of the low-lying levels ^{118}Cd was suggested to be the first candidate for a perfect vibrator [Apr87]. However, this picture was destroyed by the life-time measurements of Mach et al. [Mac89].

Kusnezov et al. [Kus87] have studied the intruder band in ^{110}Cd both experimentally and theoretically. In their IBM mixed-configuration calculations the mixing between the bands is so strong that the identity of the ground-state band and intruder band is lost, and the distinction into different bands has no physical meaning any more.

The experimental (t,p) transfer intensities to the 0^+ states in ^{112}Cd, ^{114}Cd and in ^{116}Cd have been interpreted by O'Donnel et al. [ODo88]. Their results from the three-state mixing calculations show weak mixing and thus allow a clear identification of the 0^+ levels as being rotational or vibrational.

Fahlander et al. [Fah88] have extensively studied ^{114}Cd via Coulomb excitation. They conclude that the vibrational model provides an overall better description of the data than the models mixing the vibrational and intruder states.

No consistent picture has emerged from these numerous theoretical interpretations of the data. Different kinds of mixing have been introduced in the various studies, and even different states have been assigned as the intruders. There are still open questions: Which one of the 0^+ states among the quintuplet of states (0_2^+, 2_2^+, 4_1^+, 0_3^+, 2_2^+) can be characterized as the two-phonon 0^+ state and which one as the intruder 0^+ state having the proton 2p-4h configuration? What is the role of mixing?

In locating intruder states, for example in the Pt-Pb region, studies of level systematics have been of crucial importance. For the even-mass Cd isotopes, attempts to establish the systematics of the suggested intruder states have failed mainly because of the scarce experimental information, especially on the neutron deficient isotopes (see e.g. Fig. 1 in Ref. [Apr84] and Fig. 5 in Ref. [Rou84]).

In the present work, a comprehensive experimental study of low-lying levels in ^{106}Cd, ^{108}Cd, ^{110}Cd and ^{112}Cd, and a few complementary experiments on ^{116}Cd were carried out at JYFL. The main emphasis in this work has been in the systematic behaviour of the (0_2^+, 2_2^+, 4_1^+, 0_3^+, 2_2^+) quintuplet of states. Inelastic proton scattering, (p,2n) and (α,2n) reactions, as well as EC/β^+-decay of odd-odd In isomers, were found particularly advantageous in the population of low-lying non-yrast levels in Cd nuclei. Various tools for in-beam and off-beam γ-ray and conversion-electron spectroscopy developed at JYFL were especially suitable for this kind of study.

As a result, new spin and level assignments as well as branching ratios obtained in this work render it possible to relate low-lying levels of similar characteristics in even $^{106\text{-}120}$Cd. For the first time, the systematic behaviour of the aforementioned quintuplet of states can be followed from ^{106}Cd to ^{120}Cd. The new data for ^{112}Cd reveal the candidate for the intruder band, enabling us to look at the intruder band systematics up to spin 6^+ in the even ^{110,112,114}Cd isotopes. The role of intruder states within the picture of simple collective models is discussed.

Part of the material presented in this work has been published in Ref. [Kum90] and reported in the JYFL Annual Reports 1988 and 1989. In preparation are two papers giving a detailed description of our experimental results on the Cd isotopes.

2. Experimental methods and data analysis

The light ions (p, d, ^{3}He, α) available from the JYFL MC-20 cyclotron are well suited to study low-lying levels in nuclei. Inelastic scattering of protons populates collective and non-yrast states. Therefore proton-gamma coincidence measurements were chosen as a tool for investigating all the stable even-mass Cd isotopes from ^{106}Cd to ^{116}Cd (except ^{114}Cd) in the present work. Although inelastic proton scattering has been applied to Cd isotopes, detailed conversion-electron and γ-ray spectroscopy studies have not been performed [DeF88, Hae82, DeG83, DeF89, Bla81]. The light stable Cd isotopes, ^{106}Cd and ^{108}Cd, we studied using for the first time the (p,2n) reaction on the ^{107}Ag and ^{109}Ag target nuclei.

So far extensive gamma-ray spectroscopy following the EC/β^{+} decay of the odd-odd In isotopes has been carried out for Cd isotopes [DeF88, Hae82, DeG83, DeF89], while the electron spectroscopy only for ^{106}Cd and ^{108}Cd [Rou84]. We used the (p,n) reaction to produce odd-odd ^{106,108,110}In isotopes and measured γ-ray and electron spectra following the EC/β^{+} decay of ^{106,108,110}In isomers.

The existence of the stable Pd isotopes enable the (^{3}He,xn) and (α,xn) reactions to be utilized in the study of the Cd isotopes. However, those reactions already preferably populate yrast states. The (α,2n) reaction has previously been used mainly in the study of the high-spin yrast states of the even $^{106\text{-}112}$Cd isotopes [DeF88, Hae82, DeG83, DeF89]. In the present work the (α,2n) reaction was performed for ^{110}Cd and ^{112}Cd to verify the results of Refs. [Kus87, Gei74].

A summary-list of the experiments carried out in the present study of low-lying levels in even-mass Cd isotopes is presented in Table 1.1. The properties of targets are collected in Table 1.2. In the following the different methods are briefly explained.

Table 1.1: List of the experiments for even-mass $^{106\text{-}112,116}$Cd in the present work

Reaction	Type of spectroscopy [a]	Mass number of Cd isotope investigated
(p,p')	e^-, γ	106, 108, 110
	pγ coin	106, 108, 110, 112, 116
(p,2n)	γ	106, 108
	$\gamma\gamma$ coin [b]	106, 108
	$\gamma(\theta)$	106, 108
	$\gamma(E_p)$	106, 108
(α,2n)	γ	110, 112
	$\gamma\gamma$ coin	110, 112
	$\gamma(\theta)$	110, 112
	$\gamma(E_\alpha)$	110, 112
In decay	e^-, γ	106, 108, 110

[a] e^- indicates electron spectroscopy, singles mode; γ indicates γ-ray spectroscopy, singles mode; $\gamma(\theta)$ and $\gamma(E)$ mean γ-ray angular-distribution and excitation-function measurements, respectively.

[b] Compton-suppressed $\gamma\gamma$ coincidences.

Table 1.2: Summary of targets used in different reactions.

Isotope studied	Target nucleus	Enrichment (%)	Target thickness (mg/cm^2)	Reactions performed
^{106}Cd	^{106}Cd	90	1.1	(p,p') ; In decay
	^{107}Ag	97.8	9.3	(p,2n)
^{108}Cd	^{108}Cd	73.7	1.4	(p,p') ; In decay
	^{109}Ag	98.8	7.6	(p,2n)
^{110}Cd	^{110}Cd	95.6	1 ; 3	(p,p') ; In decay
	^{108}Pd	99.0	6.8	(α,2n)
^{112}Cd	^{112}Cd	95.5	1.6	(p,p')
	^{110}Pd	99.0	5.8	(α,2n)
^{116}Cd	^{116}Cd	94.2	2	(p,p')

2.1. Inelastic proton scattering

An efficient method in locating levels and obtaining branching ratios was the detection of gamma-rays and conversion electrons from inelastic proton scattering at low bombarding energies. This method was especially useful for the ^{106}Cd and ^{108}Cd isotopes, due to the relatively high (p,n)-reaction threshold (7.5 MeV and 5.9 MeV, respectively).

2.1.1. Gamma-ray spectroscopy

Gamma-rays were measured in coincidence with scattered protons. The coincidence arrangement shown in Fig. 2.1 consisted of one Ge detector and three Si(Li) detectors. A 19% Ge detector was placed at about 3 cm from the target at 90 degrees to the beam direction and three 200 mm^2 x 3 mm Si(Li) particle detectors were positioned at 2.5 cm from the target at an angle of 140 degrees with respect to the beam. One Si(Li) detector covers about 2.4% of the 4π solid angle. Targets were 1 - 2 mg/cm^2 thick metallic foils of enriched ^{106}Cd, ^{108}Cd, ^{110}Cd, ^{112}Cd and ^{116}Cd (Table 1.2). Beam energies of E_p = (7 - 9) MeV and intensity of about 1.5 nA were used. A Cu absorber of about 1 mm was used in front of the Ge detector. Most of the delta electrons from the target were absorbed by means of a 0.5 mg/cm^2 thick Ni foil in front of the Si(Li) detectors.

The typical net collection-time of pγ coincidence events was about 25 hours. The data including 4 parameters (gamma and 3 proton detectors) were recorded in event-by-event mode on magnetic tapes and sorted off-line. The proton-gamma matrix was produced by summing up the three properly gain-shifted proton spectra during the data sorting.

The energy resolution in the summed Si(Li) spectra was about 200 keV, which allowed a sufficient level selection. In Fig. 2.2 (a) the proton gated γ-ray spectrum is

shown, and in Fig. 2.2 (b), (c) and (d) typical proton-gated γ-ray spectra corresponding to 0.3 MeV wide proton gates from ^{106}Cd(p,p') are illustrated. The gate of protons equivalent to the excitation energy of (1.6 - 1.9) MeV in ^{106}Cd is shaded in the γ-ray gated proton spectrum of Fig. 2.3 and corresponds to γ-ray spectrum in Fig. 2.2 (b).

The arrangement tends to moderate proton-gamma angular-correlation effects, which were estimated to cause about a 10% uncertainty to the γ-ray intensities deduced from the proton gated γ-ray spectra. This was evaluated in the case of ^{108}Cd.

From the γ-ray gated proton spectra gamma-ray placements and branching ratios were confirmed. Some γ-ray gated proton spectra from the ^{106}Cd(p,p') reaction are shown in Fig. 2.3. Moreover, the gamma-ray population of a state from higher-lying levels could be observed directly, as can be seen in Fig. 2.3: the gate of 1163 keV γ-ray de-exiting the level at 1.8 MeV shows that the level is fed from a state at 2.4 MeV.

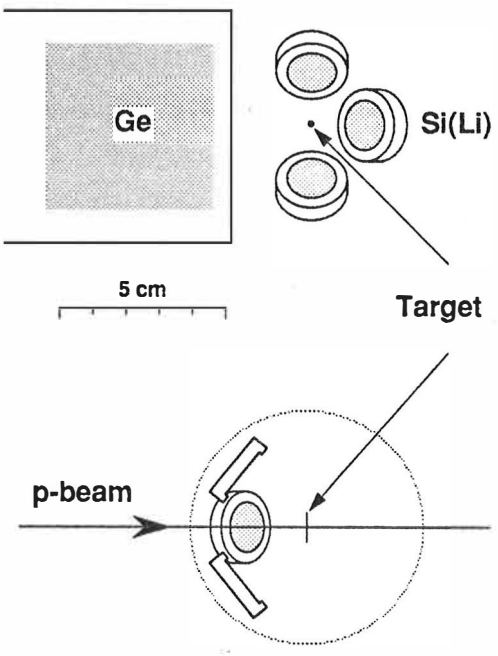

Fig. 2.1: The detector setup for proton-gamma coincidence measurements. **Top:** The Si(Li) detectors at 140° backward angles and the Ge detector at 90° with respect to the beam. **Bottom:** The Si(Li) detectors seen from the Ge-detector side.

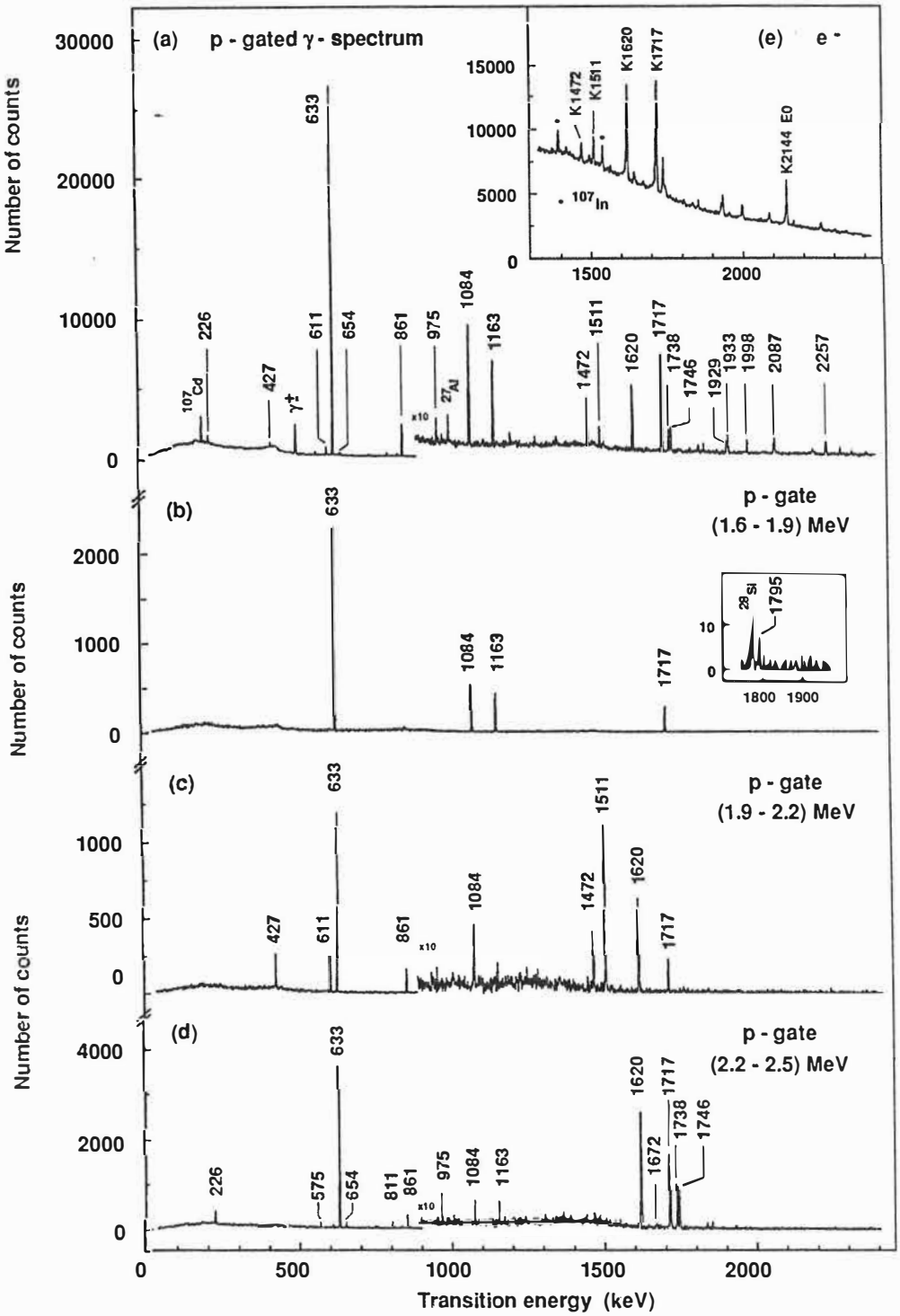

Fig. 2.2: Proton gated γ-ray spectra (a - d) and singles conversion-electron spectrum (e) from the ^{106}Cd(p,p') reaction at E_p = 7.5 MeV. Proton gates correspond to the excitation energies in ^{106}Cd indicated in the figure.

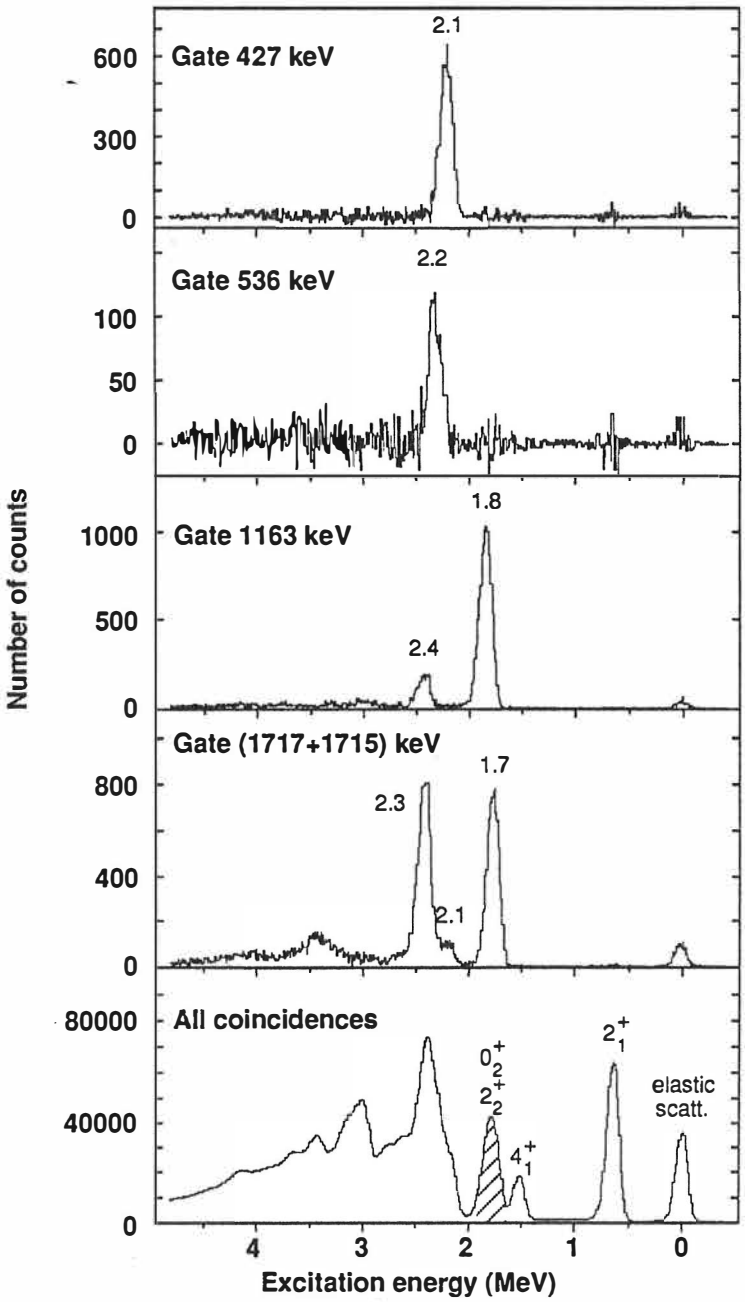

Fig. 2.3: Gamma-ray gated proton spectra from the ^{106}Cd(p,p') reaction. Spectra of protons in coincidence with the indicated γ rays are shown. In the total proton projection few of the excited levels in ^{106}Cd are marked; the protons in the hatched area (gate) are in coincidence with the γ rays in Fig. 2.2. (b); the events in the peak denoted as elastic scatt. originate from random coincidences.

In this geometry the summing of γ-rays in cascade was not negligible. Especially it caused an irritating spurious γ-ray peak at the energy corresponding to the transition from the excited 0^+ state to the ground state 0^+, where no γ-transition is allowed at all. One example is shown in the insert of Fig. 2.2 (b), where the 1795 keV line is the sum peak of the 633 keV and 1163 keV transitions. The angular correlation of the γ-rays in the (0^+-2^+-0^+)-cascade is more strongly peaked around 0 degrees (the angle between the γ-rays) than for example in the (4^+-2^+-0^+)- or the (2^+-2^+-0^+)-cascade. Thus the sum peak in the first case appeared to be even larger than in the (4^+-2^+-0^+)-cascade. Typically the sum-peak area corresponding to the (4^+-2^+-0^+)-cascade was 1.5% of the area of the less intense γ-ray peak involved, while the sum-peak area corresponding to the (0^+-2^+-0^+)-cascade was about 3%. Furthermore, the different de-excitation paths were considered in evaluating the sum peaks. The areas of the γ-ray peaks were carefully checked to subtract the sum-peak contribution and give the true γ-ray intensity.

The relative efficicncy calibrations for the γ-ray detectors were done with the calibration sources of ^{133}Ba, ^{152}Eu and ^{56}Co by placing the source into the target place. The final energy calibration was done by means of internal calibration or with the aforementioned sources.

Our proton-gamma coincidence setup was also successfully utilized in the study of the 0^+ states near 5 MeV in ^{208}Pb [Jul87] and in the study of the low-spin states of ^{198}Pt [Yat88].

2.1.2. Electron spectroscopy

Our combination electron-spectrometer system [Jul88] which includes a Siegbahn-Slätis type of magnetic lens and a cooled 110 mm^2 x 3 mm Si(Li) detector was employed in the conversion-electron measurements. The maximum transmission for the detector used is about 7%, and the momentum bandwidth about 17%. The resolution of Si(Li) detector was about 2.8 keV at 1 MeV. To suppress the delayed β^--

background, a narrow time gate, typically about 20 ns, synchronized with the cyclotron beam micropulse (rf) was used. Energy selection correlated with the momentum window was used in the sweeping mode of the spectrometer in order to reduce the background originating from the Faraday cup.

The relative efficiency calibration for the electron spectrometer was done with the sources ^{207}Bi and ^{152}Eu. The final energy calibration was done by means of the internal calibration.

Electron spectra following the inelastic proton scattering were obtained for the ^{106}Cd, ^{108}Cd and ^{110}Cd isotopes. The conversion-electron spectrum covering the energy range from 1.4 MeV to 2.3 MeV in Fig. 2.2 (e) and the energy range 0.3 MeV to 2.3 MeV in Fig. 2.4 is shown for the ^{106}Cd(p,p') reaction.

In order to deduce absolute E0 and E2 transition rates from a 0^+ state one should know the lifetime of the decaying state. When the lifetime is not known the experimental ratio X of the competing E0 and E2 transitions de-exciting the 0^+ states can be deduced from the K internal-conversion electron intensities as follows [Kan84]:

$$X_{ijk} = \frac{B(E0;0_i^+ - 0_j^+)}{B(E2;0_i^+ - 2_k^+)} = 2.56 \cdot 10^{-6}\, A^{4/3}\, E_\gamma^5(E2) \frac{\alpha_K(E2)\, I_K(E0)}{I_K(E2)\, \Omega_K(E0)} ,$$

where the E2 transition energy E_γ (E2) is given in keV, the I_K(E0) and I_K(E2) are the observed K conversion-electron intensities, and the α_K(E2) is the theoretical E2 K internal-conversion coefficient [Rös78] and Ω_K(E0) is the electronic factor for the E0 transition from Ref. [Bel70].

The E0/E2 branching ratios were extracted from the (p,p') electron spectra, as well as from the In decay measurements. The experimental K internal-conversion coefficients, $\alpha_K = I_{e^-} / I_\gamma$, were also deduced from both the (p,p') and indium decay measurements (see the chapter 2.4 for In decay). The γ-ray and electron intensities were normalized to give the theoretical α_K [Rös78] corresponding to E2 multipolarity for the $2_1^+ - 0_1^+$ transition.

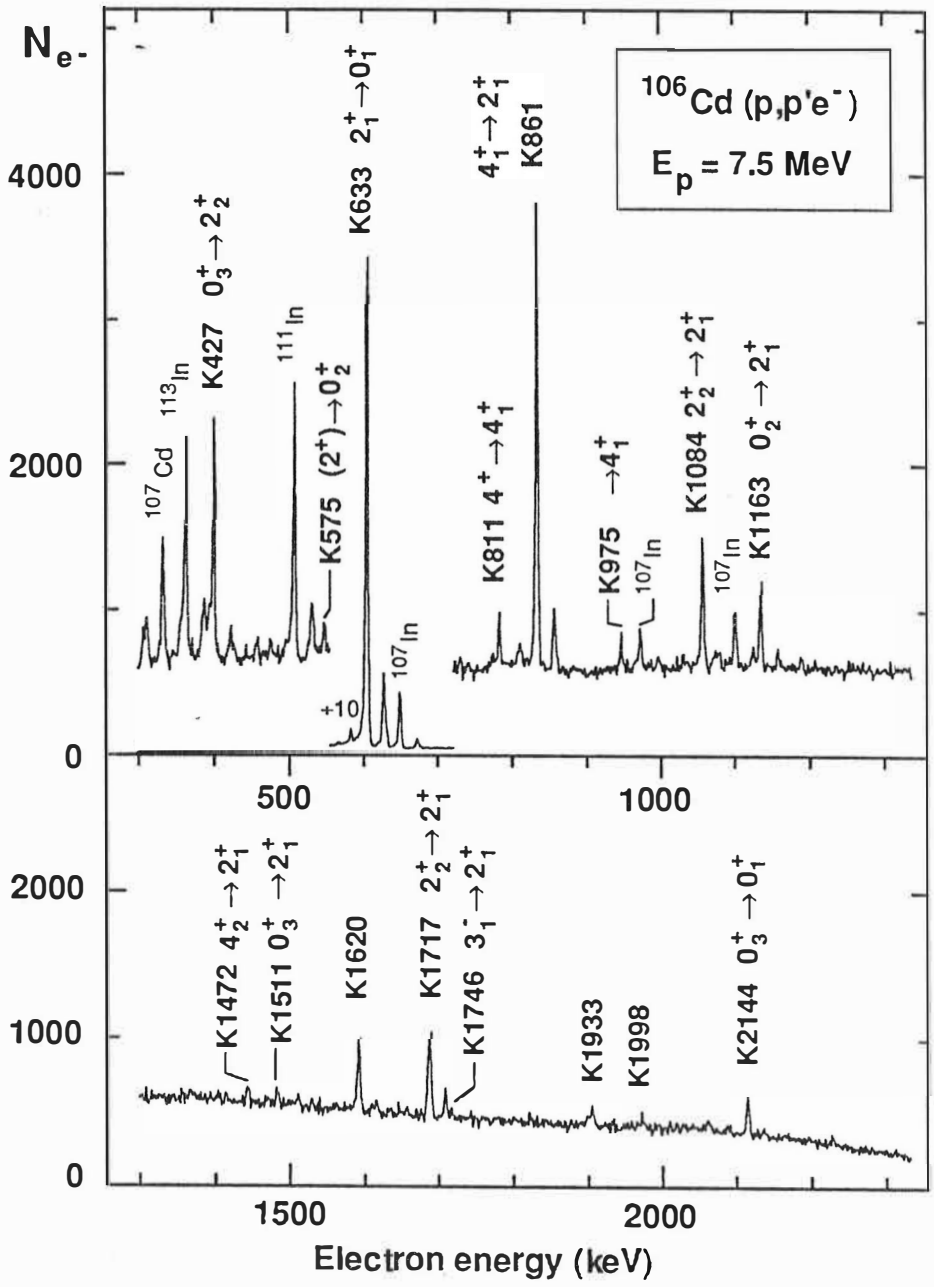

Fig. 2.4: The singles electron spectrum from the ^{106}Cd(p,p'e$^-$) at E_p = 7.5 MeV.

2.2. (p,2n) reaction

To further study low-spin properties of the ^{106}Cd and ^{108}Cd isotopes, the (p,2nγ)-reaction was employed. The targets were enriched self-supporting ^{107}Ag and ^{109}Ag foils (Table 1.2). With this reaction gamma-gamma coincidences, angular-distribution and excitation-function curves for γ-rays were measured.

2.2.1. Gamma-gamma coincidence measurements

The performance of large Compton suppressed Ge detector arrays has been found particularly useful in the study of high-spin states of fast rotating nuclei. In those studies high multiplicity of γ-rays and Doppler effects normally do not allow detector to source distances to be less than 15 cm [Eji89]. Consequently, the way to increase the detection efficiency and enhance the detection of high-multiplicity events in coincidence experiments, is to add as many detectors as possible around the target. On the other hand, in this geometry there is space enough to surround Ge detectors by BGO anti-Compton shields (for such setups, see e.g. Ref. [Eji89]).

In the study of low-spin non-yrast states via light-ion reactions, the γ-ray multiplicity is low and the Doppler effects are small. Therefore, the coincidence efficiency is often maximized by using a close-geometry detector setup. At JYFL three or four Pb-shielded Ge detectors at a distance of about 5 cm from the target have normally been used. In that geometry there is no space for anti-Compton shields.

For the aforementioned arguments it was interesting to apply the two Compton-suppressed Ge detectors (20-25 %) (designed for the NORDBALL array [Mos89]) to the typical low-spin experiments. The coincidence arrangement is shown in Fig. 2.5. The BGO+Ge units are positioned at about 115 degrees to the beam direction. The distance of Ge-crystal to target is about 8 cm, corresponding to an effective solid angle of about a factor of two smaller than that at the distance of 5 cm in the conventional

close-geometry setup. In a two-detector coincidence measurement it corresponds to a loss of a factor of four in the coincidence efficiency. The use of anti-Compton mode further reduces the coincidence rate by a factor of 7.

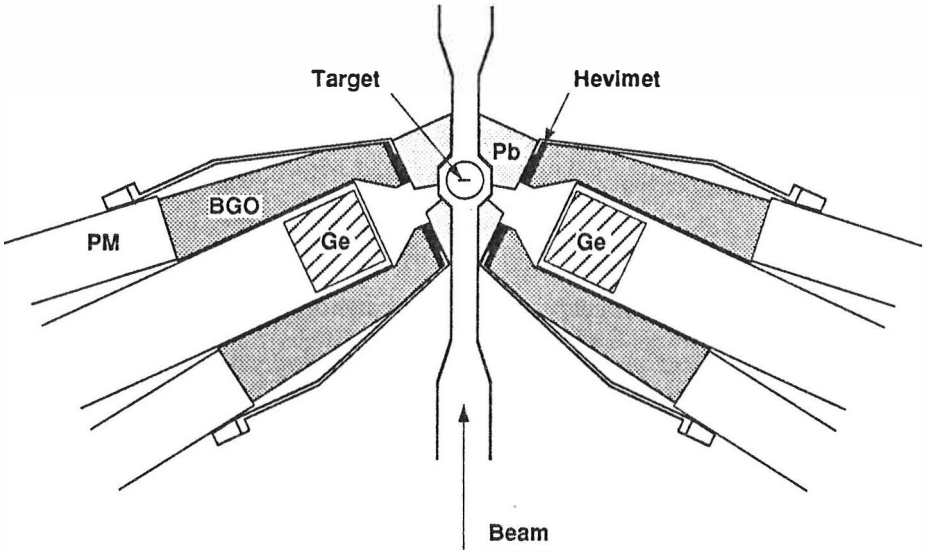

Fig. 2.5: The arrangement of two Compton-suppressed Ge detectors of the NORDBALL type.

The comparison of the three detectors in the close-geometry setup and the two NORDBALL-type detectors in the new setup was made in the $^{115}Sn(\alpha,n)^{118}Te$ reaction. In a few days about 3 x 10^6 coincidence events were recorded in the new setup, which was about 10 times less events than in the old geometry. In spite of the smaller number of events in the anti-Compton experiment, a much better peak-to-background ratio was achieved, especially for the low-energy peaks (Fig.2.6). Moreover, the number of tapes to be handled was reduced from 22 to 1.

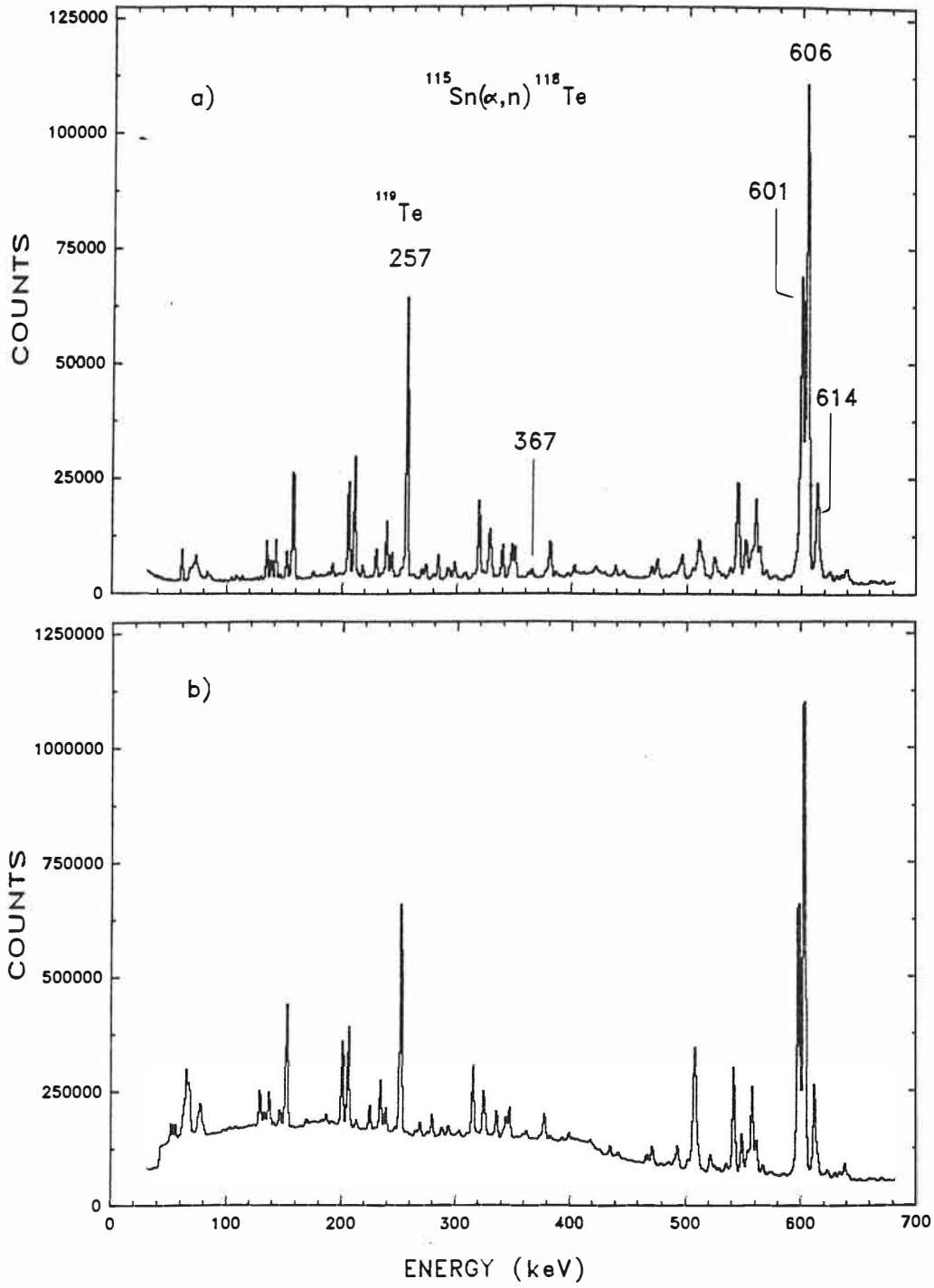

Fig. 2.6: The γ-ray coincidence spectrum from the $^{115}Sn(\alpha,n)^{118}Te$ reaction at E_α = 14.5 MeV taken with the coincidence arrangement shown in Fig. 2.5 in (a) and with the conventional three detector setup in (b).

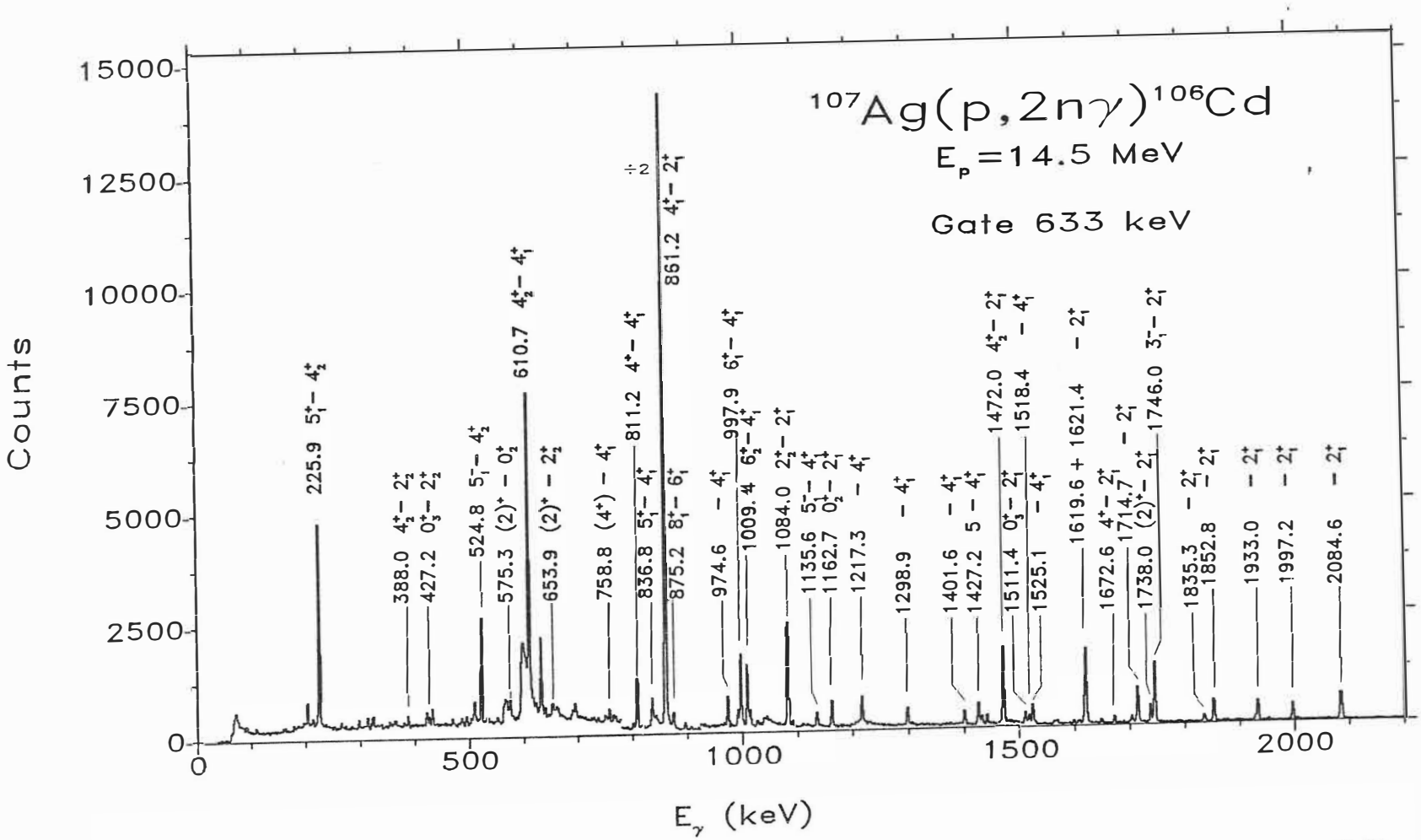

Fig. 2.7: Gamma-rays in coincidence with the $2_1^+ - 0_1^+$ γ-ray transition in ^{106}Cd from the reaction ^{107}Ag(p,2n) at E_p = 14.5 MeV. Two NORDBALL-type Compton suppression spectrometers have been used.

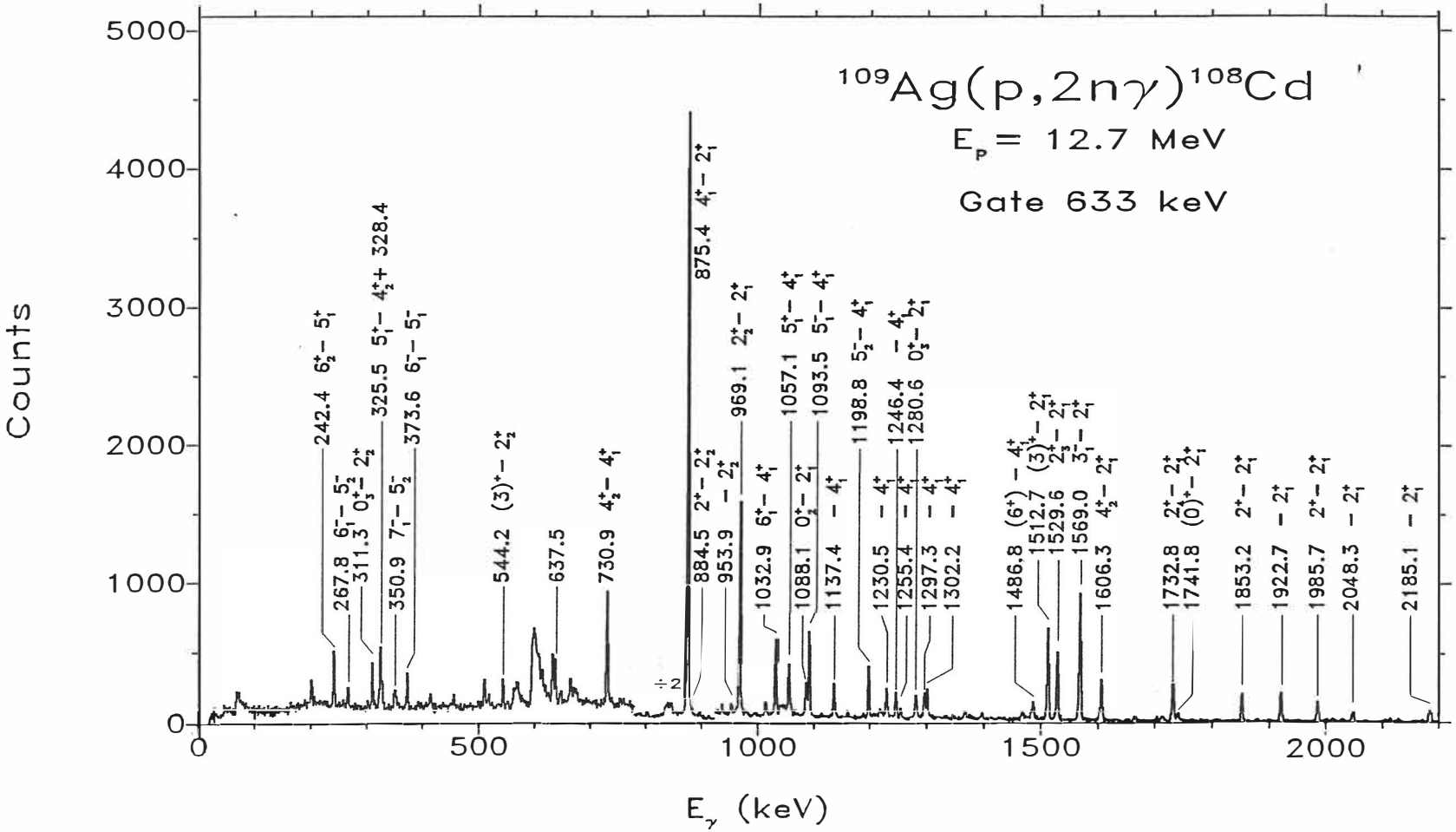

Fig. 2.8: Gamma-rays in coincidence with the 2_1^+ - 0_1^+ γ-ray transition in ^{108}Cd from the reaction ^{109}Ag(p,2n) at E_p = 12.7 MeV. Two NORDBALL-type Compton suppression spectrometers have been used.

For ^{106}Cd and ^{108}Cd, $\gamma\gamma$-coincidences with the new setup were measured at E_p = 14.5 MeV and at E_p = 12.7 MeV, respectively. About 3.3 x 10^6 and 1.4 x 10^6 Compton-suppressed coincidence events for ^{106}Cd and ^{108}Cd, respectively, were recorded in the event-by-event mode in these measurements. The E_γ-E_γ matrix sorted off-line was symmetrized before gating. Spectra corresponding to the gate set on γ-rays of the 2_1^+ - 0_1^+ transition in ^{106}Cd and ^{108}Cd are illustrated in Figs. 2.7 and 2.8, respectively. See also Fig. 3.2 in the chapter 3 showing more examples of gated coincidence γ-ray spectra in ^{106}Cd.

2.2.2. Angular-distribution measurements

The incoming projectile and the target form an excited compound nucleus which is strongly aligned in the angular momentum relative to the beam direction. The decay of the compound system, first by evaporation of neutrons and then by the emission of γ rays, has little influence on this alignment thus even the low-lying states of the final nucleus still possess a significant alignment. Consequently, γ-rays depopulating these states exhibit characteristic angular distributions depending upon the multipolarity of the radiation and the spin of the states involved.

In this work the γ-ray angular-distribution measurements for the ^{107}Ag(p,2n)^{106}Cd (E_p = 14.5 MeV) and ^{109}Ag(p,2n)^{108}Cd (E_p = 12.7 MeV) reactions were carried out at 5 different angles between 90° and 158° with respect to the beam direction. The singles γ-ray spectra were recorded with a 25% Ge detector (the resolution of 1.7 keV at 1.1 MeV) positioned at a distance of 12 cm from the target. The five spectra were normalized by using another 15% Ge detector at a fixed position at 125 degrees.

The angular-distribution of the emitted γ-rays can be expressed in terms of Legendre polynomials as

$$W(\theta) = 1 + Q_2A_{22}P_2(\cos\theta) + Q_4A_{44}P_4(\cos\theta),$$

when the first term is normalized to unity. The angle of the detector with respect to the beam direction is θ. The $A_{22} = \alpha_2 A_2^{max}$ and $A_{44} = \alpha_4 A_4^{max}$ are the angular-distribution coefficients, where α_2 and α_4 are the attenuation factors due to the spin de-alignment, and the A_2^{max} and A_4^{max} are the coefficients in the case of complete alignment. Useful tables for those can be found in Refs. [Yam67, Mat74]. The solid-angle corrections, Q_2 and Q_4, due to the finite size of the detector were estimated to be less than 5% [Kra72] and thus were neglected in the present analysis.

The simple "empirical rule" for the coefficients A_{22} and A_{44} is the following: a positive A_{22} value with a smaller negative A_{44} value indicates a $\Delta I = 2$ transition; a negative A_{22} value with a positive A_{44} value close to zero indicates a $\Delta I = 1$ transition; pure dipole $\Delta I = 0$ transition has a large positive A_{22} value with a negative A_{44} value close to zero. One must apply the rule with caution, since it assumes pure transitions, which is not often the case. The effect of mixed multipolarities can be found in the tables by Mateosian et al. in Ref. [Mat74].

Generally the γ-rays from an aligned state are emitted anisotropically. In the special case, when the initial state has spin 0, and thus no orientation, the angular distribution of the emitted γ-rays is isotropic. This was used in several cases as an additional evidence for assigning spin 0^+ to the state. A few examples of the angular distributions of γ-rays in ^{106}Cd and ^{108}Cd are shown in Figs. 2.9 and 2.10, respectively.

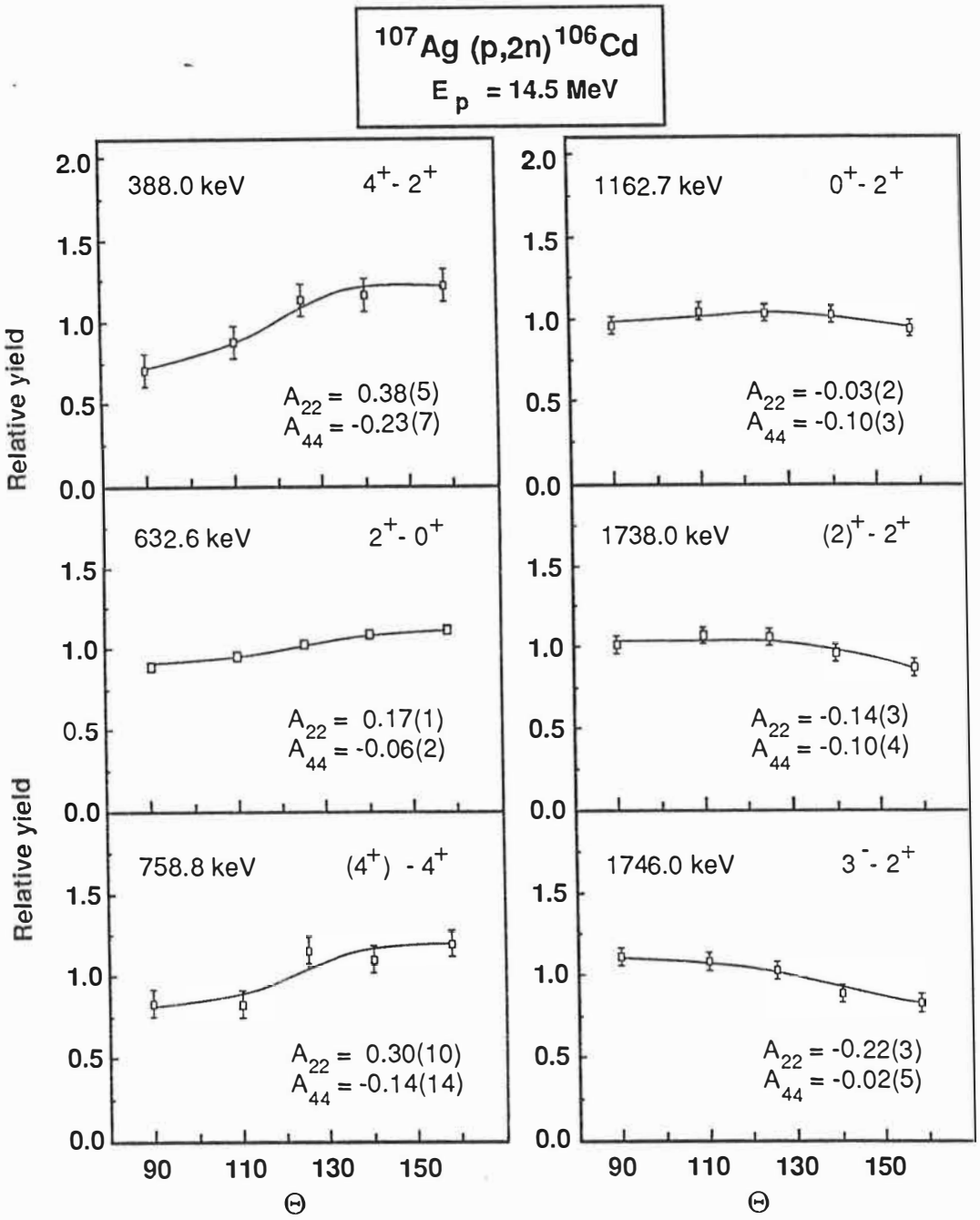

Fig. 2.9: Angular distributions and least-square fits to the W(θ) function for some γ-ray transitions in ^{106}Cd.

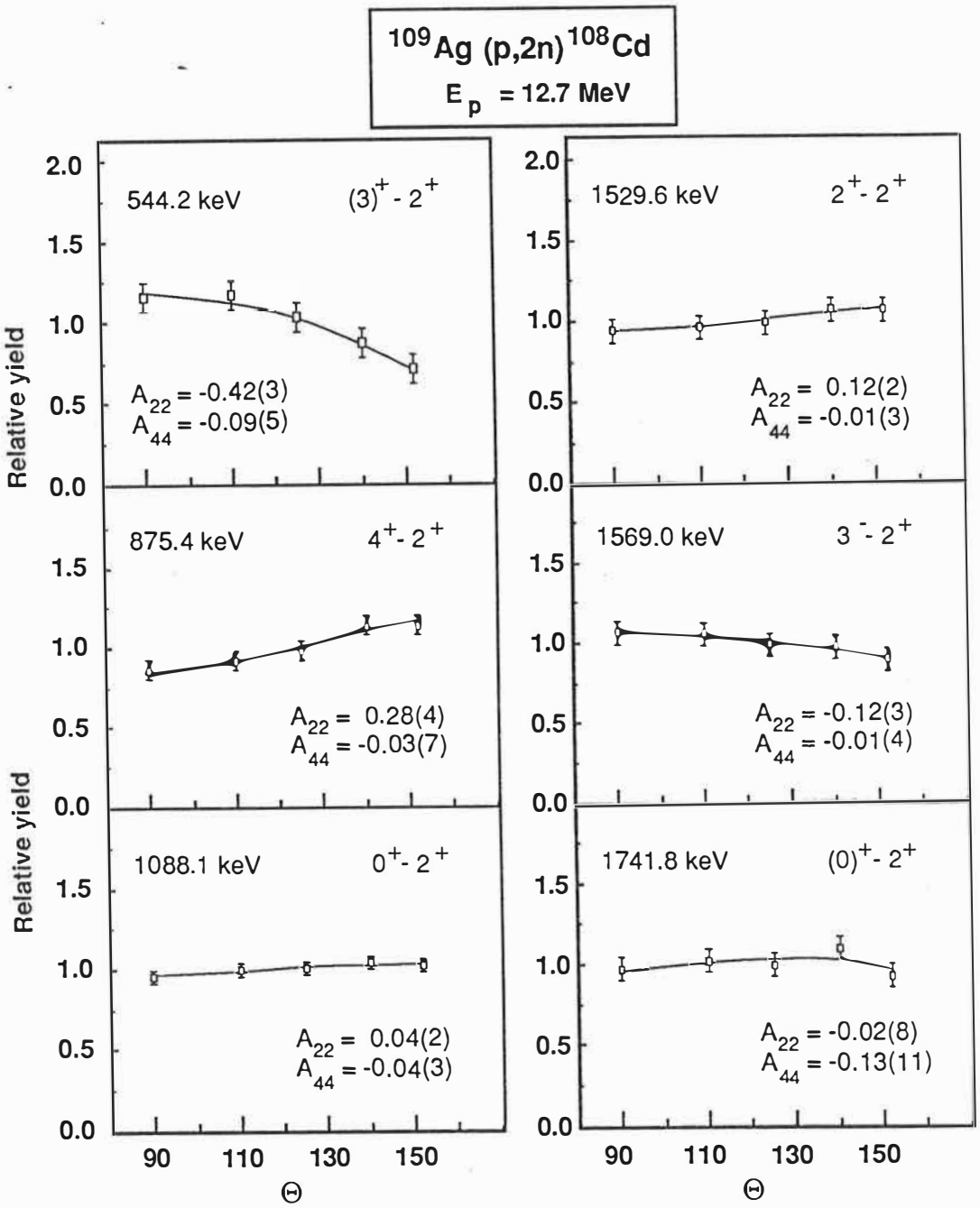

Fig. 2.10: Angular distributions and least-square fits to the W(θ) function for some γ-ray transitions in ^{108}Cd.

2.2.3. Excitation-function measurements

The increase of the projectile energy results in an increase of the angular momentum of the compound nucleus. Since the angular momentum changes little after the neutron evaporation, the dependence of the γ ray intensity on the projectile energy can be used to evaluate the spin of the residual states. Due to the increase in the angular momentum, the high-spin states are relatively more populated with increasing bombarding energy than the low-spin states.

The γ-ray excitation functions were measured for ^{106}Cd and ^{108}Cd in the (p,2n) reaction with proton energies of E_p = 12.3 MeV, 14.0 MeV, 15.7 MeV and 17.4 MeV. The same detectors as in the angular-distribution measurements were used to collect the singles γ-ray spectra at 125 degrees with respect to the beam direction and at the distance of 5 cm from the target.

Figures 2.11 and 2.12 show some typical curves obtained. The relative intensities of γ-rays are normalized to the intensities of the $2_1^+ - 0_1^+$ transition at each proton energy and to one at the lowest bombarding energy. Particularly, the spin of the first excited 0^+ state in ^{106}Cd and ^{108}Cd could be verified through the steepest downward slope in the excitation-function curve of the de-exciting ($0^+ \rightarrow 2^+$) γ ray (see the curves of the 1163 keV and the 1088 keV transitions in Figs. 2.11 and 2.12, respectively).

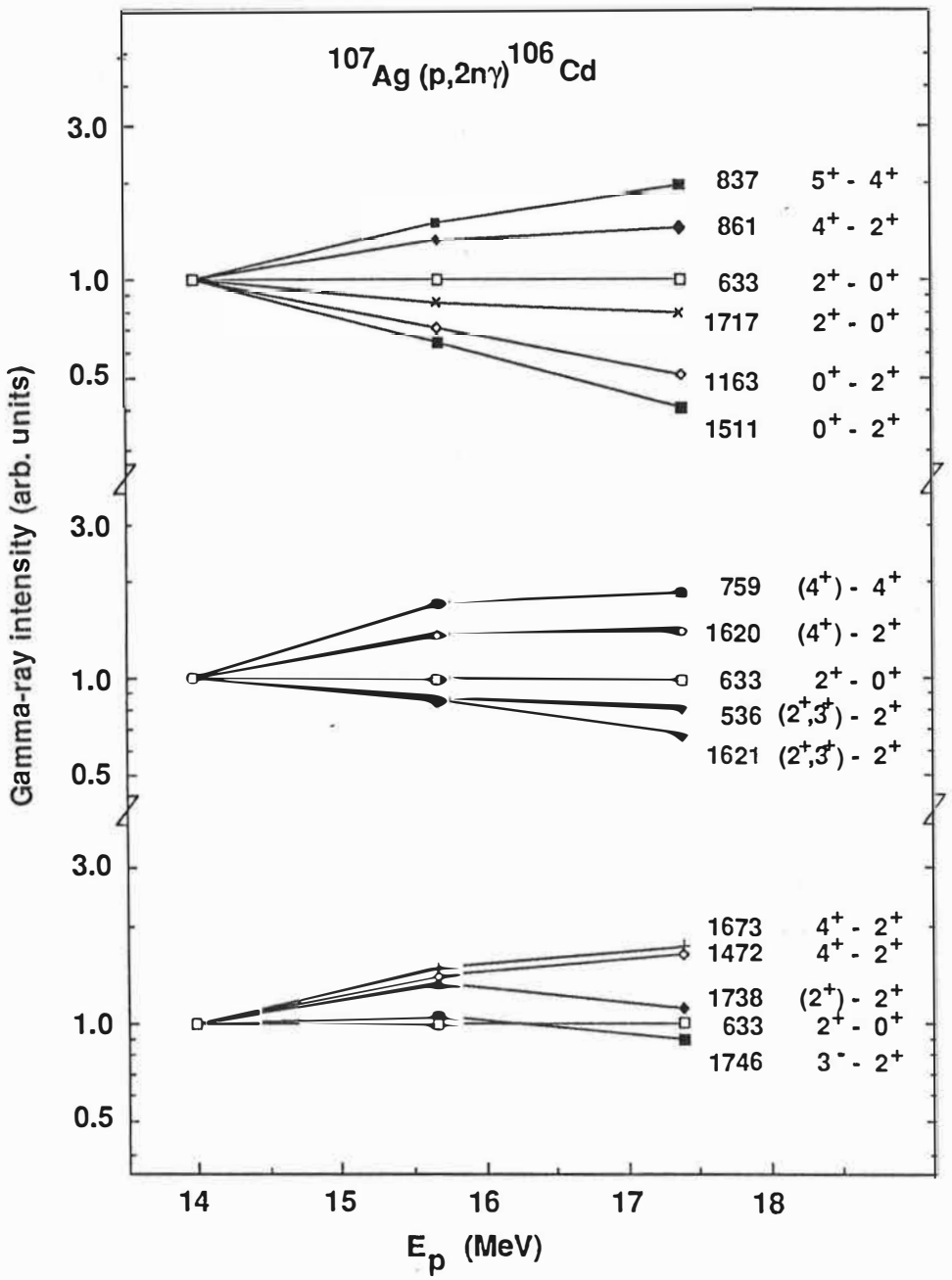

Fig. 2.11: Excitation functions for some γ-ray transitions in ^{106}Cd populated in the ^{107}Ag(p,2n) reaction. The relative yields normalized at E_p = 14 MeV are plotted.

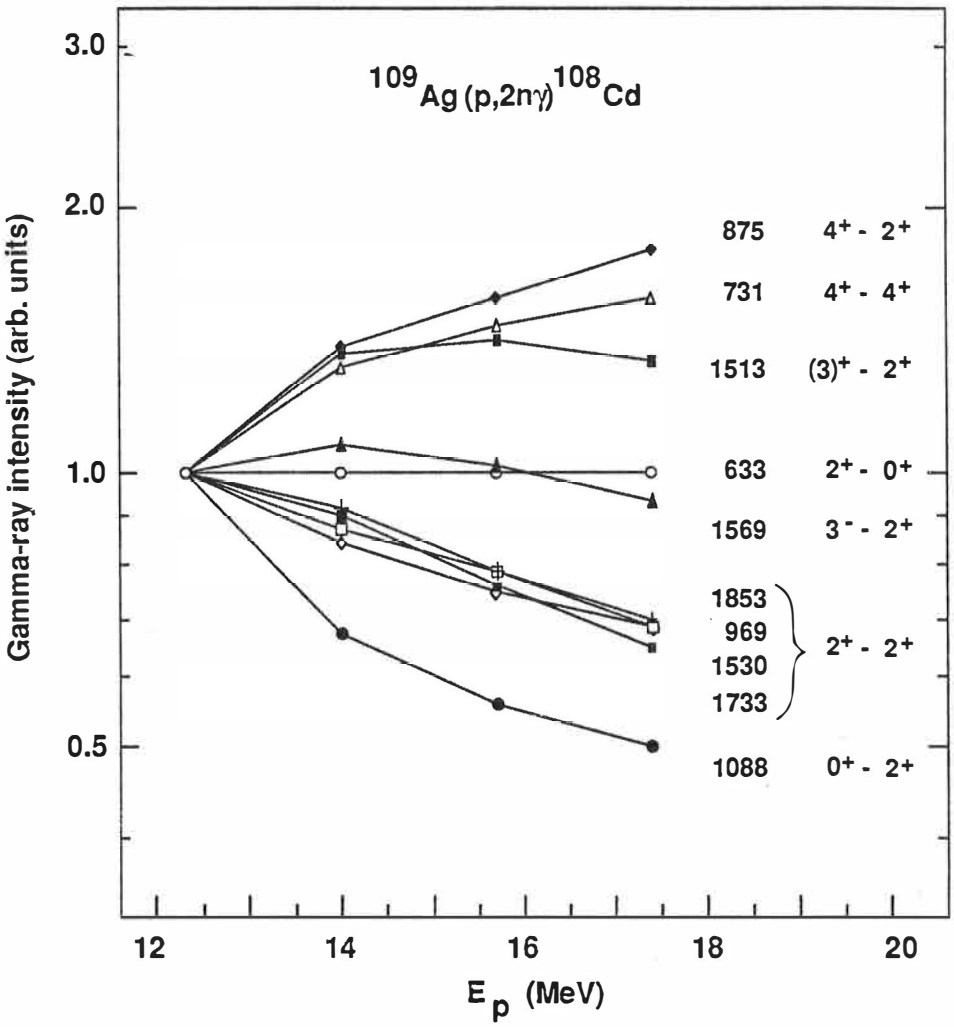

Fig. 2.12: Excitation functions for some γ-ray transitions in ^{108}Cd populated in the ^{109}Ag(p,2n) reaction. The relative yields normalized at E_p = 12.3 MeV are plotted.

2.3. (α,2n) reaction

For the study of low-lying levels of the ^{110,112}Cd isotopes, the (α,2nγ) reaction on an enriched ^{108,110}Pd target (Table 1.2) was also used. The γγ-coincidence, angular-distribution and excitation-function measurements were performed.

About 18 x 10^6 gamma-gamma coincidences were recorded for ^{110}Cd at E_α = 18 MeV by employing 20 % and 25 % Ge-detectors in the conventional close-measurement geometry without anti-Compton shields. In the γγ-coincidence measurement for ^{112}Cd at E_α = 20 MeV, three Ge-detectors were used in close geometry (40%, 25% and 15%) and about 60 x 10^6 γγ-coincidences were recorded. Examples of the spectra are shown in Figs. 3.6 and 3.8 later in chapter 3.

In the γ-ray excitation-function measurements α-beam energies from 17.0 MeV to 20.0 MeV were used (Figs. 2.13 and 2.14). In the angular-distribution measurement, γ-ray spectra at 5 angles between 90° and 155° were measured at E_α = 18 MeV and E_α = 20 MeV for ^{110}Cd and ^{112}Cd, respectively. In Fig. 2.15 a few angular distributions are shown for ^{112}Cd. The analysis of those measurements was done like the one for ^{106,108}Cd in the (p,2n) reaction described in the previous chapter.

2.4. Decay measurements

In addition to the in-beam experiments, valuable information for ^{106}Cd, ^{108}Cd and ^{110}Cd was obtained in off-beam measurements of γ-ray and conversion-electron spectra following the EC/β^+-decay of odd-odd In isomers. The decaying isomers were the 2^+ state and the 7^+ ground state, the half-lives of which are collected in Table 2.1. The data is from Nuclear Data Sheets [DeF88, Hae82, DeG83] if not mentioned otherwise. The Q_{EC} given also in Table 2.1 shows that there is enough energy available to populate the excited levels in ^{106,108,110}Cd isotopes through the EC/β^+-decay.

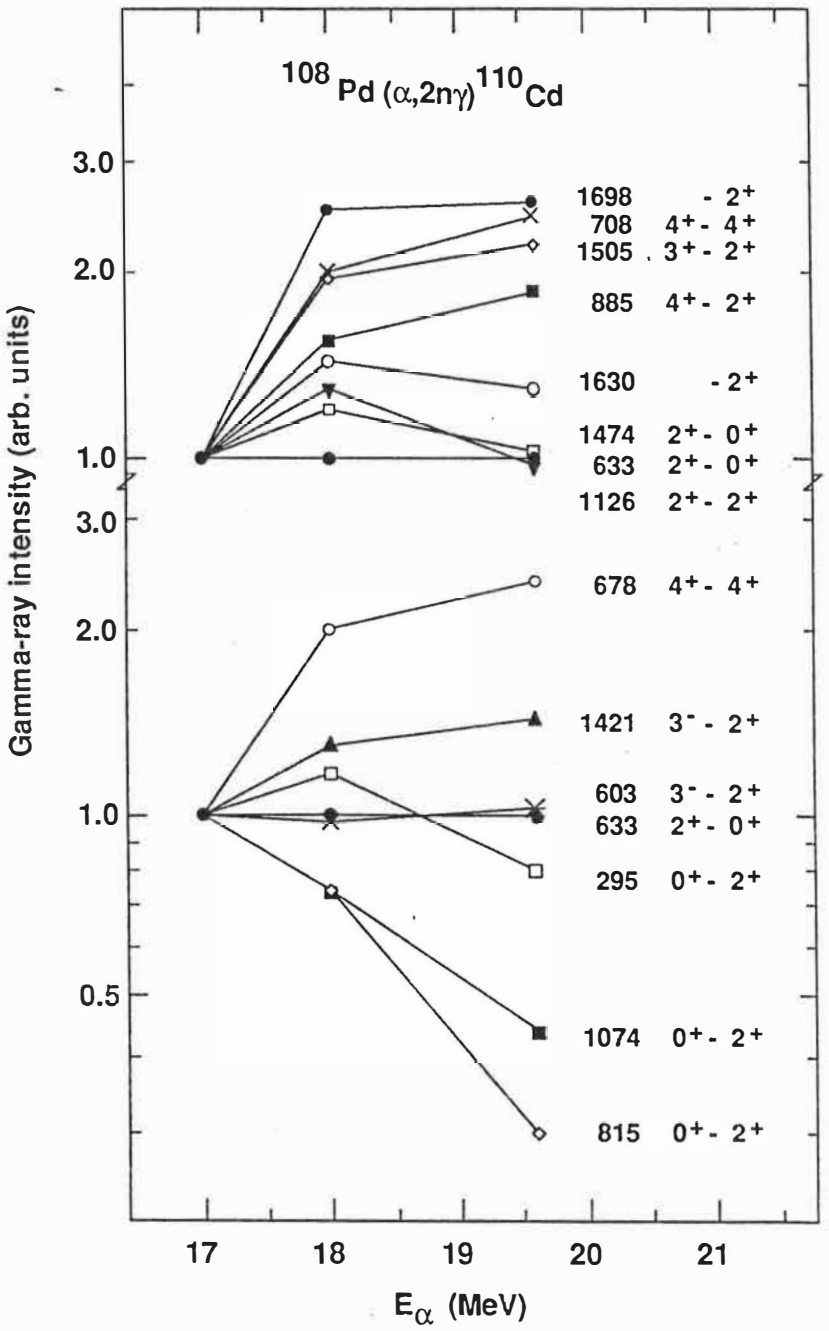

Fig. 2.13: Excitation functions for some γ-ray transitions in ^{110}Cd populated in the ^{108}Pd(α,2n) reaction. The relative yields normalized at E_α = 17 MeV are plotted.

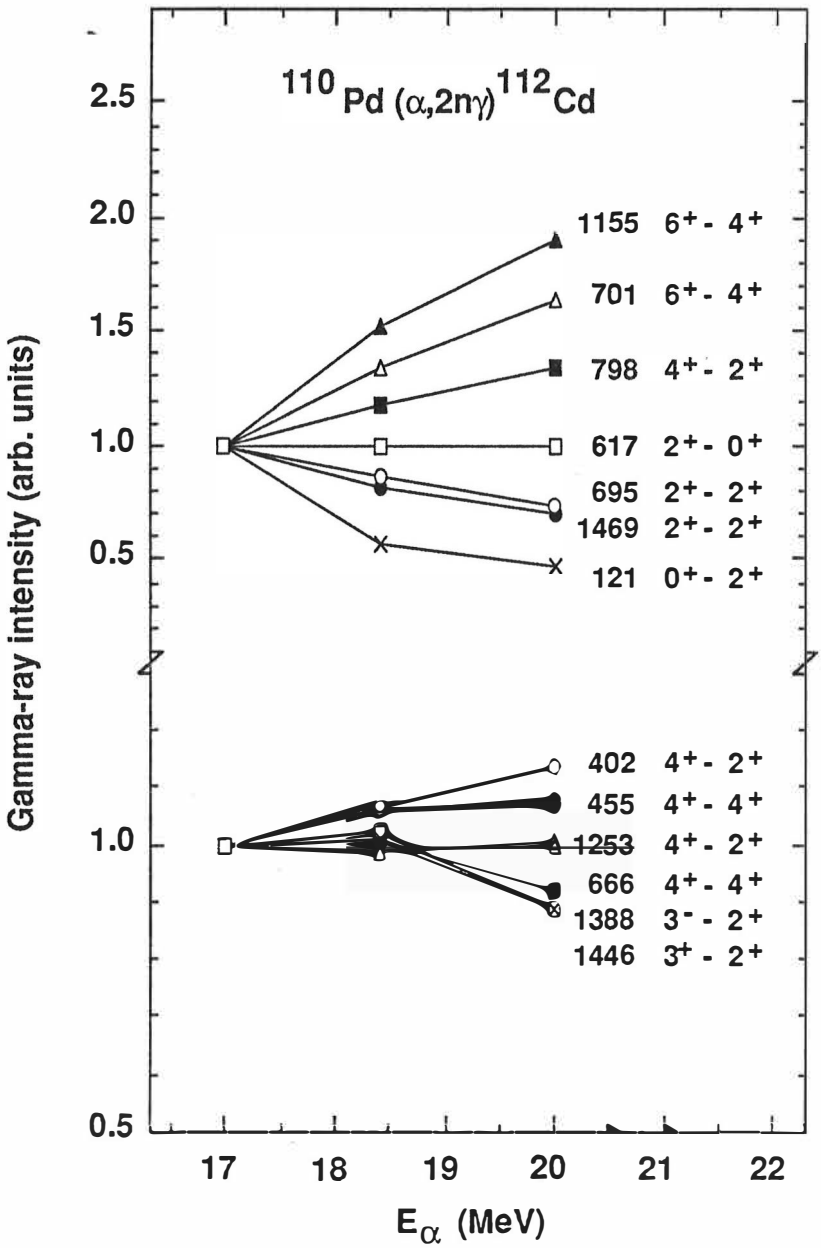

Fig. 2.14: Excitation functions for some γ-ray transitions in ^{112}Cd populated in the ^{110}Pd(α,2n) reaction. The relative yields normalized at E_α = 17 MeV are plotted.

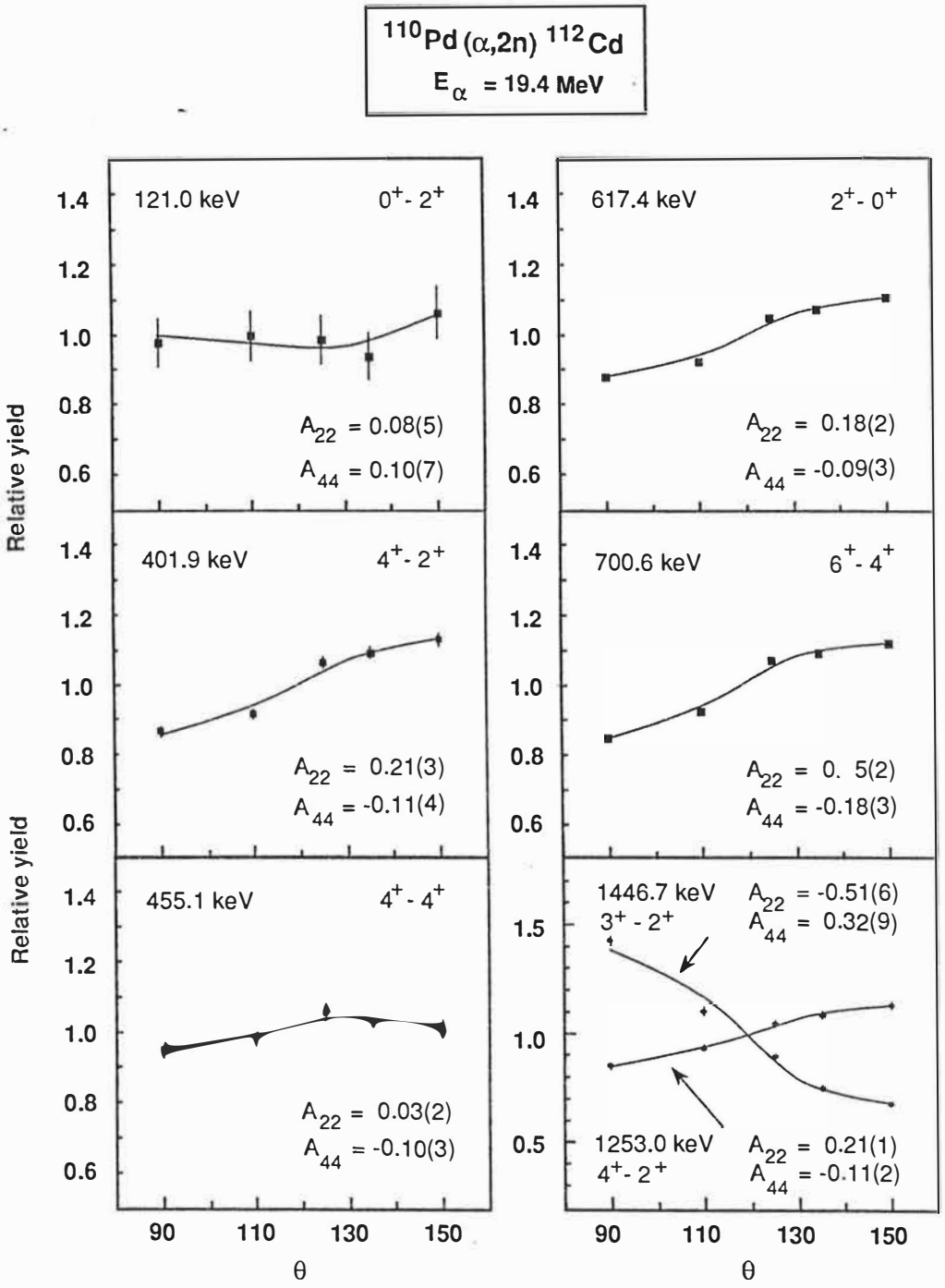

Fig. 2.15: Angular distributions and least-square fits to the W(θ) function for selected γ-ray transitions in ^{112}Cd.

Table 2.1. Properties of decaying isomers in ^{106,108,110}In.

	^{106}In	^{108}In	^{110}In
I^{π}	$(2)^+$ [a]	2^+ [b]	2^+ [c]
$T_{1/2}$ [min]	5.2	39.6	69.1
$I^{\pi}_{g.s.}$	7^+	7^+ [b]	7^+ [c]
$T_{1/2}$ [min]	6.2	58.0	294
Q_{EC} [MeV] [d]	6.5	5.1	3.9

a From Ref. [Gul90]
b From Ref. [Kra89a]
c From Ref. [Kra89b]
d Only one value given, since the decaying isomers are within 50 keV.

The decaying isomers were produced in bombardments of enriched, rolled ^{106}Cd, ^{108}Cd and ^{110}Cd foils (Table 1.2) by the (10 - 12.5) MeV protons. In the γ-ray measurements multispectra were recorded which allowed us to deduce half-lives. The information was used to identify the transition into the right nucleus, not for the exact value of the half-lives (which are already known). In the conversion-electron measurements, the aforementioned magnetic lens plus Si(Li) electron spectrometer was employed. In the measurements, the activation, waiting and collection periods were as follows, respectively: 9 min, 3 min and 12 min for ^{106}Cd; 50 min, 20 min and 80 min for ^{108}Cd; 70 min, 30 min and 80 min for ^{110}Cd. In Fig. 2.16 parts of a γ-ray and a conversion-electron spectrum following the EC/β^+ decay of ^{108}In are presented.

The K-conversion coefficients, $\alpha_K = I_{e^-} / I_\gamma$, were determined from these In decay measurements. The intensities for γ-rays and electrons were normalized to give E2 multipolarity for the 2^+_1 - 0^+_1 transition according the values given in the tables of Rösel et al. [Rös78]. Since both of the isomers decaying were produced, the α_K-values were corrected for different decaying half-lives (Table 2.1) in the case of ^{110}Cd

due to different collection times of the electron and γ-ray spectra. For other isotopes the correction is within the experimental errors and was neglected. An example of α_K-coefficients is in Fig. 2.17, where the theoretical (curves) [Rös78] and the experimental (markers) α_K-values are shown for transitions in ^{108}Cd. As one can see in the figure the multipolarities M1 and E2 can not be distinguished experimentally. However, the angular distribution data combined with the conversion coefficients often permit us to make a unique determination.

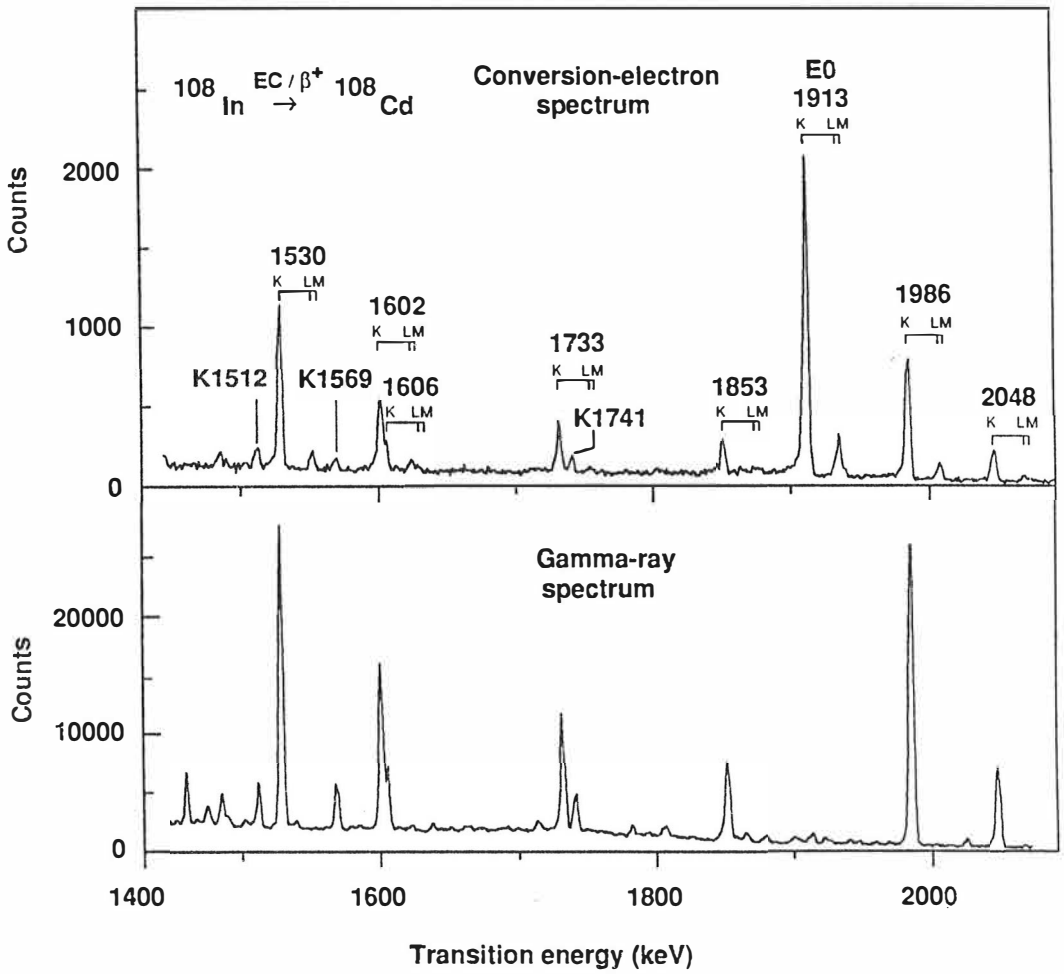

Fig. 2.16: The singles γ-ray (bottom) and conversion-electron (top) spectra following the EC/β+ decay of ^{108}In. The electron spectrum is shifted so that the K conversion-electron peaks coincide with the corresponding γ-rays.

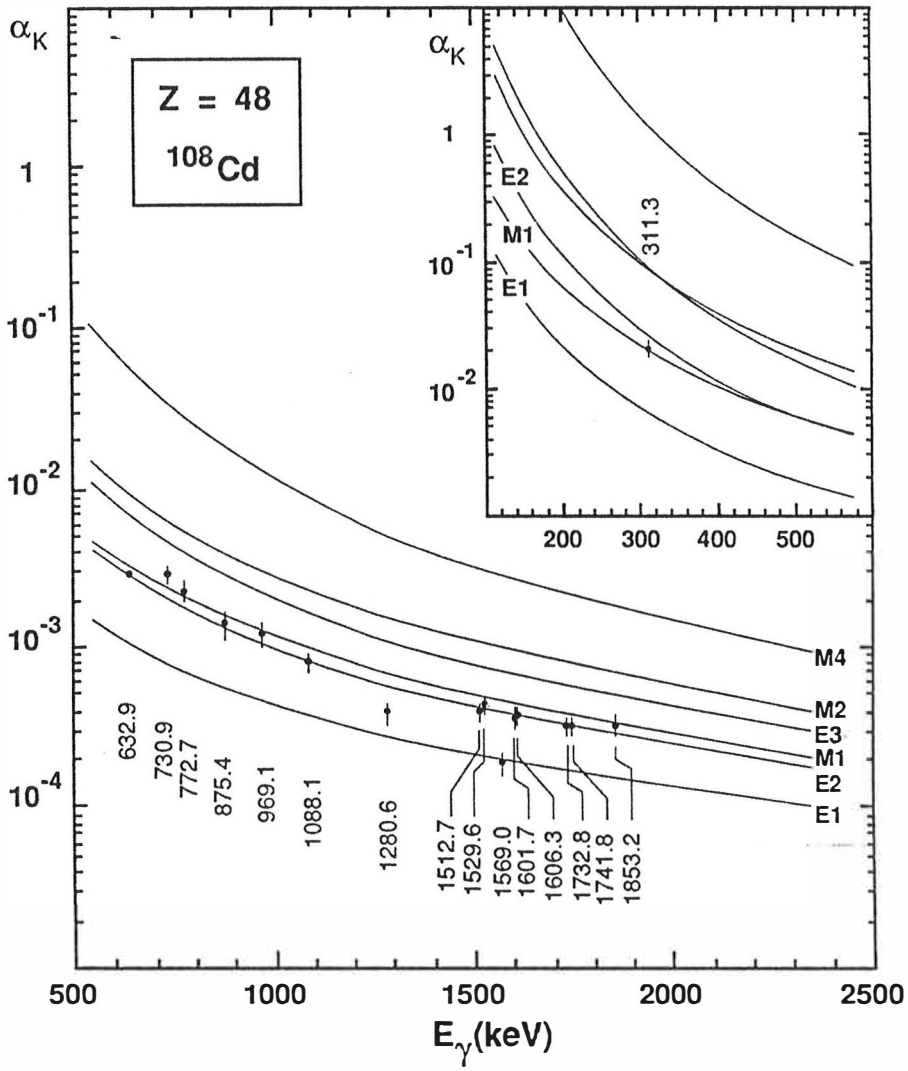

Fig. 2.17: The internal K-conversion coefficients for transitions in ^{108}Cd.

3. Experimental results

In this chapter we discuss in detail the experimental results for Cd isotopes obtained in this work. A short review of the earlier studies is also given.

A summary of the results is given in Tables 3.1 - 3.5 for each isotope. As only the low-lying collective states were of interest we limited level-energy range to that below about 2.5 MeV for ^{106}Cd, ^{108}Cd and ^{110}Cd and below 2 MeV for ^{112}Cd and ^{116}Cd. Above that energy the non-collective two quasi-particle excitations become more important. The γ-ray intensities from different reactions applied in this work are given in those tables. One should note that the γ-ray intensities obtained from the (p,p') reaction correspond to the direct level population and are thus related to the (p,p') cross section, since they do not include γ-ray feeding. However, the γ-ray branching ratios from each level can be compared in different reactions. The internal K-conversion coefficients presented in the tables are from the present decay studies of odd-odd In and from the (p,p') measurements. Theoretical K-conversion coefficients for Cd are shown in Fig. 2.17. The angular-distribution coefficients A_{22} and A_{44} are from the (p,2n) reaction for ^{106,108}Cd (see also Figs. 2.9 and 2.10) and from the (α,2n) reaction for ^{110}Cd and ^{112}Cd (Fig. 2.15). The excitation-function curves shown in Figs. 2.11 (^{106}Cd), 2.12 (^{108}Cd) and 2.13 (^{110}Cd) illustrate at least one transition from each level, when possible. Only a few curves which are relevant for the discussion on ^{112}Cd are shown in Fig. 2.14. The last column in Tables 3.1 - 3.5 gives the multipolarity deduced in this work.

The level schemes of the even-mass Cd isotopes obtained in this work are presented in Figs. 3.1 (^{106}Cd), 3.3 (^{108}Cd), 3.5 (^{110}Cd), 3.7 (^{112}Cd) and 3.9 (^{116}Cd). The placements of the transitions are based on the γγ- and pγ-coincidence data. The adopted γ-ray branching ratios shown in the level schemes are obtained by averaging the values from different experiments. The spin and parity assignments are

inferred from the excitation functions and the angular distributions of γ-rays and from the conversion-electron data.

3.1. The nucleus ^{106}Cd

The level scheme of the nucleus ^{106}Cd has previously been studied mainly by γ-spectroscopic methods via the EC/β^+ -decay of ^{106}In [Fla76, Hua78, Wis80, Rou84]. Roussiere et al. [Rou84] have also measured the conversion electrons. The high-spin states and the yrast-level structure have been investigated in compound-nucleus reactions: ^{104}Pd(α,2nγ) [Dan77], ^{97,96}Mo(^{12,13}C, 3nγ) [Sam79], ^{94}Zr(^{16}O, 4nγ) [Sam79] and ^{93}Nb(^{16}O, p2nγ) [And85]. Particle spectroscopy has been applied by Fielding et al. [Fie77] via the (^{3}He,n) two-proton transfer reaction, where excited levels above 3 MeV were strongly populated. Inelastic scattering of protons on ^{106}Cd was examined by Lutz et al. [Lut69], and inelastic scattering of alpha particles by Spear et al. [Spe77]. In many Coulomb-excitation experiments only the first three excited levels have been populated (e.g. ref. [Mil69, Esa76]). The majority of the data mentioned above has been summarized in the recent compilation of A = 106 [DeF88].

The experiments presented in this work have revealed two new levels in the level scheme of ^{106}Cd below the 2.4 MeV excitation, while no evidence was found on two levels reported earlier. For 6 levels the I^π value is new or revised and 8 new transitions were observed. In the next paragraphs details of the assignments obtained will be discussed.

Table 3.1. Properties of levels and transitions in ^{106}Cd as obtained in this work.

E_{level} [a] (keV)	J_i^π	E_{trans} [a] (keV)	J_f^π	γ-intensity [b] (p,p') [c]	(p,2n)	In decay	$10^3 \cdot \alpha_K$ [d]	Ang. Distr. Coeff. A_{22}	A_{44}	Multi-polarity
632.6	2_1^+	632.6	0_1^+	1000	1000	1000	3.0(1) *	0.17(1)	-0.06(2)	E2
1493.8	4_1^+	861.2	2_1^+	128	390	313	1.4(1)	0.24(1)	-0.06(2)	E2
1716.6	2_2^+	1084.0	2_1^+	197	43	27	0.84(10)	-0.14(1)	-0.06(2)	E2/M1
		1716.6	0_1^+	168	47 [e]	154 [f]				
1795.3	0_2^+	1162.7	2_1^+	164	14	12	0.68(9)	-0.03(2)	-0.10(3)	E2
2104.6	4_2^+	388.0	2_2^+	1.8(4)	2.5	2.3		0.38(5)	-0.23(7)	E2
		610.7	4_1^+	34	65	28	3.7(4)	0.09(1)	-0.04(2)	E2/M1
		1472.0	2_1^+	20	37	16	0.37(5)	0.27(1)	-0.06(1)	E2
2143.9	0_3^+	427.2	2_2^+	33	3.9	1.4	8.4(10) [d]	0.14(7)	-0.05(10)	E2
		1511.4	2_1^+	101	7.3	3.4	0.40(15)[d]	-0.08(6)	-0.03(9)	E2
		2143.9	0_1^+			< 0.1	> 42 [g]			E0
2252.2(6)	(4^+)	758.8	4_1^+	9.5	2.3	1.9		0.30(10)	-0.14(14)	(E2/M1)
		1619.6(6)	2_1^+	190(90)	44	39 [h]	0.34(5) [i]			
2254.0(5)	$(2^+,3^+)$	536.2	2_2^+	6.5	2.2			-0.48(23)	0.01(36)	(E2/M1)
		1621.4(4)	2_1^+	100(50)	15	h	i			
2305.1	4^+	811.2	4_1^+	38	28	9.6	1.8(3)	-0.14(7)	0.08(1)	E2/M1
		1672.6	2_1^+	4.8	3.7	1.9	< 0.45	0.34(5)	-0.16(7)	E2
2330.5	5_1^+	225.9	4_2^+	28	31	17	55(6)	-0.77(3)	-0.005(44)	E2/M1
		836.8	4_1^+	8.3	22	6.5	2.6(4)	-0.37(3)	-0.06(5)	E2/M1
2347.3		1714.7	2_1^+	185	24(6) [e]	f				
2370.6	$(2)^+$	575.3	0_2^+	25	1.8	3.7	3.6(5) [d]			E2
		653.9	2_2^+	30	2.6	4.6		0.05(5)	-0.12(7)	E2/M1
		1738.0	2_1^+	90	8.2	12		-0.14(3)	-0.10(4)	E2/M1
		2370.6	0_1^+	6.3	1.0					
2378.6	3_1^-	1746.0	2_1^+	121	43	12	< 0.15	-0.22(3)	-0.02(5)	E1

[a] Energy uncertainties typically 0.3 keV.

[b] Intensity error typically 15 %. Intensity of the $2_1^+ - 0_1^+$ transitions normalized to 1000.

[c] Gamma-ray intensities from the (p,p') reaction correspond to the direct level population.

[d] The K internal-conversion coefficients determined from the In decay experiminents except the ones marked with [d] are from the (p,p') experiments.

[e] Intensity determined from the γγ-coincidence spectra.

[f] Intensity contains the 1716.6 keV and 1714.7 keV transitions; see the data for the 1716.6 keV transition.

[g] E0 transition; $\alpha_K > 35 \times \alpha_K(M4)$.

[h] Intensity contains the 1619.6 keV and 1621.4 keV transitions; see the data for the 1619.6 keV transition.

[i] Conversion coefficient for the sum of the 1619.6 keV and 1621.4 keV transitions.

* Conversion coefficient normalized to $\alpha_K = 3.0(1)$ for the 632.6 keV line.

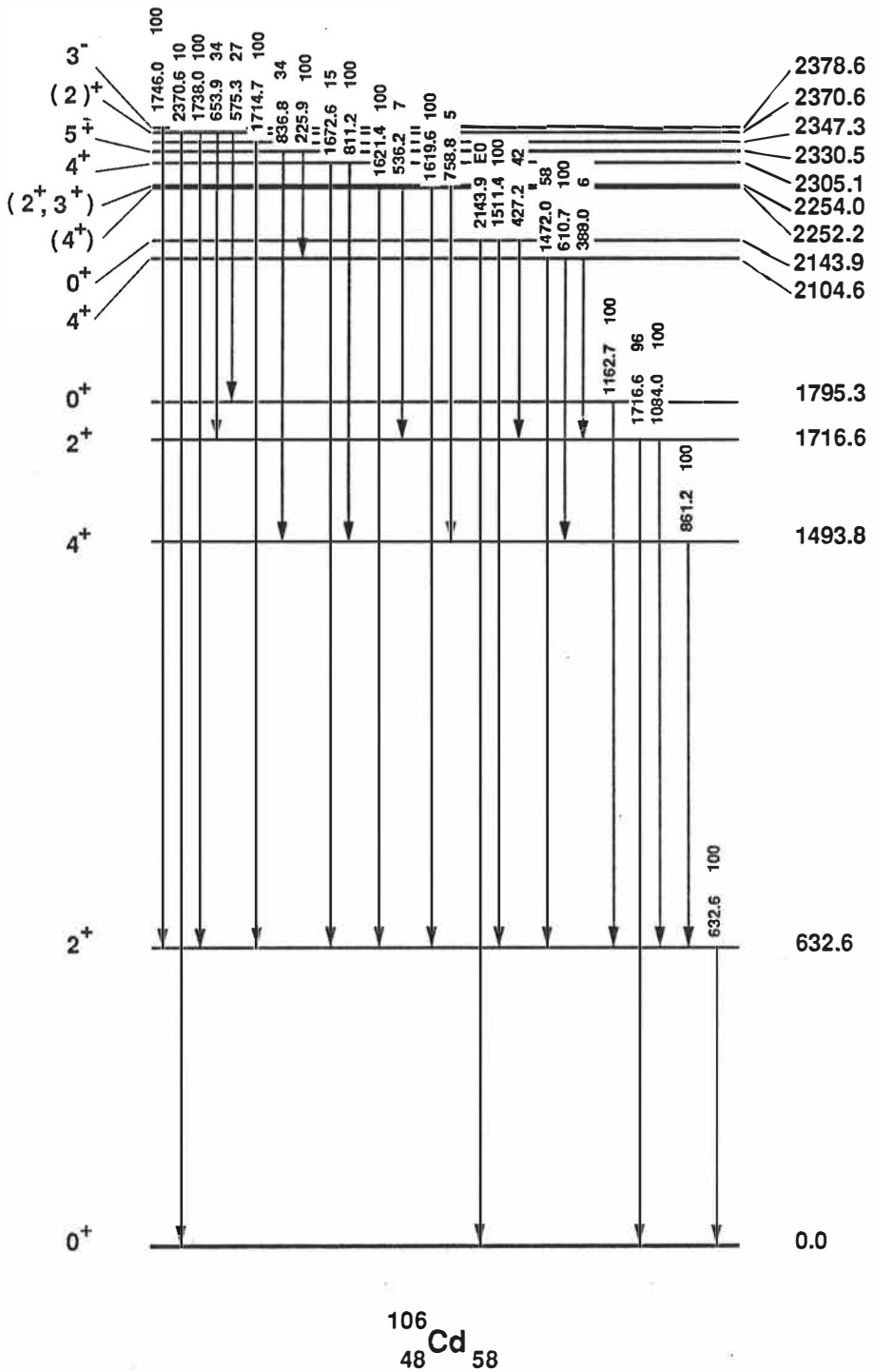

Fig. 3.1: The level scheme of ^{106}Cd as obtained in this work. The relative γ-ray intensities of the depopulating transitions are marked for each level .

The earlier assignments of 4^+ and 2^+ for the 1493.8 keV and 1716.6 keV levels [DeF88] are in agreement with the data given in Table 3.1 and the excitation-function data of Fig. 2.11. The present average value of 0.96(15) for the γ-ray branching ratio of the 1716.6 keV and 1084.0 keV transitions from the 2^+ (1716.6 keV) level is somewhat smaller than the value of 1.4(3) adopted in Ref. [DeF88] (although within the experimental errors). This may be due to the difficulties in the analysis of close-lying 1716.6 keV and 1714.7 keV lines.

The 1795.3 keV level has previously been populated in the beta decay of the low-spin isomer of ^{106}In [Rou84,Fla76,Hua78] and in the inelastic scattering of alpha particles [Spe77]. The spin and parity assignment of 4^+ for this state was proposed in Ref. [Fla76]. However, the present angular distribution of the depopulating 1162.7 keV transition is nearly isotropic (Fig. 2.9). Moreover, the excitation function of this transition shows a clear I = 0 character (Fig. 2.11). Thus, this state can be identified with the first excited 0^+ state in ^{106}Cd. In spite of the relatively strong population of this 0^+ state in the inelastic proton scattering any E0 transition from this state to the ground state is not observed in our conversion-electron measurements, which must be due to the fast competing 1162.7 keV E2 transition de-exciting this level. In the 1162.7 keV γ-ray gated proton spectrum in Fig. 2.3 one observes a peak at E_x = 2.4 MeV indicating feeding of this level from a level at about 2.4 MeV (see the discussion for the 2370.6 keV level).

No evidence for the 2034.8 keV level reported in Ref. [Rou81, Rou84] is found in this work. The level has been tentatively assigned as $I^\pi = 0^+$ in Ref. [Rou81], but was not confirmed in the later study of the same authors [Rou84]. Fig. 3.2 shows that the 1402.1 keV transition which was suggested to depopulate the 2034.8 keV level in fact is in coincidence with both of the 632.6 keV and 861.2 keV transitions, thus depopulating a level at higher excitation energy. The pγ-coincidence data confirms this result .

For the 2104.6 keV level we confirm $I^\pi = 4^+$ through the excitation functions, angular distributions and conversion-electron coefficients of the depopulating 388.0

keV, 610.7 keV and 1472.0 keV transitions. The γ-ray branchings of that level are in agreement with Ref. [DeF88].

We identify a new level at 2143.9 keV for which we firmly assign $I^{\pi} = 0^+$. From the conversion-electron and γ-ray data in the (p,p') reaction a new 2143.9 keV E0 transition could be established (Figs. 2.2 (e) and 2.4). In the pγ-coincidence experiments the corresponding new 1511.4 keV and 427.2 keV E2 transitions to the 2_1^+ and 2_2^+ states (Fig. 2.2 (c)) are observed, and the placement is confirmed by the γγ-coincidence measurements. The slope of the 1511 keV γ-ray excitation-function curve in the (p,2n) reaction (Fig. 2.11) is typical for γ-rays from a 0^+ level. The connecting E0 transition between the 0_3^+ and 0_2^+ states is not observed in our electron spectra from the (p,p') reaction or from the ^{106}In EC/β^+ decay. The 427.2 keV γ-ray gated proton spectrum (Fig. 2.3) shows no feeding of this level from higher lying levels in the (p,p') reaction.

For the 2252.2(6) keV level we tentatively assigned $I^{\pi} = (4^+)$, mainly on the basis of the (p,2n) excitation functions for the depopulating 758.8 keV (new) and 1619.6 keV γ-transitions to the 4_1^+ and 2_1^+ states, respectively (Fig. 2.11). This level is probably the same as the 2252.7 keV (3, 4^+) level seen in an earlier in-beam γ-ray study of the ^{97}Mo(^{12}C,3n) reaction [Sam79], and the same as the 2252.9 keV level observed in the ^{106}In decay study [Rou84]. The present pγ- and γγ-coincidence data show that this level is fed from the level at about 3020 keV (which is beyond the energy region considered here) by the 767 keV transition (see the gate on the 759 keV γ-ray in Fig. 3.2).

The 2254.0(5) keV level has a low-spin value $I^{\pi} = (2^+, 3^+)$ according to the (p,2n) excitation-functions for the depopulating 536.2 keV (new) and 1621.4 keV γ-transitions (Fig. 2.11). There is no transition to the ground state from this state, which would favor the 3^+ assignment. Also the angular distribution of the 536.2 keV transition with the large negative A_{22} is consistent with the $I^{\pi} = 3^+$. Roussiere et al. [Rou84] have reported the 1620.2 keV and 1622.1 keV transitions, of which the latter

one was not placed into their level scheme, therefore supporting our result of two close-lying levels.

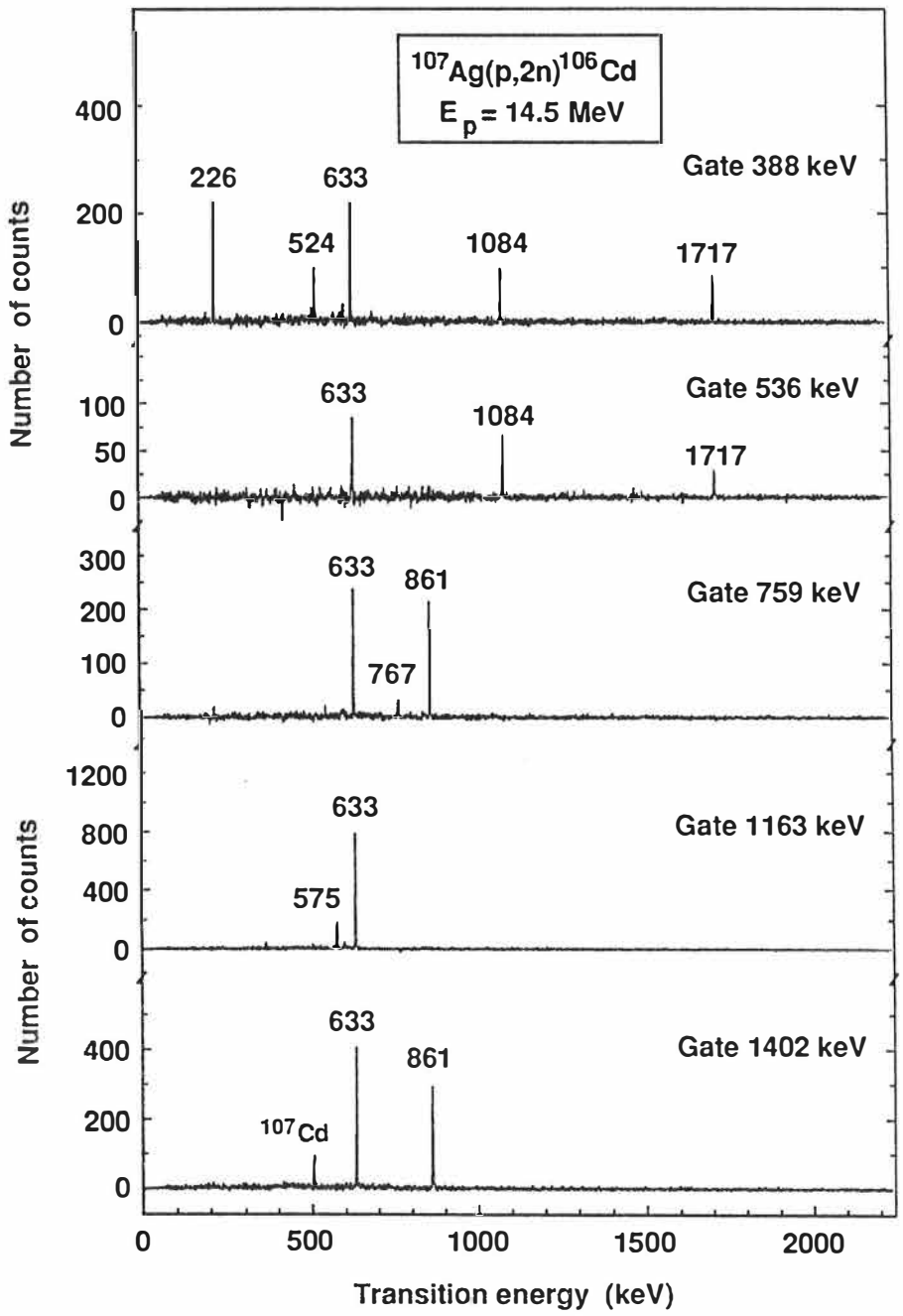

Fig. 3.2: Typical γγ-coincidence spectra from the ^{107}Ag(p,2n) reaction at E_p = 14.5 MeV measured with two NORDBALL-type Compton suppression spectrometers.

The 2305.1 keV level has earlier been assigned I = (4) in the in-beam ^{96,97}Mo(^{13,12}C,3n) study [Sam79]. The present excitation functions and the angular distributions of the 811.2 keV transition and of a new 1672.6 keV γ-transition from this level (Fig. 2.11) are in accord with the old result. In addition, the conversion coefficients of both of these transitions (Table 3.1) imply a positive parity for this state, thus revealing $I^{\pi} = 4^+$ for the state.

The present data for the 2330.5 keV level confirms the γ-ray branching ratio and $I^{\pi} = 5^+$ adopted for this level in Ref. [DeF88].

In the level scheme we have omitted the 2338.7 keV level seen in the (^{12}C,3n) and (^{13}C,3n) reactions [Sam79]. The 1704.5 keV transition which was previously suggested to de-excite this level is observed to feed the 1494 keV 4_1^+ level in our γγ-coincidence measurements and further confirmed by the pγ-coincidences.

The 2347.8 keV level is strongly populated in the present (p,p') experiment, but the $(2)^+$ assignment of Ref. [DeF88] could not be verified due to the complexity of the depopulating 1714.7 keV transition (close-lying 1716.6 keV transition).

The level at 2370.6 keV has been associated with a L=3 state at 2366 keV observed in a (p,p') experiment [Lut69] and thus suggested to be the first excited 3^- state [Dan77]. However, in addition to the 1738.0 keV transition to the 2_1^+ state and a new 653.9 keV transition to the 2_2^+ state, we observe the 575.3 keV transition to the newly assigned 0_2^+ state and 2370.6 keV transition to the ground state (see the 1163 keV gate in Figs. 2.3 and 3.2). The measurement of the K internal conversion-coefficients for these transitions is obscured by the L-conversion lines of the strong E2 transitions (552 keV, 633 keV and 1717 keV). However, the K conversion-coefficient for the 575.3 keV transition could be obtained in the (p,p') reaction where the 3044 keV $(8)^+$ level decaying by the interfering 552.4 keV transition is not populated in difference to the ^{106}In decay. The E2 multipolarity of the 575.3 keV transition definitively rules out the 3^- assignment. Consequently, a tentative (2^+) assignment for this state is suggested in this work.

The 2378.6 keV level is strongly populated in our (p,p') experiment. The level has been observed in Refs. [Fla76] and [Hua78], but no spin and parity assignments have been proposed. The conversion-coefficient limit definitely gives an E1 multipolarity for the 1746.0 keV transition from this state to the 2_1^+ state. Also the negative A_{22} angular-distribution coefficient implies a $\Delta I = 1$ character for this transition (Fig.2.9 and Table 3.1). The (p,2n) excitation-function curve indicates an I = 3 for this state (Fig. 2.11). Thus, this state can firmly be assigned $I^\pi = 3^-$. The state could well be the same one as the proposed 3^- state at 2366 keV of Ref. [Lut69], where the levels separated by less than 50 keV were not resolved.

3.2. The nucleus ^{108}Cd

The level scheme of ^{108}Cd has been established in the EC/β^+ decay of ^{108}In using γ-ray spectroscopy [Fla75, Wis80, Rou84] and also using electron-spectroscopy methods [Rou84]. The high-spin yrast states are examined via ^{96}Zr(^{16}O,4nγ) [Sam78] and ^{106}Pd(α,2nγ) [And85] reactions. The ^{108}Cd has been studied also in the one-proton (^{3}He,d) [Aub72] and the two-proton (^{3}He,n) [Fie77] transfer reactions, as well as in the (d,^{6}Li) alpha-transfer reaction [Jän79] through particle spectroscopy. Also inelastic scattering of protons [Lut69] and alpha-particles [Spe77] have been applied. The three lowest-lying levels has been populated in Coulomb-excitation (e.g. Ref. [Mil69]). The results of these experiments, excluding those of Ref. [Rou84], have been compiled by Haese et al. [Hae82].

Based on the measurements of the present work we have established for the ^{108}Cd isotope three new levels below the 2.5 MeV excitation energy, four new or revised I^π assignments and about 10 new transitions. One level previously reported was not confirmed. Some details of the results that are summarized in Table 3.2 and Fig. 3.3 are discussed below.

Table 3.2: Properties of levels and transitions in ^{108}Cd as obtained in this work.

E_{level} [a] (keV)	J_i^π	E_{trans} [a] (keV)	J_f^π	γ-intensity [b] (p,p') [c]	(p,2n)	Decay	$10^3 \cdot \alpha_K$	Ang. Distr. Coeff. A_{22}	A_{44}	Multi-polarity
632.9	2_1^+	632.9	0_1^+	1000	1000	1000	3.0(1) *	0.18(3)	-0.02(4)	E2
1508.3	4_1^+	875.4	2_1^+	61	343	230	1.4(3)	0.28(4)	-0.03(7)	E2
1601.7	2_2^+	969.1	2_1^+	141	68	46	1.2(2)	-0.09(2)	-0.05(3)	E2/M1
		1601.7	0_1^+	123	62	47	0.36(5)	0.14(3)	-0.01(5)	E2
1721.0	0_2^+	1088.1	2_1^+	127	15	14	0.8(1)	0.04(2)	-0.04(3)	E2
1913.3	0_3^+	311.3	2_2^+	46	4(1) [d]	7.4	21(3)			E2
		1280.6	2_1^+	39	5(1)	8.2	0.39(6)	-0.01(17)	-0.01(25)	E2
		1913.3	0_1^+			< 4	> 25 [e]			E0
2145.6	$(3)^+$	544.2	2_2^+	8.3	6.0	1.5		-0.42(3)	-0.09(5)	E2/M1
		637.3	4_1^+	[f]	4(1) [d]	[f]				
		1512.7	2_1^+	62	48	12	0.40(5)	-0.36(2)	-0.00(4)	E2/M1
2162.5	2_3^+	1529.6	2_1^+	80	30	81	0.43(5)	0.12(2)	-0.01(3)	E2/M1
		2162.5	0_1^+	2.5(10)	1.7	6.2				
2201.9	3_1^-	600.2	2_2^+	1.8(3)	3.0					
		1569.0	2_1^+	54	62	12	0.19(3)	-0.12(3)	-0.01(4)	E1
2239.2	4_2^+	637.5	2_2^+	5.5 [f]	3(1) [d]	6.3 [f]				
		730.9	4_1^+	13	27	21	2.9(4)	0.12(4)	-0.03(5)	E2/M1
		1606.3	2_1^+	8.4	23	17	0.37(5)	0.26(1)	-0.08(2)	E2
2365.7	2_4^+	1732.8	2_1^+	57	17	39	0.32(4)	0.13(4)	0.01(5)	E2/M1
		2365.7	0_1^+	8.5(25)	2.7	5.3		0.06(6)	-0.16(9)	
2374.7	$(0)^+$	772.7	2_2^+	4.6	1.0	5.6	2.3(4)			(E2)
		1741.8	2_1^+	34	5.4	13	0.32(4)	-0.02(8)	-0.13(11)	(E2)
2486.1	2^+	884.5	2_2^+	3(1)	2.7					
		1853.2	2_1^+	34	15	28	0.33(5)	-0.10(2)	-0.00(3)	E2/M1
		2486.0	0_1^+	1.0(5)						

[a] Energy uncertainties typically 0.3 keV.

[b] Intensity error typically 15 %. Intensity of the $2_1^+ - 0_1^+$ transitions normalized to 1000.

[c] Gamma-ray intensities from the (p,p') reaction correspond to the direct level population.

[d] Intensity determined from γγ-coincidence spectra.

[e] E0 transition; $\alpha_K > 17 \times \alpha_K(M4)$.

[f] Intensity contains the 637.3 keV and 637.5 keV transitions; see the data for the 635.7 keV transition.

* Conversion coefficient normalized to $\alpha_K = 3.0(1)$ for the 632.9 keV line.

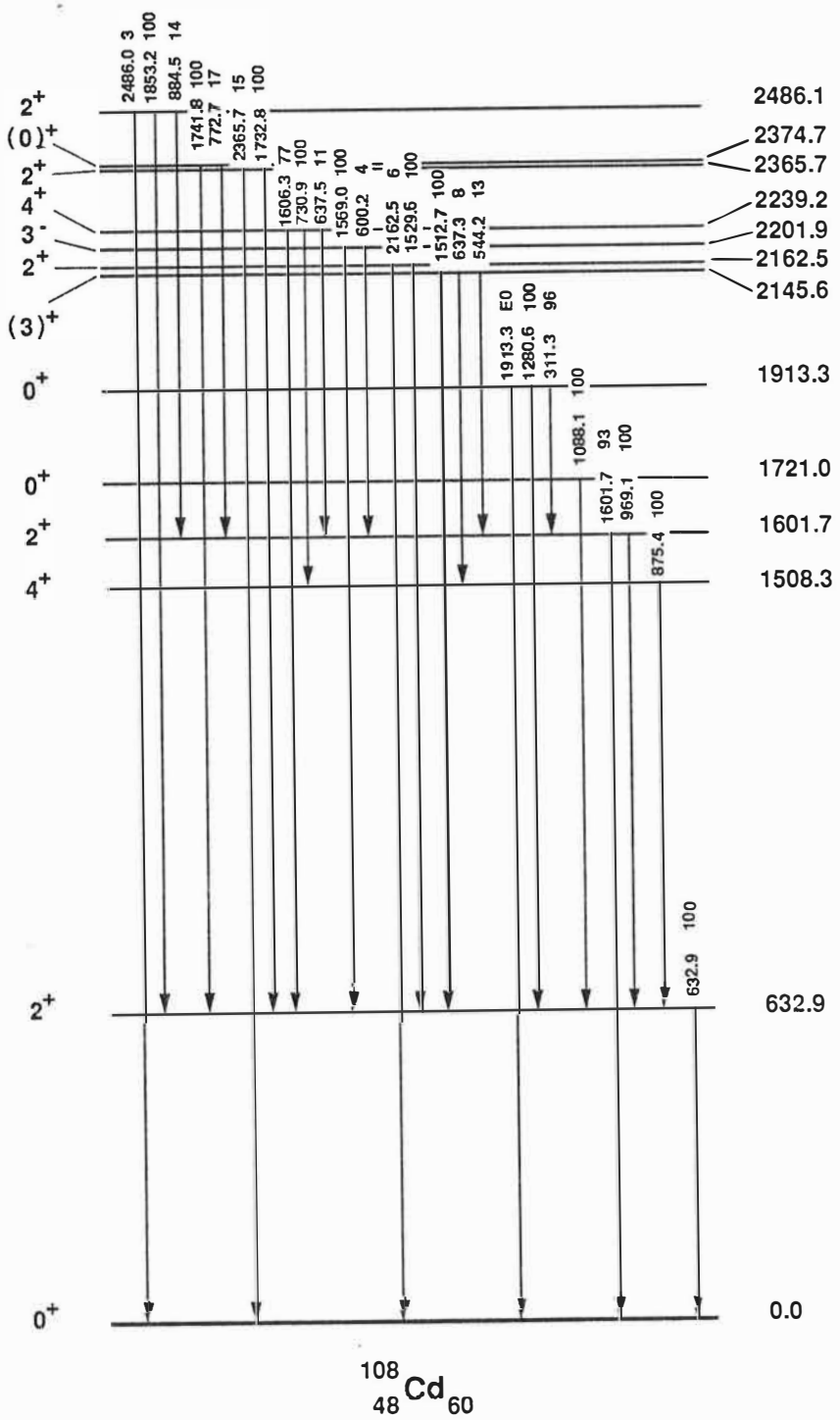

Fig. 3.3: The level scheme of ^{108}Cd as obtained in this work. The relative γ-ray intensities of the depopulating transitions are marked for each level.

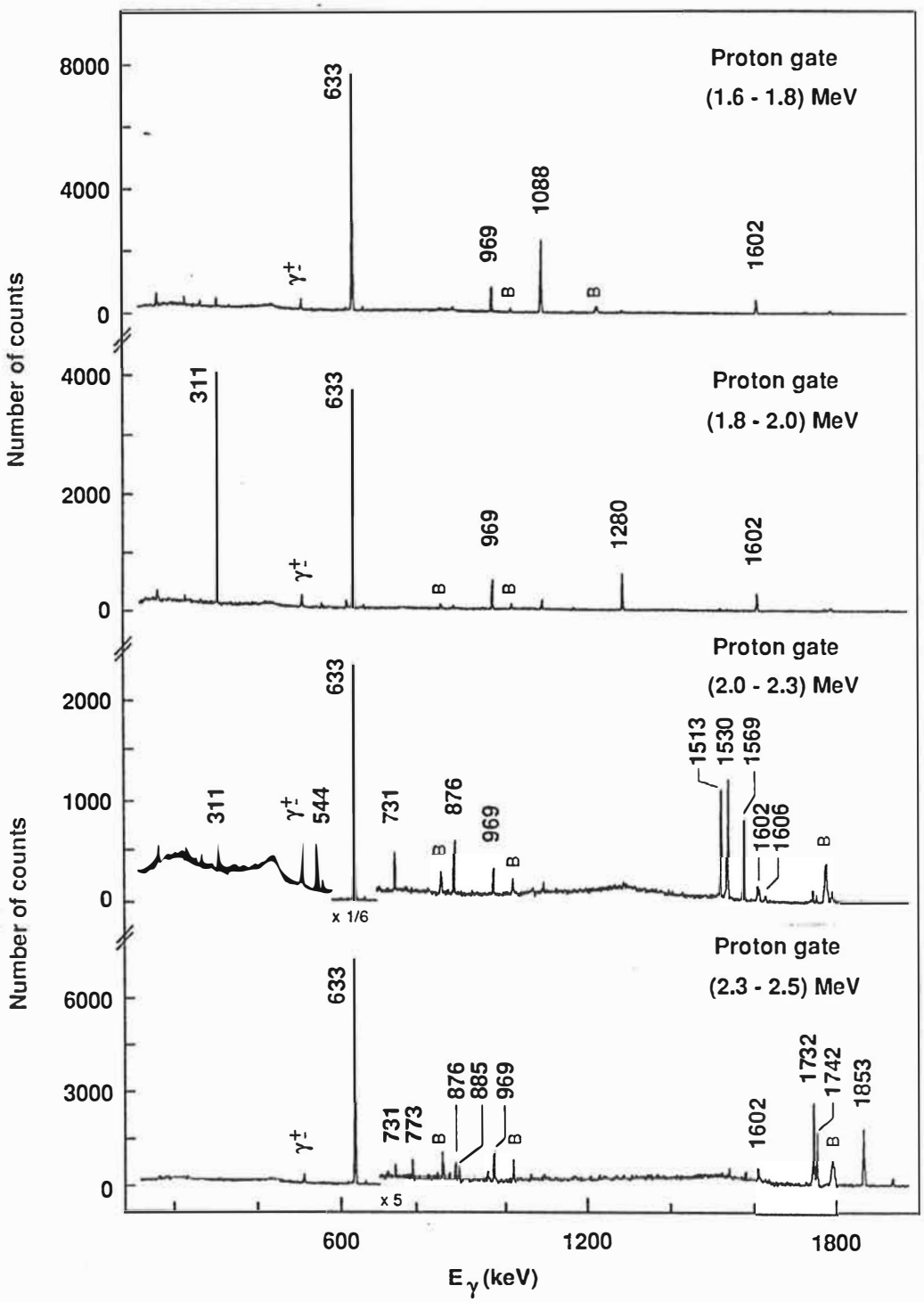

Fig. 3.4: Proton gated γ-ray spectra from the ^{108}Cd(p,p') reaction at E_p= 7.5 MeV; proton gates which correspond to the excitation energies in ^{108}Cd are indicated in the figure.

The data of Table 3.2 and of Fig. 2.12 are consistent with the earlier assignments of 4_1^+ and 2_2^+ [Hae82] for the 1508.3 keV and 1601.7 keV states, respectively.

The 1721.0 keV level is strongly populated in the (^{3}He,d) proton-transfer reaction and suggested to have $I^\pi = (0 - 2)^+$ [Aub72]. A level at 1704(25) keV has been observed in the (d,^{6}Li) alpha-transfer reaction [Jän79], which could be considered to be the same level. From the proton gated γ-ray spectra (Fig. 3.4) we establish a strong 1088.1 keV transition from this state to the 2_1^+ state. The $\gamma\gamma$-coincidence measurement in the (p,2n) reaction confirms the placement. This agrees with the information for the 1087.6 keV γ-ray given by B. Roussiere et al. [Rou84], although it was not placed into their level scheme. In our work, both the isotropic angular-distribution (Fig. 2.10) and the excitation-function curve (Fig. 2.12) of the 1088.1 keV gamma-ray determine I = 0 for this level. Consequently, the state must be the first excited 0^+ state in ^{108}Cd. As in the case of the 0_2^+ state in ^{106}Cd, no E0 transition from this state to the ground state is observed.

The 1913.3 keV level has previously been assigned as $I^\pi = 0^+$ by B. Roussiere et al. [Rou84] based on the observed E0 transition to the ground state. Our data confirm the assignment. The E0 transition can be seen in Fig. 2.16 which shows the conversion-electron and γ-ray spectra from the ^{108}In decay. The γ-ray branching ratio of the 311.3 keV and 1280.6 keV E2 transitions is consistent with the results of Ref. [Rou84].

The 2020.7 keV level and the depopulating 1387.8 keV transition reported in Ref. [Rou84] are not observed in any of our experiments. Thus, the level was omitted from the level scheme of ^{108}Cd.

At 2145.6 keV we find a new level which de-excites to the 2_1^+, 4_1^+ and 2_2^+ levels. These transitions are placed on the basis of the $\gamma\gamma$- and pγ-coincidence experiments (Fig. 3.4). From the present conversion coefficient of the 1512.7 keV transition, positive parity is deduced for this state. On the basis of the negative A_{22} angular-distribution coefficients for the 544.2 keV (Fig. 2.10) and 1512.7 keV γ-rays and the

excitation-function curve (Fig. 2.12) of the 1512.7 keV γ-ray, we propose an I = 3 for this state, thus suggesting $I^{\pi} = (3)^{+}$.

The level at 2162.5 keV has earlier been assigned as 3^{-} [Rou84, Mum85]. From the conversion-electron and γ-ray spectra of Fig. 2.16, one clearly sees that the 1529.6 keV transition from this state to the 2_1^+ state has a multipolarity of E2/M1 rather than E1 (see also Fig. 2.17). In Ref. [Rou84] the E1 multipolarity is determined for the 1529.7 keV transition based on their experimental K-conversion coefficient. This value is the only one reported in Ref. [Rou84], which is in serious disagreement with our results. Since the transition from this state to the ground state is observed in the present work, a spin and parity 2^+ is adopted. The excitation function (Fig. 2.12) and the angular distribution (Fig. 2.10) of the 1529.6 keV γ-ray are in agreement with the 2^+ assignment.

The 2201.9 keV level is confirmed to have $I^{\pi} = 3^{-}$ by the 1569.0 keV E1 transition to the 2_1^+ state, which is shown in Figs. 2.16 and 2.17. Moreover, a new 600.2 keV transition to the 2_2^+ level is observed in the present work.

The 2239.2 keV level has previously been assigned as 4^+ [Rou84], which agrees with our data.

For the 2365.7 keV level, our experiments have confirmed the 2^+ assignment reported in Ref. [Mum85]. The γ-ray branching ratio agrees with Ref. [Hae82].

At 2374.7 keV a new level is located. The level is depopulated by the 1741.8 keV and 772.7 keV transitions to the 2_1^+ and 2_2^+ states, respectively (Fig. 3.4). In Ref. [Rou84] the unplaced transition of 1741.8 keV is reported. The E2/M1 multipolarity (Table 3.2 and Figs. 2.16 and 2.17) for both of the transitions indicate positive parity. The angular distribution of the 1741.8 keV transition (Fig. 2.10) favors a spin of 0, but the assignment is not conclusive.

The new level at 2486.1 keV might be the 2481 keV level observed in the (^{3}He,d) reaction [Aub72]. We have seen the depopulating transitions of 1853.2 keV and 884.5 keV to the 2_1^+ and 2_2^+ states (Fig. 3.4), respectively, and the transition to the ground state. This, together with the excitation-function curve for the 1853.2 keV

transition (Fig. 2.12), reveals $I^{\pi} = 2^+$ for the state. Also the E2/M1 multipolarity of the 1853.2 keV transition is consistent with the 2^+ assignment.

3.3. The nucleus ^{110}Cd

The level scheme of ^{110}Cd has previously been deduced mainly from the ^{110}In EC/β^+- and ^{110}Ag β^--decay studies [Sar69, MeyPC, Kaw72, Ver79, Mal81]. The (n,n'γ) measurements have been performed by Demidov et al. [Dem76, Dem78]. A study of high-spin yrast states has been carried out with the ^{96}Zr(^{18}O,4nγ) reaction [Lum74]. The energy levels and I^{π} assignments have been evaluated in one- and two-proton transfer reactions: (^{3}He,d) in Ref. [Aub72] and (^{3}He,n) in Ref. [Fie77]. Also inelastic scattering of p, d, and alpha particles has been studied in Refs. [Lut69, Kim66, Spe77]. Only the few lowest-lying states were excited through Coulomb excitation [Mil69, DeG83]. The results of all the above mentioned experiments are included in the A=110 compilation of P. DeGelder et al. [DeG83]. Some data from the (α,2nγ) reaction study have been reported by Kusnezov et al. [Kus87], and the details of those experiments have been recently published by Kern et al. [Ker90]. The results of our measurements are briefly discussed in the following paragraphs, and summarized in Table 3.3 and in Fig. 3.5.

The second excited level at 1473.2 keV has previously been identified as a 0^+ state through a γ-ray angular-correlation measurement in the ^{110}Ag decay [Kaw72] and a proton-transfer reaction study [Aub72]. The excitation-function curve (Fig. 2.13) and the angular distribution (Table 3.3) for the 815.4 keV transition to the 2^+_1 state in our (α,2n)-reaction experiments are in accordance with this assignment. As in the case of the 0^+_2 states in ^{106}Cd and ^{108}Cd, we could not observe the E0 transition to the ground state.

Table 3.3: Properties of levels and transitions in ^{110}Cd as obtained in this work.

E_{level} [a] (keV)	J_i^π	E_{trans} [a] (keV)	J_f^π	γ-intensity [b] (p,p') [c]	(α,2n)	Decay	$10^3 \cdot \alpha_K$	Ang. Distr. Coeff. A_{22}	A_{44}	Multi-polarity
657.8	2_1^+	657.8	0_1^+	1000	1000	1000	2.7(1) *	0.23(2)	-0.15(3)	E2
1473.2	0_2^+	815.4	2_1^+	75	12	2.8	1.6(2) [d]	0.08(12)	-0.08(17)	E2
1475.9	2_2^+	818.1	2_1^+	81	71	9.8	[d]	-0.23(1)	-0.10(1)	E2/M1
		1475.9	0_1^+	40	42	5.7	0.46(3)	0.18(3)	-0.11(4)	E2
1542.5	4_1^+	884.8	2_1^+	15	560	50	1.2(2)	0.28(3)	-0.22(5)	E2
1731.3	0_3^+	255.4	2_2^+	2.7	1.0	0.12	23(7)			E2
		1073.7	2_1^+	20	6.7	1.1	0.85(8)	0.01(6)	-0.07(9)	E2
1783.6	2_3^+	1125.8	2_1^+	33	35	11	0.43(5)	0.21(2)	-0.10(2)	E2/M1
		1783.6	0_1^+	11	9.7	3.4	0.18(3)	0.18(2)	-0.01(2)	E2
2078.6	0_4^+	295.3	2_3^+	9.2	3.3	0.4	28(5)	-0.06(4)	-0.18(5)	E2
		605.4	0_2^+			< 0.3	> 50 [e]			E0
		2078.4	0_1^+			< 0.17	> 7 [f]			E0
2078.9	3_1^-	602.9	2_2^+	6.9	5.5	0.7		-0.3(2)	-0.3(3)	E1
		1421.2	2_1^+	43	39	4.6	0.19(2)	-0.28(3)	-0.04(5)	E1
2162.8	3_1^+	687.0	2_2^+	3.6	8.0	0.7		-0.70(5)	-0.01(2)	E2/M1
		1505.0	2_1^+	12	25	1.1	0.50(5)	-0.55(4)	-0.03(7)	E2/M1
2220.2	4_2^+	677.8	4_1^+	3.6	26	2.5		0.05(1)	-0.13(2)	E2/M1
		744.3	2_2^+	1.5	14	1.1	2.0(3)	0.28(1)	-0.27(1)	E2
		1562.3	2_1^+	<0.7	3.0	0.3		0.22(6)	-0.19(8)	E2
2250.5	4_3^+	467.0	2_3^+		7(3) [g]			0.28(4)	-0.29(5)	E2
		708.0	4_1^+	2.4	38 [g]			0.45(3)	-0.14(4)	E2/M1
		774.7	2_2^+		2(1)					
		1592.7	2_1^+		5(1)			0.22(3)	-0.16(4)	E2
2287.5		1629.7	2_1^+	15	10	1.0		0.01(5)	0.01(8)	
2332.1		1674.3	2_1^+	12	2.2	0.2		0.14(10)	-0.18(15)	
2355.8		1698.0	2_1^+	13	6.9	3.0	0.27(5)	-0.02(1)	-0.12(2)	E2/M1

[a] Energy uncertainties typically 0.3 keV.

[b] Intensity error typically 15 %. Intensity of the $2_1^+ - 0_1^+$ transitions normalized to 1000.

[c] Gamma-ray intensities from the (p,p') reaction correspond to the direct level population.

[d] Conversion coefficient for the sum of the 815.4 keV and 818.1 keV transitions; see the data for the 815.4 keV transition.

[e] E0 transition; $\alpha_K > 1.6 \times \alpha_K(M4)$.

[f] E0 transitions; $\alpha_K > 38 \times \alpha_K(M4)$.

[g] Intensity deduced from γγ-coincidence spectra.

* Conversion coefficient normalized to $\alpha_K = 2.7(1)$ for the 657.8 keV line.

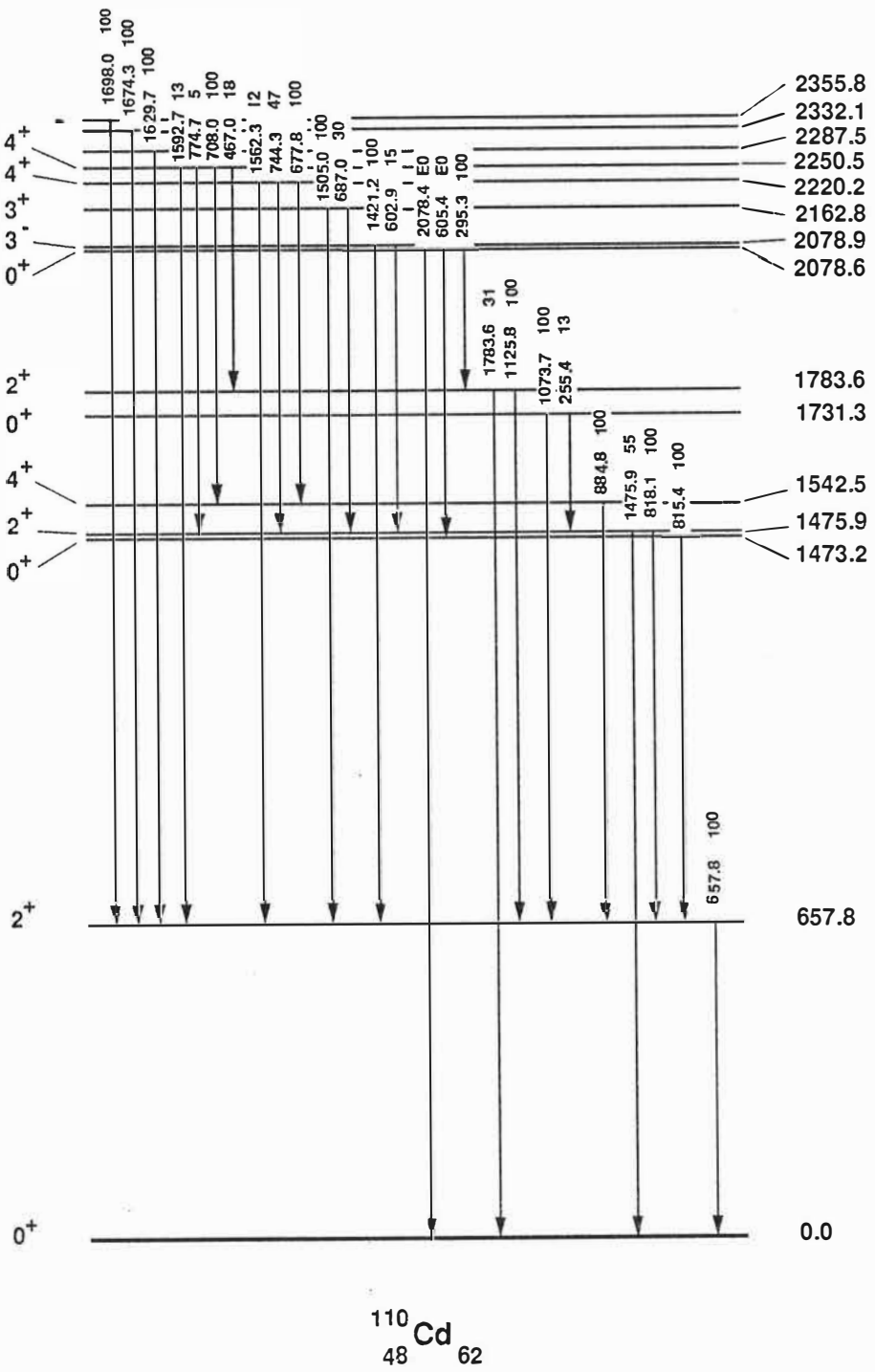

Fig. 3.5: The level scheme of ^{110}Cd as obtained in this work. The relative γ-ray intensities of the depopulating transitions are marked for each level .

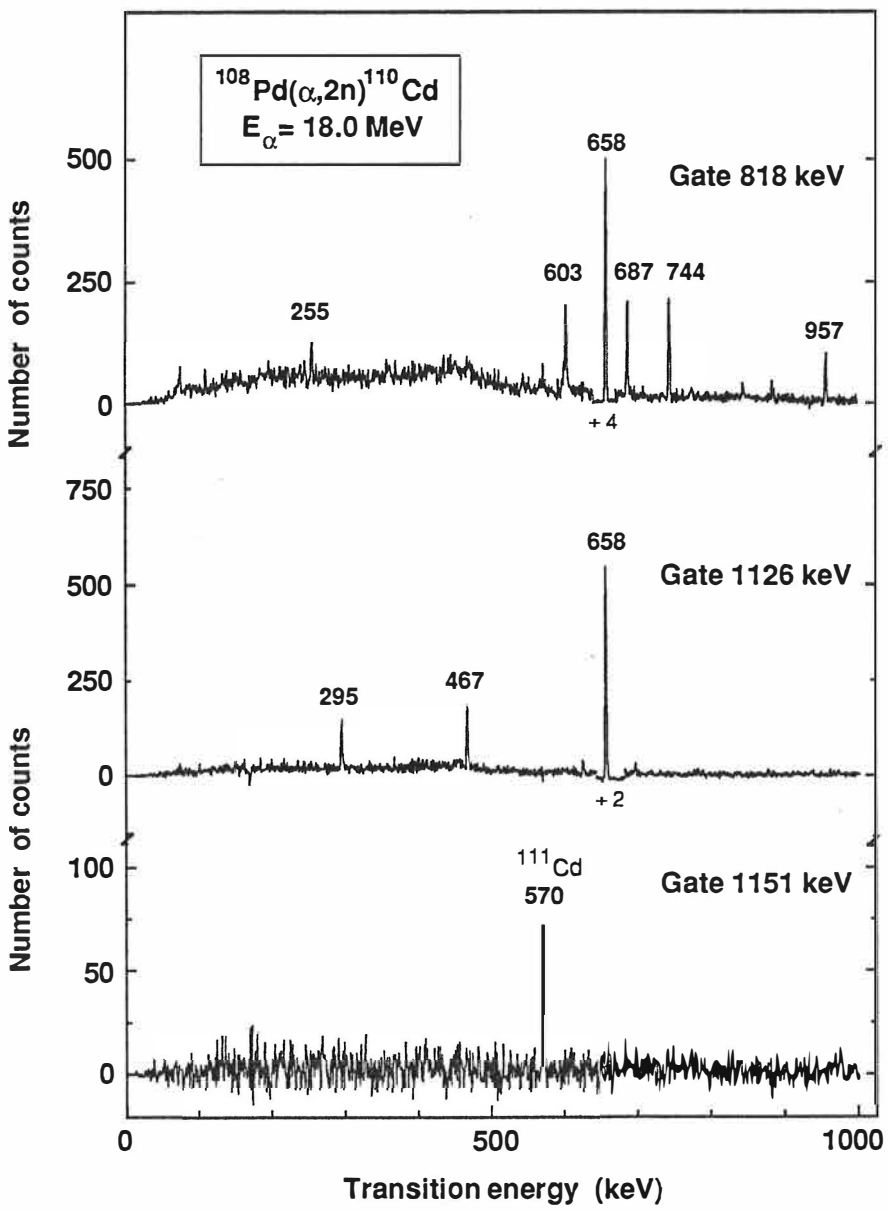

Fig. 3.6: Gamma-gamma coincidence spectra from the ^{108}Pd(α,2n)^{110}Cd reaction at E_α = 18.0 MeV.

Our results for the 1475.9 keV 2_2^+ and 1542.5 keV 4_1^+ states agree with the previous results on these levels [DeG83].

The spin of the 1731.3 keV level was assigned tentatively as $(0)^+$ based on the (^{3}He,d) data and the level systematics of even Cd isotopes [DeG83]. Our excitation-function (Fig. 2.13) and angular-distribution (Table 3.3) measurements for the 1073.7 keV transition to the 2_1^+ state in the (α,2n) reaction prove that this level has $I^\pi = 0^+$. Moreover, we have observed a new 255.4 keV E2 transition to the 2_2^+ state (Fig. 3.6). The E0 transitions to the 0_2^+ state and to the ground state were not observed.

The 1783.6 keV level is known as the third 2^+ state [DeG83]. Our data agree with this assignment.

We do not observe the 1809.5 keV level seen in the ^{110}In decay by Meyer [MeyPC]. According to our $\gamma\gamma$-coincidence measurements in the (α,2n) reaction the proposed depopulating 1151.7 keV transition does not belong to the ^{110}Cd nucleus but most probably to ^{111}Cd (Fig. 3.6). Furthermore, there is no evidence for this state in our pγ-coincidence spectra.

The 2078.6 keV level has been assigned spin 0^+ in the ^{110}Ag (1+;24.6 s) decay [Kaw72] and in the (^{3}He,d) reaction [Aub72], where it is strongly populated. In our study of the ^{110}In EC/β^+-decay, we have observed new E0 transitions from this state to the ground state and to the 1473 keV 0_2^+ state. Our value for the conversion coefficient of the 295 keV transition (Table 3.3) supports the earlier placement of (0_4^+ - 2_3^+). Other possible E2 transitions from this 0_4^+ state are hampered by transitions from the close-lying 3^- state.

The 2078.9 keV level has been identified in many experiments [DeG83] as a 3^- state. We have observed two depopulating transitions, the 602.9 keV transition to the 2_3^+ state and the 1421.2 keV transition to the 2_1^+ state. According to our conversion electron data, the latter transition has definitively an E1 character (Table 3.3) confirming the 3^- assignment.

Our data agree with the earlier assignments of 3^+ for the 2162.8 keV level and 4^+ for the 2220.2 keV and 2250.0 keV levels [DeG83].

For the monopode levels at 2287.5 keV and 2332.1 keV, quite strongly populated in our (p,p') experiments, we are not able to get any definite spin and parity assignments. In the (n,n'γ) study the assignments of 2^+ and 0^+ were given to these states [Dem78], respectively.

The level at 2355.8 keV is assigned as 2^+ in Ref. [Dem78]. The conversion coefficient of the 1698.0 keV transition feeding the 2_1^+ level defines positive parity (Table 3.3). The excitation-function curve of this transition indicates $I \geq 4$, but the angular-distribution coefficient A_{22} is not consistent with that.

3.4. The nucleus ^{112}Cd

The level scheme of ^{112}Cd has been deduced from the ^{112}In EC/β^+- and ^{112}Ag β^--decay studies [Kaw72, Wal72]. The (n,n'γ) and (γ,γ') examinations have been performed by Demidov et al. [Dem76, Dem78] and [Mor71], respectively. The study of yrast states has been carried out only in the (α,2nγ) reaction [Gei74]. The levels have been evaluated in the two-proton transfer reaction (^{3}He,n) in Ref. [Fie77], in the (d,p) reaction by Barnes et al. [Bar67] and, recently, in the (t,p) reaction by Medsker et al. [Med87]. Also inelastic scattering of p, d, and alpha particles has been studied in Refs. [DeL89, Pig84, Kim66, Spe77]. Only low-lying states were excited through Coulomb excitation [Mil69, Jul80, DeF89]. The low-lying 0^+ states have been examined via the EC/β^+-decay of ^{112}In and the (d,p) reaction [Jul80]. The results of all the above mentioned experiments are included in the newest A=112 compilation of DeFrenne et al. [DeF89].

We used the ^{112}Cd nucleus as a reference case for our (p,p'γ) experiments. Especially, we could examine the population of 0^+ levels by this reaction. Since no electron spectroscopy is applied in the present work for ^{112}Cd, the E0 transitions are not included in Table 3.4 nor in Fig. 3.7 summarizing our results. The earlier study of Julin et al. [Jul80] is referred for the E0 measurements. The new data from our recently

performed (α,2n) reaction revealed one new level below 2.1 MeV excitation energy and several new transitions. The results of our measurements are briefly discussed in the following paragraphs.

The results obtained in this work for the four lowest excited levels are consistent with the data given in the A = 112 compilation. The γ-ray branching ratio for the transitions from the 0_3^+ level obtained in our (α,2n) experiment are in disagreement while those obtained from the (p,p') reaction are in agreement with the results of Ref. [DeF89]. The (p,p') results have been adopted to the level scheme (Fig. 3.7), since in the (α,2n) case the 815 keV line is a doublet with the other transition being higher in the level scheme. Contrary to the (α,2n) study by Geiger et al. [Gei74], performed at similar alpha-beam energies as our experiments, we populated clearly the first two excited 0^+ levels.

The 1468.8 keV 2^+ level has previously been observed to decay to the 0_2^+, 2_1^+ and the ground states [DeF89]. Our result is consistent with that. The branching ratios of the depopulating transitions agree with the adopted values [DeF89].

The 1870.8 keV level has been assigned as 0^+ in several experiments: via the γ-ray angular-distribution measurements in the photoexcitation study [Mor71], via the γ-ray angular-correlation measurements in the ^{112}In (1^+) decay [Kaw72], in the ^{112}Ag (2^-) decay [Wal72], and earlier through particle spectroscopy in the (d,p) reaction [Bar67]. It has also been populated in the proton-scattering experiments by Pignanelli et al. [Pig84], and recently in two-neutron (t,p) transfer-reaction [Med87].

In the earlier (α,2n) study Geiger et al. [Gei74] report that the first two excited 0^+ states are not populated while the 1870 keV 0^+ state is. The 402 keV, 558 keV and 1253 keV transitions to the 2_3^+, 2_2^+ and 2_1^+ levels, respectively, have been observed to depopulate this level [Gei74]. In addition to those transitions, we found a new 455 keV transition to the 4_1^+ level in our γγ-coincidence measurements from the (α,2n) reaction (see the gates 455 keV and 701 keV in Fig. 3.8). This result is in serious disagreement with the 0^+ assignment for the 1870 keV level. Therefore, we repeated the γ-ray

angular-distribution and excitation-function measurements to figure out the spin of the level: The angular distributions of the 402 keV and 1253 keV transitions are definitely of $\Delta I = 2$ character and not isotropic (Fig. 2.15 and Table 3.4) as reported in Ref. [Gei74]. The angular distribution of the 455 keV transition is consistent with $\Delta I = 0$ (Fig. 2.15). The excitation functions indicate spin 4 for the level (Fig. 2.14), but are not conclusive. Moreover, the 1870 keV state is fed from the 2570.9 keV level (Fig. 3.8), which we assign as a 6^+ state based on the angular-distributions and excitation-functions of the depopulating 701 keV and 1155 keV transitions (Figs. 2.14 and 2.15, Table 3.4). Thus, we adopt $I^\pi = 4^+$ for the 1870 keV state.

We conclude, however, that there are two levels at about 1870 keV excitation energy: the 0^+ and 4^+ levels. The very strong evidence for the 0^+ level is deduced from different experiments as stated above, but the 4^+ level is clearly populated in the (α,2n) reaction . Most probably in our (p,p') experiment it is the 0^+ level that is populated, since the γ-ray branchings for the depopulating transitions are quite different than those in the (α,2n) reaction. Based on the energies of the transitions to the 2_1^+ state observed in the (p,p') and (α,2n) reactions the 4^+ state would be 0.6 keV lower in energy than the 0^+ state.

The 2005.1 keV level has been previously assigned as the first 3^- state. We observed the 692.7 keV and 1387.6 keV transitions to the 2_2^+ and 2_1^+ state. In both of our experiments the intensity of the 692.7 keV transition is higher than reported in Ref. [DeF89].

Our data for the 2064.1 keV level is in agreement with the assignment of 3^+ for the level and the γ-ray branchings are about the same as in [DeF89].

The 2081.5 keV level has been assigned as 4^+ [DeF89]. In addition to the 666.1 keV transition to the 4_1^+ level, we observed in the (α,2n) reaction three new transitions: the 211 keV, 612.8 keV and 769.3 keV transitions to the 4_2^+ , 2_3^+ and 2_2^+ states, respectively (see the 852 keV gate in Fig. 3.8). The γ-ray results for those transitions are consistent with the 4^+ assignment.

Table 3.4: Properties of levels and transitions in ^{112}Cd as obtained in this work.

E_{level} [a] (keV)	J_i^π	E_{trans} [a] (keV)	J_f^π	γ-intensity [b] (p,p') [c]	(α,2n)	Ang. Distr. Coeff. A_{22}	A_{44}	Multi-polarity
617.4	2_1^+	617.4	0_1^+	1000	1000	0.18(2)	-0.09(3)	E2
1224.2	0_2^+	606.7	2_1^+	12	6.3 [d]	-0.02(7) [f]	-0.08(10)	E2
1312.3	2_2^+	694.8	2_1^+	24	92	-0.24(2)	0.00(3)	E2/M1
		1312.3	0_1^+	7.8	32	0.13(2)	-0.06(3)	E2
1415.3	4_1^+	797.9	2_1^+	17	670	0.24(2)	-0.12(3)	E2
1433.2	0_3^+	121.0	2_2^+	2.5	1.4	0.08(5)	0.10(7)	E2
		815.8	2_1^+	4.1	5.1 [e]			
1468.8	2_3^+	244.8	0_2^+	< 0.4	1.7 [e]			
		851.2	2_1^+	8.0	34	0.16(1)	-0.02(2)	E2/M1
		1468.8	0_1^+	3.8	19	0.18(2)	-0.06(2)	E2
1870.4	4_2^+	401.9	2_3^+		24	0.21(3)	-0.11(4)	E2
		455.1	4_1^+		11	0.03(2)	-0.10(3)	E2/M1
		558.3	2_2^+		32 [e]	0.08(2) [f]	-0.09(3)	E2
		1253.0	2_1^+		30 [e]	0.21(1) [f]	-0.11(2)	E2
1871.0	0_4^+	402.0	2_3^+	< 0.2				
		558.0	2_2^+	< 0.3				
		1253.6	2_1^+	4.9				
2005.1	3_1^-	692.7	2_2^+	11	15	-0.06(1)	0.03(2)	E1
		1387.7	2_1^+	18	33	-0.22(3)	-0.00(5)	E1
2064.1	3_1^+	649.0	4_1^+		7 [e]			
		751.8	2_2^+	1.6	21 [e]			
		1446.8	2_1^+	1.3	13	-0.51(6)	0.32(9)	E2/M1
2081.0	4_3^+	211.0	4_2^+		1.9 [e]			
		612.8	2_3^+		6.4 [e]			
		666.0	4_1^+	< 0.7	30	0.05(2)	-0.03(4)	E2/M1
		769.3	2_2^+		23 [e]	0.24(3) [f]	-0.11(4)	E2
2570.9	6_2^+	403.8	6_1^+		< 1.7	0.2(2)	0.1(2)	E2/M1
		700.6	4_2^+		47	0.25(2)	-0.18(3)	E2
		1155.5	4_1^+		53	0.02(4)	-0.13(6)	E2

a Energy uncertainties typically 0.3 keV.

b Intensity error typically 15 %.

c Gamma-ray intensities from the (p,p') reaction correspond to the direct level population.

d Intensity contains also the higher lying 607 keV transition.

e Intensity deduced from the γγ-coincidence spectra.

f Doublet line: The angular distribution coefficients determined from singles gamma-ray intensities containing both transitions.

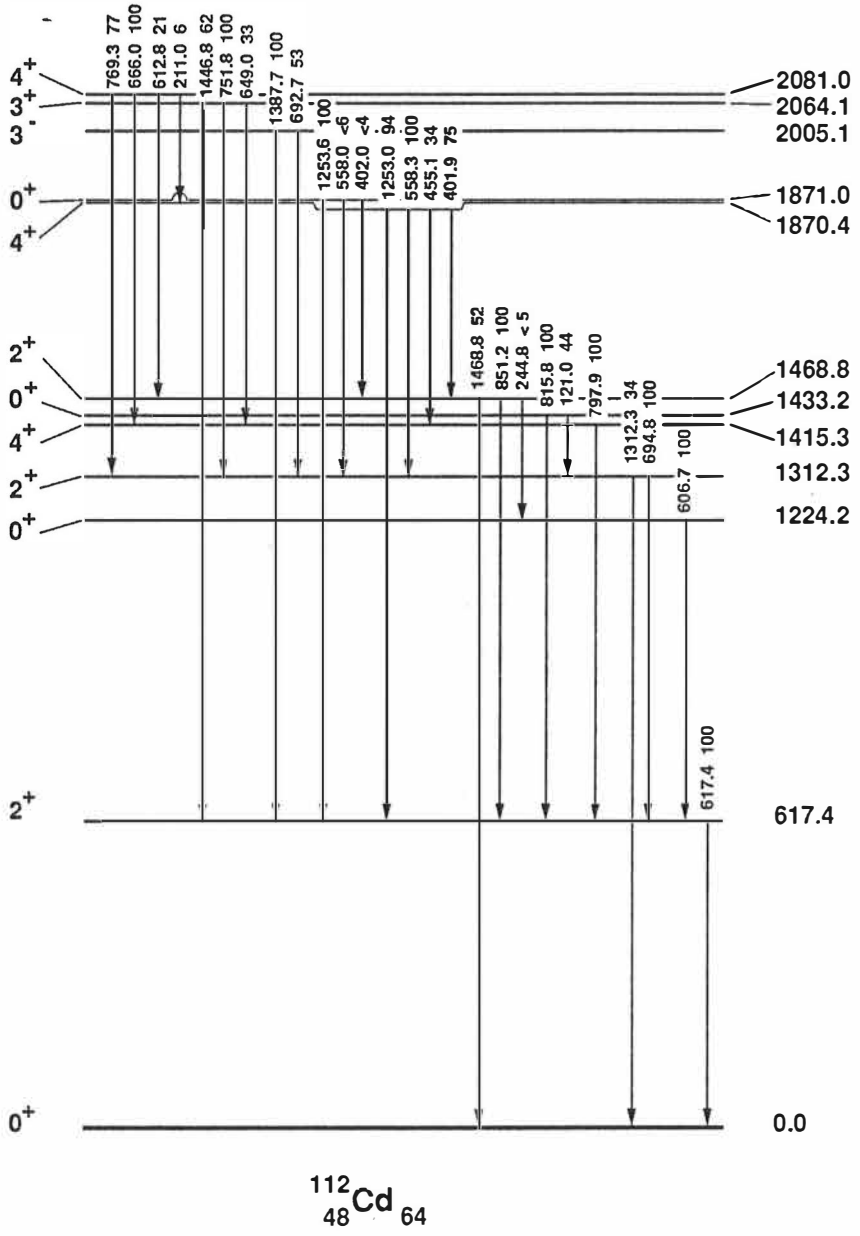

Fig. 3.7: The level scheme of ^{112}Cd as obtained in this work. The relative γ-ray intensities of the depopulating transitions are marked for each level. Note, that the E0 transitions measured in Ref. [Jul80] are not included in the figure.

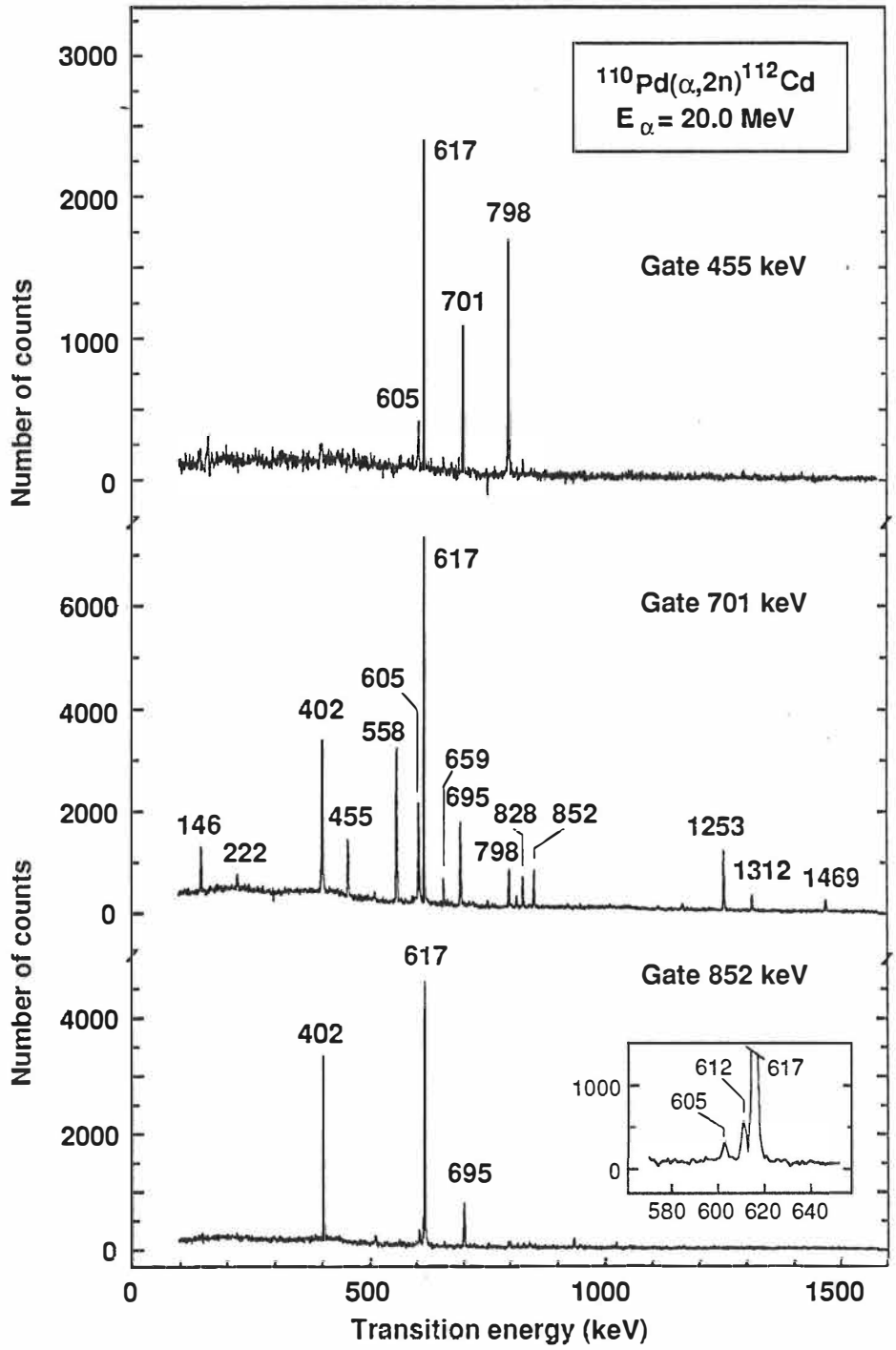

Fig. 3.8: Gamma-gamma coincidence spectra from the ^{110}Pd(α,2n)^{112}Cd reaction at E_α = 20.0 MeV.

3.5. The nucleus ^{116}Cd

The nucleus ^{116}Cd has been studied in the β^--decay of ^{116}Ag [Brü82, Mac89, Wal85], and in the inelastic scattering of protons [Dey72, Lut69], deuterons [Kim66] and alpha-particles [Spe77]. Deye et al. performed also pγ-coincidence measurements for this nucleus [Dey73]. Deminov et al. [Dem76a, Dem78] and Newton et al. [New80] have performed the (n,n'γ) studies. The levels of ^{116}Cd were examined also in the (d,^{6}Li) [Jän79] and (t,p) [Wat87] transfer reactions. In Coulomb excitation of the ^{116}Cd nucleus [McG65, Mil69] the 0^+ state at 1380 keV was populated [McG65] among the few other low-lying states. Most of this data has been summarized in the latest compilation of A=116 [Bla81].

For ^{116}Cd we carried out only a short experiment to complete our (p,p'γ) results. The in-beam conversion electron spectra from the (p,p') reaction were obscured by the dominating β^- background. The beta-decaying ^{116}In is produced through the (p,n) reaction. Thus, for this Cd isotope we could not observe any E0 transitions like for the other Cd isotopes. The spin assignments given in the Table 3.5 and the level scheme of ^{116}Cd (Fig. 3.9) are based on the previous results [Bla81, Wat87]. Generally, the gamma-ray branchings obtained in this work are in agreement with those of Ref. [Bla81].

The 1282.5 keV level has earlier been assigned tentatively as the first excited 0^+ state [Bla81]. We do not observe the 68.9 keV transition to the 2_2^+ state as reported from the ^{116}Ag decay in [Wal85, Brü82]. Our upper limit for the γ-ray intensities of the depopulating transitions is I_γ(69 keV)/I_γ(769 keV) < 0.005 compared to the value of 0.22 in Ref. [Brü82]. Moreover, the proposed 669 keV transition feeding this 0_2^+ level from the 1951 keV 2^+ level is not observed in the present work. Instead, the 769 keV γ-ray gated proton spectrum shows a weak population from a level around 2430 keV (this energy region is not included into our table nor the level scheme). In the recent

(t,p) work [Wat87], a new level at 2431(10) keV was found and it was assigned as $I^{\pi} = 2^+$. The observed coincidence relations in Ref. [Brü82] would place the 1151.7 keV transition between the 2431 keV and 1283 keV levels in contradiction to the original placement in Ref. [Brü82].

Table 3.5: Properties of levels and transitions in ^{116}Cd as obtained in this work.

E_{level} [a] (keV)	J_i^{π}	E_{trans} [a] (keV)	J_f^{π}	γ-intensity [b] (p,p')
513.5	2_1^+	513.5	0_1^+	1000
1212.7	2_2^+	699.4	2_1^+	129
		1212.6	0_1^+	75
1219.0	4_1^+	705.5	2_1^+	4.3
1282.5	0_2^+	769.0	2_1^+	40
1380.2	0_3^+	866.7	2_1^+	31
1641.5	2_3^+	422.7	4_1^+	< 1.3
		1128.5	2_1^+	15
		1641.5	0_1^+	13
1915.2	3_1^+	702.7	2_2^+	< 1.3
		1401.8	2_1^+	< 2.7
1921.2	3_1^-	708.7	2_2^+	15
		1407.5	2_1^+	50
1927.8	(0^+)	1414.3	2_1^+	103
1951.0	2_4^+	1437.5	2_1^+	9

[a] Energy uncertainties typically 0.3 keV.

[b] Intensity error typically 15 %. Gamma-ray intensities from the (p,p') reaction correspond to the direct level population.

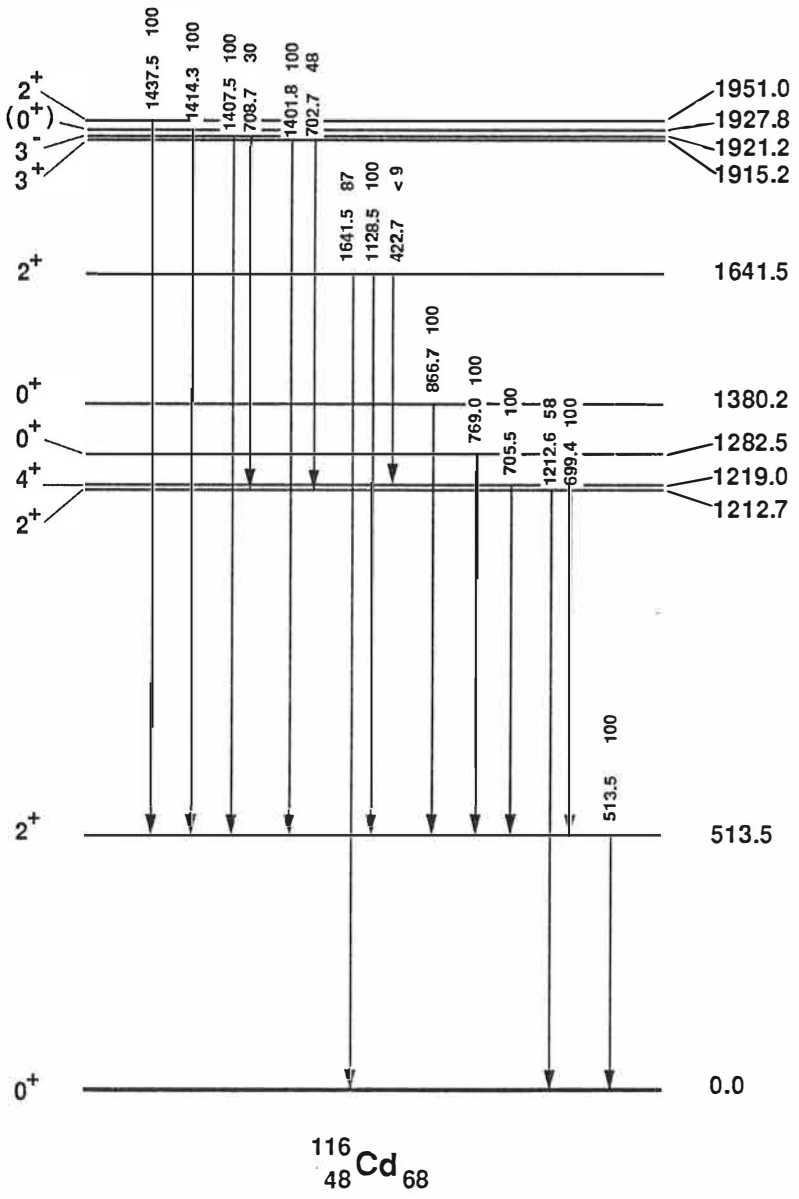

Fig. 3.9: The level scheme of ^{116}Cd as obtained in this work. The relative γ-ray intensities of the depopulating transitions are marked for each level.

The 1380.2 keV level has been unambiguously assigned as 0^+ [Bla81, Wat87]. In addition to the 866 keV 0_3^+ - 2_1^+ transition we do not observe any new depopulating transitions from this state. While we especially searched for the 167 keV transition to the 2_2^+ state, it is not observed; only an upper limit of the γ-ray intensity is determined.

The 1927.8 keV level, strongly populated in our (p,p'γ) experiment, is most probably the 0_4^+ state. In a (n,n'γ) study [New80], the 1414.3 keV transition has an isotropic angular-distribution and, in a (t,p) study [Wat87], the 1924 keV proton group has a definite L = 0 component. In the other (n,n'γ) work [Dem78] the 1929.0(5) keV level has been assigned as a probable 0^+ state.

4. Level systematics

With the present results included, the information on even-mass $^{106\text{-}120}$Cd nuclei is now sufficient to correlate low-lying levels of similar characteristics. The main emphasis in this work has been on the systematic behaviour of the (0_2^+, 2_2^+, 4_1^+, 0_3^+, 2_3^+) quintuplet of states. In particular, we have clarified the energy and the de-excitation pattern of the 0_2^+ and 0_3^+ states.

4.1. The quintuplet of states: (0_2^+, 2_2^+, 4_1^+, 0_3^+, 2_3^+)

In ^{110}Cd, ^{112}Cd, ^{114}Cd and in ^{116}Cd the states of the aforementioned quintuplet are well separated from higher lying states. When going from ^{108}Cd (Fig. 3.3) to ^{106}Cd (Fig. 3.1), the 2_3^+ state rises fast in excitation energy. In ^{108}Cd it lies above the 2146 keV $(3)^+$ state, while in ^{106}Cd, there are difficulties in identifying it from the group of the other states. In ^{106}Cd also the 0_3^+ state lies above the 4_2^+ state. Level-energy and energy-ratio systematics of this quintuplet and the 2_1^+ states in the even-mass $^{106\text{-}120}$Cd are presented in Fig. 4.1. The level energies for ^{114}Cd are taken from Refs. [Mhe84, Fah88]. For ^{118}Cd and ^{120}Cd the level energies are from Refs. [Apr87, Apr85].

Perhaps the most conspicuous feature of the level systematics is the behaviour of the excited 0^+ states (Fig. 4.1 (b)): These states cross when going from ^{114}Cd to ^{116}Cd, i.e. the 0_3^+ and 0_2^+ states fully exchange their properties, which is discussed later in this chapter. For this reason, the notation 0_A^+ for the 0_2^+ state in $^{106\text{-}114}$Cd and the 0_3^+ state in $^{116\text{-}120}$Cd is adopted in Fig. 4.1 and in the following discussion. The 0_3^+ states in $^{106\text{-}114}$Cd and the 0_2^+ states in $^{116\text{-}120}$Cd are labelled 0_B^+. In the (t,p) two-neutron transfer-study O'Donnel et al. [ODo88] suggested the change in level ordering between ^{110}Cd and ^{112}Cd based on the assumption of Ref. [Apr84] that the intruder levels in Cd follow a "V" shape pattern. However, according to the present data, no corresponding crossing occurs on the neutron-deficient side in Cd isotopes.

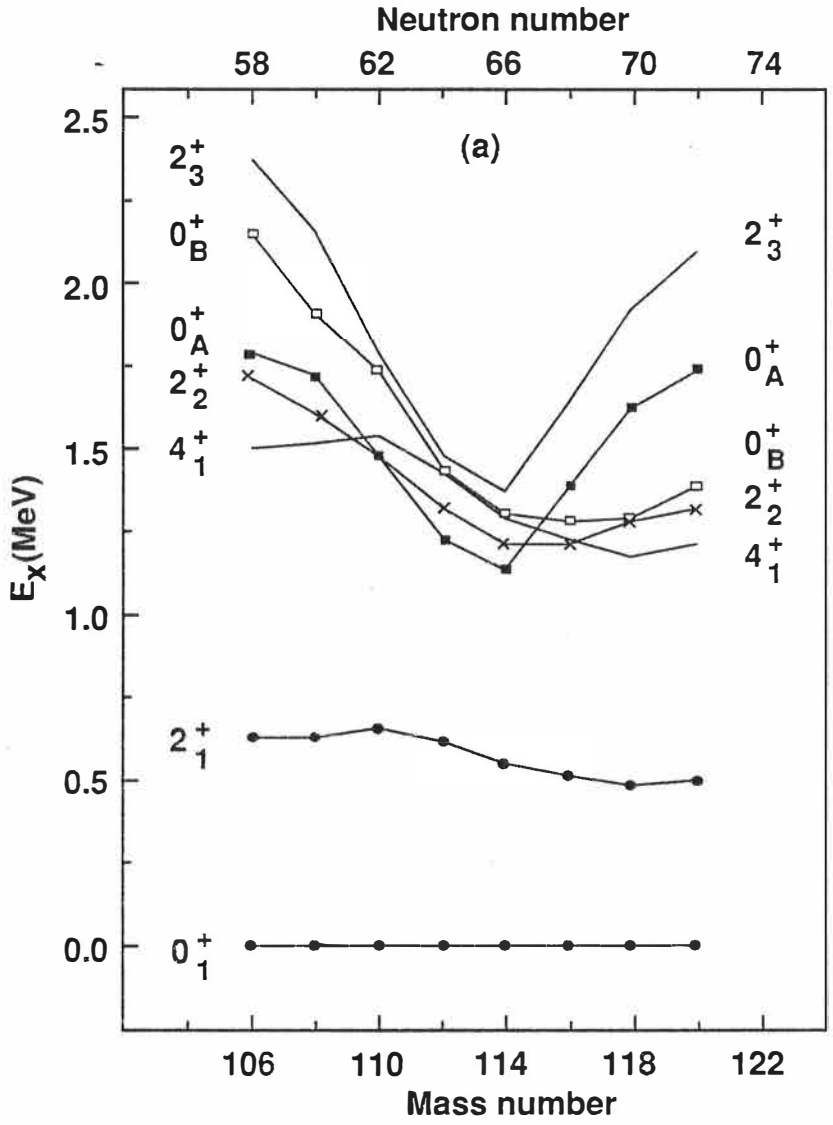

Fig. 4.1: (a) The systematics of low-lying low-spin states in the even $^{106\text{-}120}$Cd. For clarity of presentation symbols marking the 2^+_3 and 4^+_1 levels are omitted.

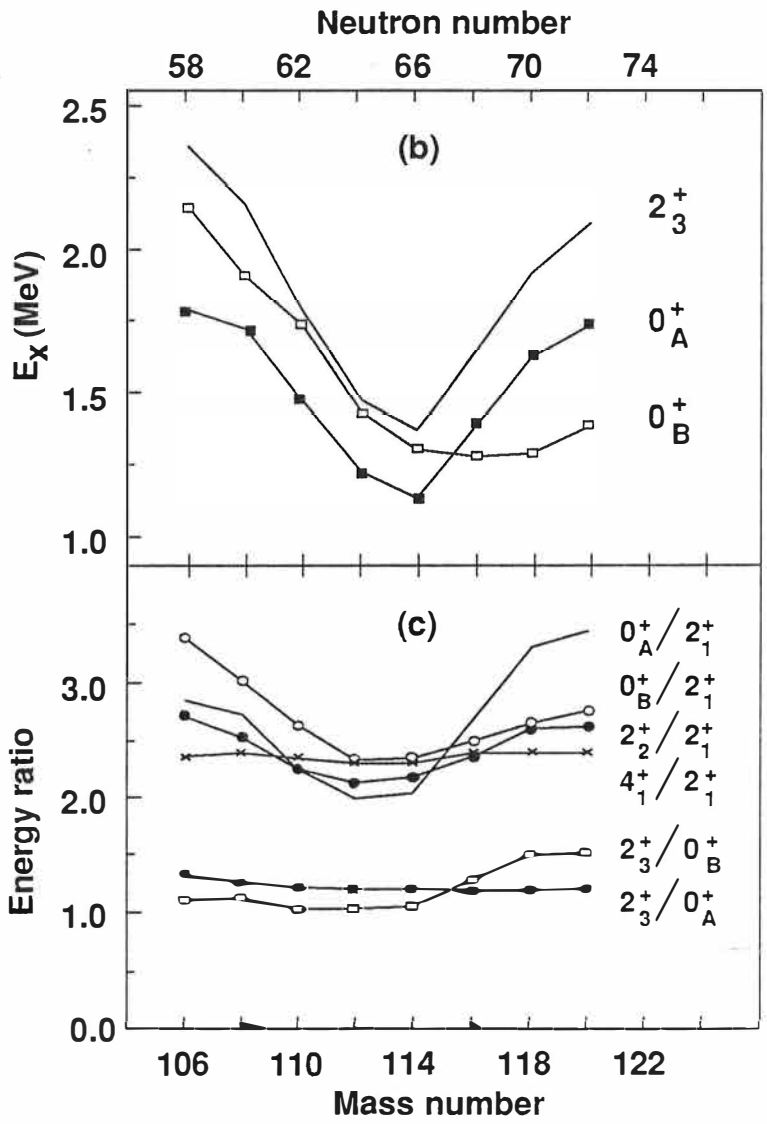

Fig. 4.1: (b) The systematics of the 2^+_3, 0^+_A and 0^+_A states in the even $^{106\text{-}120}$Cd.
(c) The energy ratios of the selected levels in even $^{106\text{-}120}$Cd.

Another important feature is the relationship between the 0^+_A and the 2^+_3 states. The ratio of the excitation energies of these states is almost constant, which can be seen in Fig. 4.1 (b) and (c).

A small subshell effect at N=64 is revealed by a local maximum in the energies of the 2^+_1 and 4^+_1 levels in ^{110}Cd (N = 62). A small bump is also visible in the energies of the 2^+_2 and 0^+_B levels, while the 2^+_3 and 0^+_A levels behave smoothly at N=62. However, between ^{108}Cd and ^{106}Cd a slight change in the slope of the energy curves of the 2^+_3 and 0^+_A states is observed. Also the rearrangement of the 4^+_1, 2^+_2 and 0^+_2 states is taking place at ^{110}Cd: There the 0^+_2 state is the lowest one and the 4^+_1 state the highest one among those three excited state, whereas their sequence is reversed in the ^{106,108}Cd isotopes. At the neutron-rich side the similar rearrangement is again happening at ^{116}Cd and ^{118}Cd so that in ^{118}Cd the 4^+_1 state is the lowest one and the 0^+_2 state the highest one.

Ratios of absolute E2 transition rates ($\propto I_\gamma / E^5_\gamma$) from the 0^+_2, 2^+_2, 0^+_3, 2^+_3 states relevant to the following discussion are presented in Table 4.1. The values for ^{114}Cd are from Ref. [Fah88], and for ^{118}Cd and ^{120}Cd, the results of Refs. [Apr87, Apr85] are used. The values for $^{106\text{-}112}$Cd and ^{116}Cd are from the present work. Our data for the B(E2; 2^+_2 - 2^+_1) / B(E2; 2^+_2 - 0^+_1) values are in agreement with the earlier values of Refs. [DeF88, Hae82, DeG83, DeF89]. The values for the 0^+_2 states are new, like the ones for the 0^+_3 states in ^{106,110,116}Cd, and most of the upper limits for the 2^+_3 states (see also chapter 3). Our result of B(E2; 0^+_3 - 2^+_2) / B(E2; 0^+_3 - 2^+_1) = 170(35), in ^{110}Cd is in complete agreement with the value of 171(62) reported in Ref. [Gia89], which appeared during the course of this work. The value for the 0^+_3 state in ^{108}Cd is in good agreement with the one in Ref. [Rou84] (note that our 0^+_3 state is labelled as 0^+_2 state in Ref. [Rou84]); the values for ^{112}Cd and ^{114}Cd are somewhat larger than the ones obtained in Ref. [Jul80].

Table 4.1: Relative E2 transition rates in the even $^{106-120}$Cd isotopes. Transitions which are not energetically possible are indicated by an asterisk. The errors estimated to be between 15 % and 35 % are not marked.

	106	108	110	112	114 [a]	116	118 [b]	120 [c]
$E(2_2^+)$ [keV]	1716.6	1601.7	1475.9	1312.3	1209.7	1212.7	1269.5	1322.8
$B(E2;2_2^+\text{-}2_1^+)$	4 [d]	8 [d]	24 [d]	26 [d]	45 [d]	19 [d]	17	25
$B(E2;2_2^+\text{-}0_1^+)$	1	1	1	1	1	1	1	1
$E(0_2^+)$ [keV]	1795.3	1721.0	1473.2	1224.2	1134.5	1282.5	1285.8	1388.7
$B(E2;0_2^+\text{-}2_2^+)$	< 700	< 190	*	*	*	< 870		
$B(E2;0_2^+\text{-}2_1^+)$	1	1				1		
$E(0_3^+)$ [keV]	2143.9	1913.3	1731.3	1433.2	1305.6	1380.2	1615.0	1744.6
$B(E2;0_3^+\text{-}2_2^+)$	230	1100	170	8500	41000	< 240	< 19	< 3
$B(E2;0_3^+\text{-}2_1^+)$	1	1	1	1	1	1	1	1
$E(2_3^+)$ [keV]	2370.6	2162.5	1783.6	1468.8	1364.3	1641.5	1915.8	2093.8
$B(E2;2_3^+\text{-}0_1^+)$	1	1	1	1	1	1		1
$B(E2;2_3^+\text{-}2_1^+)$	50	< 100	< 33	< 28	< 50	< 10	<10 [f]	< 33
$B(E2;2_3^+\text{-}2_1^+)$ [g]			0.5 [d]	0.7 [d]	0.2 [d]	2.6 [e]		
$B(E2;2_3^+\text{-}4_1^+)$	< 1.5	< 70	< 1100		40	< 120	< 20	190
$B(E2;2_3^+\text{-}2_2^+)$	< 2250	< 300	< 130	< 2400	95	< 70	330	< 700
$B(E2;2_3^+\text{-}0_2^+)$	3400	< 300	< 130	710	50	< 140	< 30	
$B(E2;2_3^+\text{-}0_3^+)$	< 4000	< 3500			20	< 500		

[a] Data from Ref. [Fah88].

[b] Data from Ref. [Apr87].

[c] Data from Ref. [Apr85].

[d] E2/M1 mixing ratio from Ref. [Lan82].

[e] E2/M1 mixing ratio δ = -0.6 used from Ref. [New80].

[f] B(E2) value normalized to 10.

[g] $B(E2;2_3^+\text{-}2_1^+)$ when the E2/M1 mixing ratio used.

Table 4.2: Ratios of E0 and E2 transition rates for 0_2^+ and 0_3^+ states in the even $^{106-114}$Cd isotopes.

	Mass Number				
X_{ijk} [a]	106	108	110	112 [b]	114 [b]
X_{211} (10^{-3})	< 9	< 12	< 8	26(4)	26(5)
X_{311}	2.2(5)	10(2)	< 0.04	1.0(2)	16(3)
X_{312} (10^{-4})	70(20)	80(20)	< 6	2.6(6)	6.0(6)

[a] $X_{ijk} = B(E0;0_i^+ - 0_j^+) / B(E2;0_i^+ - 2_k^+)$

[b] From Ref. [Jul80].

The available ratios of the reduced E0 and E2 transition probabilities (X = B(E0)/B(E2); see chapter 2.1.2.) from the 0_2^+ and 0_3^+ states in the even $^{106-114}$Cd isotopes are collected in Table 4.2. The X-values for ^{106}Cd, ^{108}Cd and ^{110}Cd are new from the present work. Preliminary X-values reported [Gia89] for ^{110}Cd are not in serious disagreement with our values. For ^{112}Cd and ^{114}Cd the data is from the earlier study of Julin et al. [Jul80].

4.1.1. The 0_A^+ state

The 0_A^+ states are characterized by fast E2 transitions to the 2_1^+ states: In even $^{106-114}$Cd, this property is reflected in the small value of X for the 0_2^+ states (Table 4.2). The Coulomb-excitation values of the absolute $B(E2;0_2^+ - 2_1^+)$ in ^{112}Cd and ^{114}Cd are 51 W.u. and 41 W.u. [Jul80], respectively. The monopole strengths for the $E0(0_2^+ - 0_1^+)$ transitions are $\rho_{21}^2 = 37 \times 10^{-3}$ (^{112}Cd) and 30×10^{-3} (^{114}Cd) leading to the X_{211} value of 26×10^{-3} for both of these nuclei [Jul80]. The limits for the X_{211} values in $^{106-110}$Cd are smaller or of the same order of magnitude: 10×10^{-3} (Table 4.2). If one assumes a $B(E2;0_2^+ - 2_1^+)$ value of about 1 W.u., which is considered a slow transition, one would

need an E0(0_2^+ - 0_1^+) with a rather small monopole strength: ρ^2_{21} = 0.3 x 10^{-3}. As this value would be quite unreasonably small [Kan84], one can conclude that the E2 transition to the 2_1^+ state is fast also in $^{106\text{-}110}$Cd.

In ^{116}Cd it is the 0_3^+ state which is characterized by a fast B(E2) to the 2_1^+ state, as found in the Coulomb-excitation experiment [McG65, Bla81], and recently confirmed by Mach et al. [Mac89]: The B(E2;0_3^+ - 2_1^+) value deduced from those experiment is about 30 W.u., which is approximately the same as in ^{112,114}Cd for the 0_2^+ - 2_1^+ transition. The lifetime (τ = 94(6) ps) of the 0_2^+ level in ^{116}Cd measured by Mach et al. [Mac89] leads to the B(E2) value of about 1 W.u. for the 0_2^+ - 2_1^+ transition. The 0_2^+ level is not populated in Coulomb excitation [Bla81]. Consequently, those arguments imply the level crossing between the Cd isotopes 114 and 116, and that the 0_3^+ state in ^{116}Cd can be assigned as 0_A^+.

On the basis of the excitation energies of Refs. [Apr87, Apr85], it now seems straightforward to identify the 0_3^+ states in ^{118}Cd and ^{120}Cd as the 0_A^+ states. This interpretation is also supported by the recent (t,p) study [ODo88], where the crossing of the 0^+ levels between the ^{114}Cd and ^{116}Cd is deduced from the interpretation of the (t,p) transfer strengths.

The present findings contradict the conclusions drawn in Refs. [Apr84, Apr87, Apr85], where the 0_3^+ states of ^{118}Cd and ^{120}Cd are related to the 0_3^+ states in ^{114}Cd and ^{112}Cd. Their experimental argument has been a large value of the ratio R = B(E2;$0_3^+ \rightarrow 2_2^+$)/B(E2;$0_3^+ \rightarrow 2_1^+$) for the 0_3^+ states. In fact, the limits, R < 19 in ^{118}Cd [Apr87] and R < 3 in ^{120}Cd [Apr85] are rather small and do not completely exclude a possible strong E2 transition to the 2_1^+ state. Moreover, the short lifetime recently measured by Mach et al. [Mac89] for the 0_3^+ state in ^{118}Cd (τ < 10 ps) is in agreement with the idea of the present work.

4.1.2. The 0^+_B state:

A characteristic feature of the 0^+_B (0^+_3) states in the even $^{106-114}$Cd isotopes is the large value for ratio R (see above), which means that the E2 transition to the 2^+_2 state is much stronger than the E2 transition to the 2^+_1 state. In ^{112}Cd and ^{114}Cd the E2(0^+_3 - 2^+_1) transition has shown to be strongly hindered [Jul80] by having the B(E2;0^+_3 - 2^+_1) value of 0.017 W.u. for ^{112}Cd and 0.0038 W.u. for ^{114}Cd. Rather large X_{311} values (Table 4.2) for ^{106}Cd and ^{108}Cd reveal that this is also the case for the 0^+_3 states in these isotopes.

In ^{110}Cd (N = 62), a discontinuity in the properties of the 0^+_B (0^+_3) state is observed. In addition to the small bump in the level-energy curve at N = 62, the smooth decrease of the R-value with decreasing neutron number is disturbed by the smaller value of R = 170 in ^{110}Cd (Table 4.1). Also the limit for the X_{311} value in ^{110}Cd (Table 4.2) is exceptionally low.

The 0^+_2 - 2^+_1 transition seems to be hindered in ^{116}Cd. From the lifetime measurement [Mac89] a value of B(E2;0^+_2 - 2^+_1) = 1 W.u. in ^{116}Cd can be derived (τ = 94(6) ps), which is slow in comparison to the B(E2;0^+_3 - 2^+_1) = 30 W.u. The value of about 40 x 10^3 is obtained for the B(E2;0^+_2–2^+_2)/B(E2;0^+_2–2^+_1) ratio from the data of Ref. [Brü82]. In our work the 70 keV 0^+_2-2^+_2 transition is not observed and the upper intensity limit gives the B(E2) ratio < 870 (Table 4.1). Those properties resemble the situation of the 0^+_3 state in the ^{112,114}Cd, therefore the 0^+_2 state in ^{116}Cd is associated with the 0^+_3 state in ^{112,114}Cd. This interpretation is supported by the (t,p) transfer data [ODo88], as discussed in the previous chapter 4.1.1.

For the 0^+_B (0^+_2) states in the even ^{118}Cd and ^{120}Cd, the B(E2)-ratio is not known, since it is difficult to observe the low-energy E2(0^+_2-2^+_2) transitions (16 keV and 66 keV, respectively). The lifetime-measurement of the 0^+_B(0^+_2) state in ^{118}Cd (τ = 14(2) ps) by Mach et al. [Mac89] indicates the hindrance of the E2(0^+_2–2^+_1) transition, although one

would expect even longer lifetimes. Thus, the 0_2^+ state in ^{118}Cd and ^{120}Cd (the latter based on energy systematics) can be related to the 0_2^+ state in ^{116}Cd.

4.1.3. The 2_3^+ state:

In ^{106}Cd the 2370.6 keV $(2)^+$ state is adopted as the 2_3^+ state and the lower lying $(2^+, 3^+)$ state at 2254.0 keV is adopted in the present work as the first excited 3^+ state; see the discussion about this level in chapter 3.1. The energy systematics of the 2_3^+ state is similar to that for the 0_A^+ state, both having a sharp "V"-shape behaviour (Fig. 4.1).

The B(E2) ratios given in Table 4.1 for ^{106}Cd, ^{112}Cd and ^{114}Cd indicate that the 2_3^+ state de-excites preferably to the 0_2^+ state. From the other transitions it is difficult to make any definitive conclusions, since they are generally unobserved due to the competing transition to the ground state and the first 2^+ state.

4.2. Other states

The first 3^+ state is identified in even $^{106\text{-}118}$Cd isotopes (although somewhat tentatively in ^{106,108}Cd). The systematics of the 3^+ level energy is shown in Fig. 4.2. The energy of the 3^+ state correlates with the energy of the first 4^+ state and the second 2^+ state: there is a small bump in energy at N = 62 (^{110}Cd) similar to the 4_1^+ energy and then shifts upwards at N = 68 - 70 (^{116,118}Cd) similar to the 2_2^+ energy. Also the energy ratio $E(3_1^+)/E(4_1^+)$ or $E(3_1^+)/E(2_2^+)$ is quite constant, from which one could predict the 3^+ state in ^{106}Cd to be at approximately 2.2 MeV. The level at 2254.0 keV which is assigned in the present work as $(2^+,3^+)$ fits well to the systematics of the 3^+ states.

The 3_1^+ state de-excites to the 2_2^+ state with a higher probability than to the 2_1^+ or 4_1^+ states. This is illustrated in Table 4.3 where the relative B(E2)-ratios are given assuming pure E2 transitions.

Systematics of other 4^+ states above the first excited 4^+ state is not straightforward. In Fig. 4.2 the energy systematics of the 4_2^+ and 4_3^+ states is shown and the B(E2) ratios are collected in Table 4.3. According to the de-excitation properties the second excited 4^+ state in ^{112}Cd and ^{114}Cd is connected to the third 4^+ state in ^{110}Cd (open circles in the Fig. 4.2). This 4^+ state preferably feeds the 2_3^+ state and the energy systematics is following that of the 0_A^+ and 2_3^+ states. In ^{106,108,110}Cd the experimental data allow the connection of the 4_2^+ states in these isotopes to the 4_3^+ state in ^{112,114}Cd (filled circles in Fig. 4.2). In ^{116}Cd and ^{120}Cd the second 4^+ state was not identified. In ^{118}Cd the 1929.1 keV level was assigned tentatively $I^\pi = 4_2^+$ [Apr87]. This assignment is adopted in the present work as the 1929.1 keV level preferably de-excites to the 2_2^+ and 4_1^+ levels like the 4_2^+ level in $^{106\text{-}110}$Cd.

The energy systematics of the 0_4^+ states are illustrated in Fig. 4.3. The levels are connected only to guide the eye; no other information except the 0_4^+ energy is considered. The energy of the 0_4^+ state behaves smoothly as a function of the neutron number. In the study of ^{104}Cd via the (p,t) reaction Rotbard et al. [Rot84] observed the 0^+ states at 1882 keV and 3099 keV. The energy systematics favors the latter one to be the 0_4^+ state and the former one to be the 0_2^+state. If so, one could predict the fourth 0^+ state in ^{106}Cd to be around 2.7 MeV.

In this work the first 3^- state in ^{106}Cd and ^{108}Cd has been firmly determined. However, it required revising some previous incorrect spin assignments. The energy of the first 3^- state decreases regularly with increasing neutron number at least until ^{116}Cd which is the last case where the state is exactly known (Fig. 4.3). In ^{118}Cd the 1935 keV level is suggested as 3^- in the (d,^{6}Li) study [Jän79], but in Ref. [Apr87] spin 5^+, 6^+ or (4^+) is reported. Similarly, in ^{120}Cd the 1920(25) level is reported in Ref. [Jän79] as 3^-, but it is not confirmed by Aprahamian [Apr85].

Table 4.3: Relative E2-transition rates for the 3_1^+, 4_2^+ and 4_3^+ states in even $^{106-118}$Cd. Transitions which are not energetically possible are indicated by an asterisk. The errors estimated to be between 15 % and 35 % are not marked, and pure E2 transitions are assumed.

	Mass Number						
	106	108	110	112	114 [a]	116	118 [b]
$E(3_1^+)$ [keV]	(2254.0)	(2145.6)	2162.8	2064.1	1864.3	1915.2	2091.6
$B(E2;3_1^+ - 2_1^+)$	1	1	1	1	1	1	1
$B(E2;3_1^+ - 2_2^+)$	18	22	15	35	37	15	34
$B(E2;3_1^+ - 4_1^+)$		6		24	15		12
$E(4_2^+)$ [keV]	2104.6	2239.2	2220.2	1870.4	1732.2		(1929.1)
$B(E2;4_2^+ - 2_1^+)$	1	1	1	1	1		1
$B(E2;4_2^+ - 2_2^+)$	81	15	160	< 60	80		100
$B(E2;4_2^+ - 4_1^+)$	13	48	60	58	33		6
$B(E2;4_2^+ - 2_3^+)$	*			240	290		
$E(4_3^+)$ [keV]	(2252.2)		2250.5	2081.0	1932		
$B(E2;4_3^+ - 2_1^+)$	0.5		2×10^{-3}	$< 7\times10^{-4}$			
$B(E2;4_3^+ - 2_2^+)$			0.03	0.4	0.9		
$B(E2;4_3^+ - 2_3^+)$			1.5	0.3			
$B(E2;4_3^+ - 4_1^+)$	1		1	1	1		
$B(E2;4_3^+ - 4_2^+)$				< 20	14		

a From Ref. [Fah88, Mhe84].
b From Ref. [Apr87].

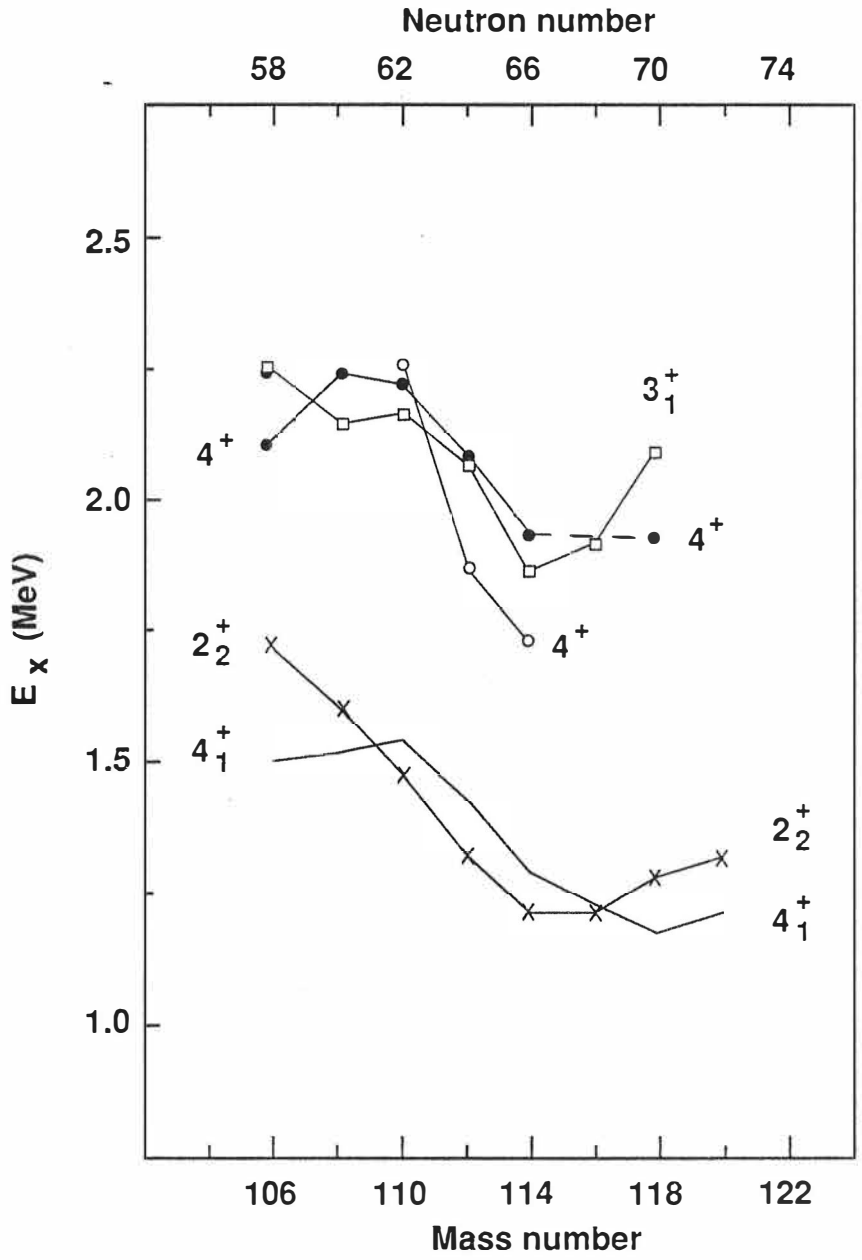

Fig. 4.2: The energy systematics of the 3_1^+, 4_2^+ and 4_3^+ states in the even $^{106\text{-}120}$Cd. The 2_2^+ and 4_1^+ states are shown for comparison.

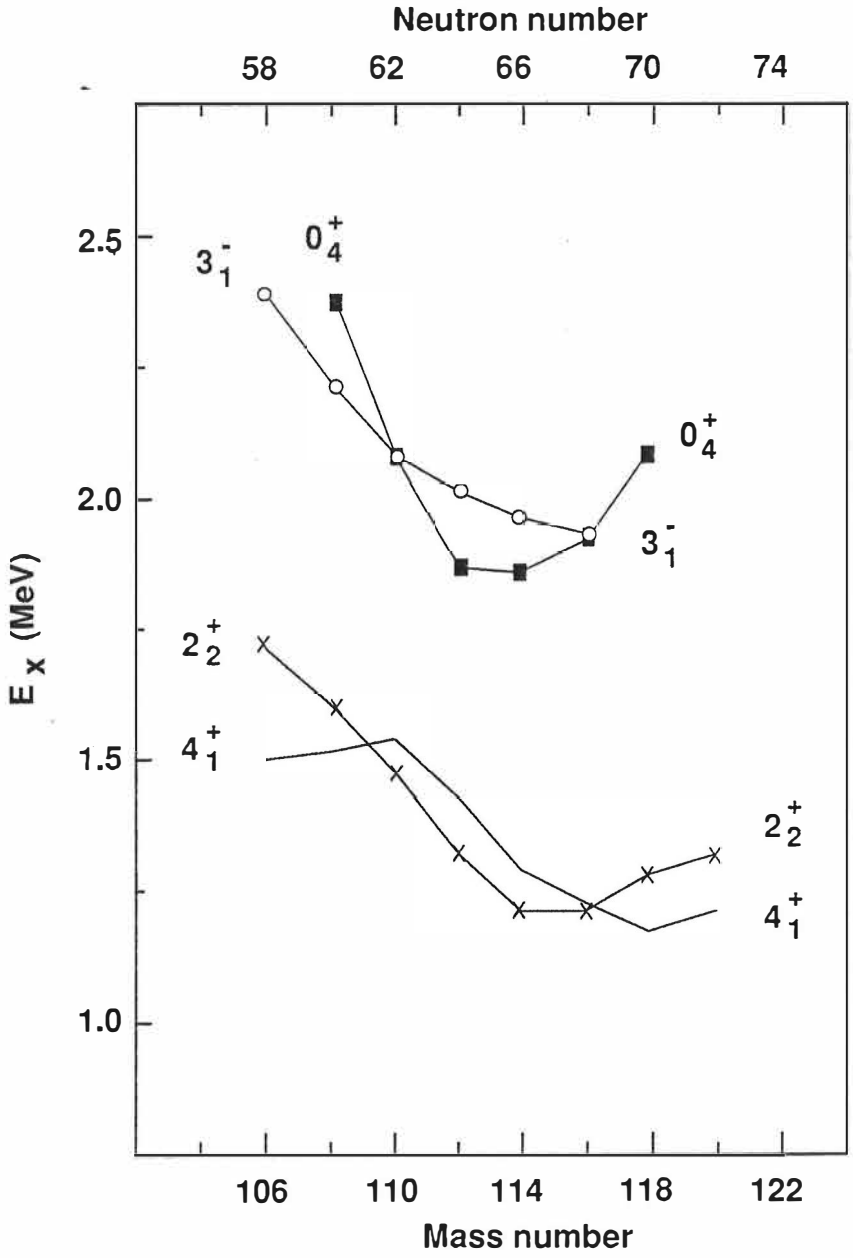

Fig. 4.3: The energy systematics of the 3^-_1 and 0^+_4 states in the even $^{106\text{-}120}$Cd. The 2^+_2 and 4^+_1 states are shown for comparison.

5. Discussion

5.1. Vibrational features in Cd isotopes

5.1.1. Quadrupole vibrations

The level structure and the relative B(E2) values for the allowed E2 transitions in a spherical quadrupole-phonon model are shown in Fig. 5.1 up to the three-phonon states [Boh75]. These predictions serve as a basis for a qualitative discussion of quadrupole vibrational features in Cd isotopes. One solution to the anharmonic effects can be found in Ref. [Bri65], and the corresponding U(5) limit of the algebraic IBA model is discussed in Refs. [Lip84, Cas88].

The quadrupole-phonon model predicts the two-phonon triplet (0^+, 2^+ and 4^+) at the energy of twice the energy of the one-phonon 2_1^+ state. The energies of the 2_2^+ and 4_1^+ states in the even $^{106\text{-}120}$Cd isotopes (Fig. 4.1 (c)) are in modest agreement with the 'energy-rule', and thus, they are considered the two-phonon states. The observed strong E2 branches from these states to the 2_1^+ state also satisfy the selection rule for E2 transitions ($\Delta n = \pm 1$) in the vibrator picture. However, the trend in the B(E2;2_2^+ - 2_1^+)/B(E2;2_2^+ - 0_1^+) values (Table 4.1) indicates that the ratio of ≈ 30 characterizing a "good vibrator" which is clearly observed at higher masses, may already be lost in ^{108}Cd.

Based on the excitation energy the 0_2^+ state should be the 0^+ state of the two-phonon triplet. But, when considering the E2 properties discussed in chapter 4.1.1. (strong E2 branch to the 2_1^+ state), one has to identify the 0_A^+ state (0_2^+ in $^{106\text{-}114}$Cd and 0_3^+ in $^{116\text{-}120}$Cd) as the two-phonon 0^+ state. In the quadrupole-phonon model the E0 transition from the two-phonon 0^+ state to the ground state is allowed according to the

selection rule for the E0 transitions ($\Delta n = 0, \pm 2$). We have not observed the $E0(0_2^+ - 0_1^+)$ transitions in $^{106,108,110}Cd$ in our conversion-electron measurements, but one should be cautious to make any definitive conclusions about that. The E0 strength might be large, even if the E0 peak in the electron spectrum is small. That has been the case for example in the $^{112,114}Cd$ isotopes [JulPC].

The interpretation of the 0_2^+ state in $^{106\text{-}114}Cd$ as being the two-phonon 0^+ state is supported by the X_{211} values (Table 4.2), which are of the order of magnitude predicted for the spherical vibrator. In the quadrupole-phonon model the ratio X for the transitions from the two-phonon 0^+ state is equal to β_{rms}^2, where β_{rms} is regarded as the rms value of deformation [Kum75]. With the β_{rms} values from Ref. [Ram87] for the even $^{106\text{-}116}Cd$ isotopes one gets the ratio X of about 0.035.

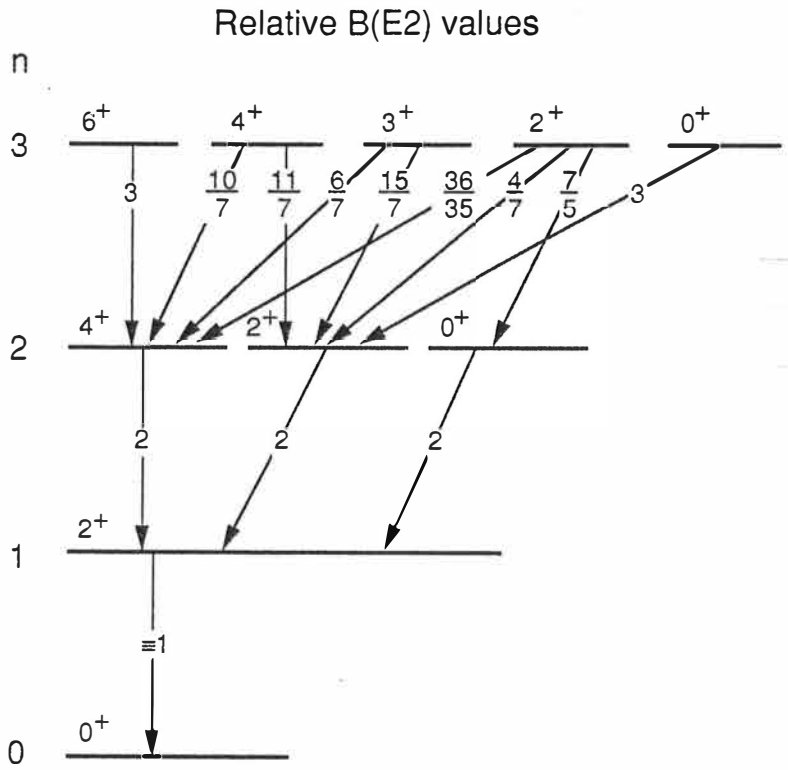

Fig. 5.1: The energy spectrum and the B(E2) ratios in the spherical quadrupole-phonon model.

In the even $^{106\text{-}120}$Cd isotopes, the 0^+_B (0^+_3 in $^{106\text{-}114}$Cd and 0^+_2 in $^{116\text{-}120}$Cd) and 2^+_3 states could play the role of the three-phonon states. In ^{112}Cd and ^{114}Cd they are pushed down in energy to form the well-known quintuplet of states in the energy region of two-phonon states. The interpretation of 0^+_B state as being a three-phonon state is supported by its strong E2 branch to the 2^+_2 state and hindered E2 decay to the 2^+_1 state (see the discussion in chapter 4.1.2). The 2^+_3 state de-excites preferably to the two-phonon states, in particular to the 0^+_2 state in ^{106}Cd, ^{112}Cd and ^{114}Cd, and to the 0^+_3 state in ^{116}Cd (Table 4.1). This is consistent with 2^+_3 state being interpreted as the three-phonon 2^+ state.

The application of the vibrator picture to the even ^{116,118,120}Cd isotopes leads to the conclusion that the three-phonon 0^+ state lies below the two-phonon 0^+ state. This interpretation of 0^+ states conflicts with Ref. [Apr87] where ^{118}Cd is introduced as an almost perfect harmonic vibrator up to the three-phonon excitations. The 0^+_3 state in Ref. [Apr87] is considered as an "extra" intruder state. The life-time measurements by Mach et al. [Mac89] support our interpretation of the 0^+ states in those heavy Cd isotopes.

The 3^+_1 level is mainly the regular quadrupole three-phonon state. This is indicated by transitions more favored to the two-phonon 2^+_2 and 4^+_1 states than to the one-phonon 2^+_1 state (Table 4.3).

The 4^+_2 level in ^{106,108,110}Cd and ^{118}Cd might be considered as the three-phonon 4^+ state. The level preferentially feeds the two-phonon 2^+_2 and 4^+_1 states (Table 4.3) via E2 transitions. However, the measured B(E2) values for those transitions are not consistent with equal B(E2) values predicted for the spherical vibrator (Fig. 5.1). The 4^+_3 levels in ^{112,114}Cd have similar properties than the 4^+_2 level in ^{106,108,110}Cd and ^{118}Cd, except the de-excitation also to the second excited 4^+ state (see the discussion in chapter 4.2).

In conclusion of this qualitative interpretation, the quadrupole-phonon model seems to work quite well for the Cd isotopes at low excitation energies. Moreover, Fahlander et al. [Fah88] have shown that all the observed levels and B(E2) values below 2.6 MeV in ^{114}Cd can be accounted for in view of a simple vibrator. The serious discrepancy arises from a large energy-splitting of the three-phonon states in ^{110,112,114}Cd as the 0^+ and 2^+ states are pushed down from the other three-phonon states (3^+, 4^+ and 6^+). The other discrepancy is the drop of the energy of the three-phonon 0^+ state below that of the two-phonon 0^+ state observed in the heavier Cd isotopes. In ^{134}Ba [Mey76] and ^{126}Te [Jac77] this kind of phenomenon is explained as caused by γ-softness of the nucleus. A similar situation can be achieved in the O(6) dynamical symmetry of the IBA [Cas88].

5.1.2. Octupole vibrations

A collective octupole vibrational state can be understood as the coherent sum of a number of one-particle-one-hole excitations which can couple to an angular momentum of 3$\hbar$. Excitations between orbits, which differ in orbital angular momentum l by 3$\hbar$ and have the same change in total angular momentum $\Delta j = \Delta l$, dominate the behaviour of low-energy octupole states [Boh75]. In Cd isotopes this kind of pair of orbits is the neutron ($d_{5/2}$ - $h_{11/2}$)-pair.

The 3^-_1 state in the even Cd isotopes show characteristics of an octupole vibrational state for this region. Its excitation energy is decreasing smoothly when adding neutrons to the $d_{5/2}$ orbit (up to N = 64) and then the energy should increase [Boh75] when the $h_{11/2}$ orbit is being filled. In Cd isotopes at least up to ^{116}Cd (N = 68) the energy of the 3^- state is monotonously decreasing (Fig. 4.3).

Recently, Zamfir et al. [Zam89] developed a phenomenological formula to estimate the energy of the octupole 3^- state: for non-magic near-spherical nuclei, when the sum of valence nucleons $N_t = N_p + N_n \geq 4$ but ≤ 18, then $E(3^+_1) = 35A^{-2/3} + 8/N_t$. It reproduces quite well the 3^- energies for the $^{106\text{-}112}$Cd isotopes, but it predicts the

turnover to the upward slope exactly in the middle of the neutron shell at N = 66, which is not in agreement with the experimental data (Fig. 4.3). Unfortunately, there is no reliable experimental data on the heavier Cd isotopes to draw further conclusions (see the discussion about the systematics of the 3^- state in chapter 4.2).

5.2. Rotational features in Cd isotopes

Recently the energy levels in the ^{106,108,110}Pd isotopes (Z = 46) have been interpreted in terms of quasi-rotational bands and a triaxially deformed shape has been suggested [Cli86, Sve89, Kot89]. Therefore it is worthwhile to look for such properties in the neighbour even-mass Cd isotopes. Fahlander et al. [Fah88] have pointed out that the quadrupole moments of the low-lying states in ^{114}Cd are large enough for an interpretation of the level structure in terms of rotational bands. Moreover, in the recent NORDBALL study of ^{110}Cd, a number of well-developed bands have been identified [Juu89].

In the rotor picture, the closely related 0^+_A and 2^+_3 states (Fig. 4.1) would represent the two lowest members of a β-band. The E0 transitions between equal spin members of a β-band and the ground state band of a deformed nucleus are allowed and known to be strong [Kum75, Kan84]. In an earlier study, Julin et al. [Jul80] measured large values for the E0($0^+_A \rightarrow 0^+_1$) transition probabilities in ^{112}Cd and ^{114}Cd. In Ref. [Mhe84], the E0 transition from the 2^+_3 state to the 2^+_1 state in ^{114}Cd was also observed to be strong. The band built on top of the 0^+_2 state in ^{110,112,114}Cd is discussed in the next chapter in the context of intruder states.

The 2^+_2 state looks like the head of a γ-band, although the Alaga-rule for B(E2) ratio, B(E2; 2^+_2 - 2^+_1)/B(E2; 2^+_2 - 0^+_1) = 1.43, is strongly violated (Table 4.1). On the other hand, as in the case of a rotational nucleus, a sizeable positive value for the quadrupole moment has been measured for this state in ^{114}Cd [Fah88]. The 3^+_1 level can be assigned to the γ-band; it is depopulated to the 2^+_2 state with a higher probability

than to the 2_1^+ state, and the energy difference $E(3_1^+) - E(2_2^+)$ is approximately equal to the energy of the 2_1^+ state.

The 4_2^+ state in ^{108,110}Cd and 4_3^+ state in ^{112,114}Cd could be the 4^+ member of the γ-band, even though the E2 branch to the 2_2^+ state is not so clearly favored over other transitions in these Cd isotopes. This state has the energy difference $E(4_\gamma^+) - E(2_2^+)$ close to the energy difference $E(4_1^+) - E(2_1^+)$. This is in accord with the Sakai's classification scheme of a quasi-gamma band [Sak81, Sak84].

In ^{108}Cd and ^{110}Cd there are candidates for the 5^+ and 6^+ members of the γ-band; at 2811 keV (5^+) and 2996 keV (6^+) in ^{108}Cd, and at 2928 keV (5^+) and 3064 keV (6^+) in ^{110}Cd. If they belong to a γ-band, there is quite a strong odd-even staggering for the levels grouped as 2^+, (3^+, 4^+), (5^+, 6^+) in the γ-band. This kind of staggering obviously follows from the Sakai's classification scheme [Sak81] for vibrational nucleus.

Evidently, the Cd isotopes have some properties which resemble, albeit only qualitatively, a slightly deformed rotor.

5.3. Intruder states in Cd isotopes

Keeping in mind the simple model pictures, it is intriguing to see if our level systematics exhibit properties characteristic of intruder states. The intruder states in the even Cd isotopes should involve proton 2p-4h excitations, i.e. 6 valence quasiprotons (Fig. 1.1). The collectivity of these states should be similar to that in the ground state band of the Ru (Z = 50 - 6) and Ba (Z = 50 + 6) isotones.

In Fig. 5.2 the energy difference between the 0^+_A and 2^+_3 states in the even Cd isotopes is compared to the energies of the known 2^+_1 states in the neighbouring isotones. Indeed, the similarities are remarkable between the Cd and the Ru and Ba isotones. This indicates that the 0^+_A and 2^+_3 states could represent the two lowest members of the intruder band. In accordance with the intruder picture, the 0^+_A state has its minimum excitation energy at N = 66, i.e., in the middle of the neutron shell. The other members of the intruder band are compared in Fig. 5.3 with the ground state band in the Ru and Ba isotones. Again, the analogy is quite impressive. Our data for ^{110}Cd confirms the previously proposed [Mey77, Kus87, Ker90] band up to spin 6^+; the continuation of the band above the 6^+ state is not yet clear. The 8^+ state of the band reported by Kusnezov et al. [Kus87] and Kern et al. [Ker90] is not observed in our work, nor in the NORDBALL study [Juu89]. The data for ^{114}Cd is taken from Refs. [Jul80, Mhe84, Fah88]. Our (α,2n) measurements revealed completely new data for ^{112}Cd. In ^{112}Cd, there is slight evidence for the 8^+ state of the band at about 3400 keV, but it still needs a verification.

Further support for associating the 0^+_A states with the intruders comes from a careful examination of the results of the two-proton transfer studies [Fie77]. For ^{110}Cd and ^{112}Cd there is no doubt that it is the 0^+_A (0^+_2) state which is strongly populated in the (^{3}He,n) two-proton transfer reaction. For ^{110}Cd the 0^+_B (0^+_3) state is not populated. For ^{112}Cd one cannot completely exclude the population of the 0^+_3 state, but it would have to be weak, if populated at all. It is not obvious why no 0^+ states are strongly populated

in the ^{106,108}Cd isotopes in the (^{3}He,n) reaction; the strength was reported [Fie77] to be fragmented over several 0^+ states. However, at least in the ^{110}Cd and ^{112}Cd the results of the (^{3}He,n) reaction can be regarded as an evidence for a strong two-proton component in the wave function of the 0^+_A state.

Moreover, in the evaluation of the (t,p) two-neutron transfer strengths, O'Donnell et al. [ODo88] have concluded that the 0^+_A state in the even $^{112\text{-}118}$Cd isotopes is the intruder 0^+ state, thus supporting the interpretation of the crossing 0^+ states between ^{114}Cd and ^{116}Cd. The order of the 0^+ states in ^{110}Cd has not been determined firmly in that work, but a crossing between ^{112}Cd and ^{110}Cd was suggested.

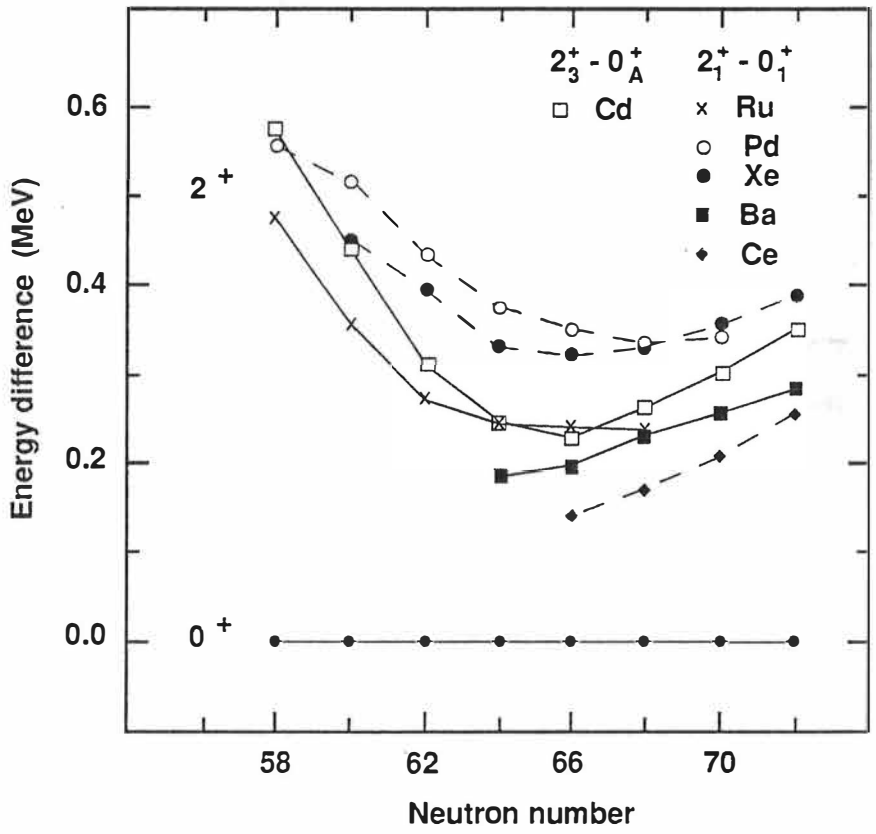

Fig. 5.2: The energy difference between the 2^+_3 and 0^+_A states in $^{106\text{-}120}$Cd compared to the 2^+_1 energy in the corresponding isotones of the neigbouring $_{44}$Ru, $_{46}$Pd, $_{54}$Xe, $_{56}$Ba and $_{58}$Ce nuclei [WooPC].

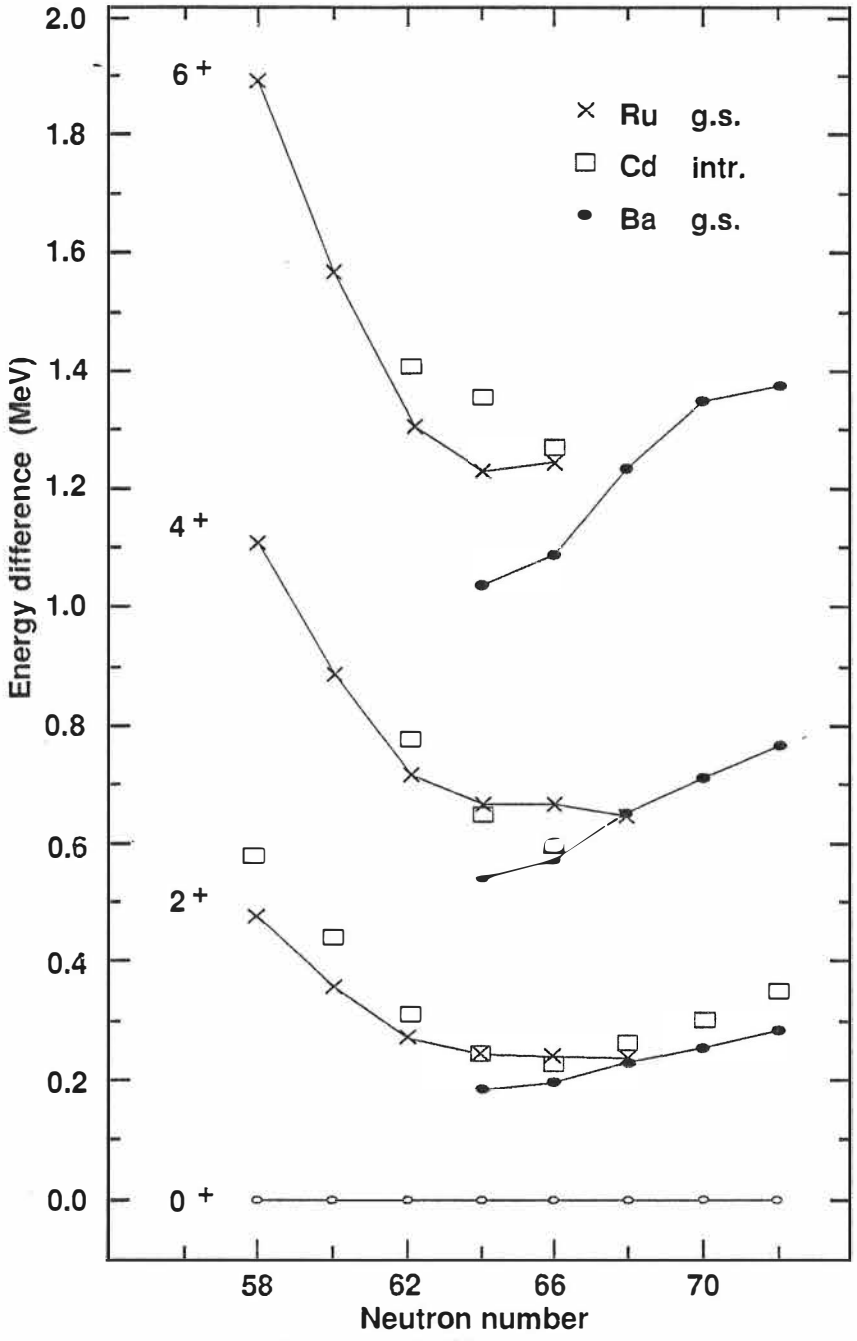

Fig. 5.3: Proposed members of the intruder band in even $^{106\text{-}120}$Cd compared to the states of the ground state band in the even Ru and Ba isotones. The intruder 0^+ state is normalized to 0 MeV. Data for Ru and Ba isotopes from Ref. [WooPC].

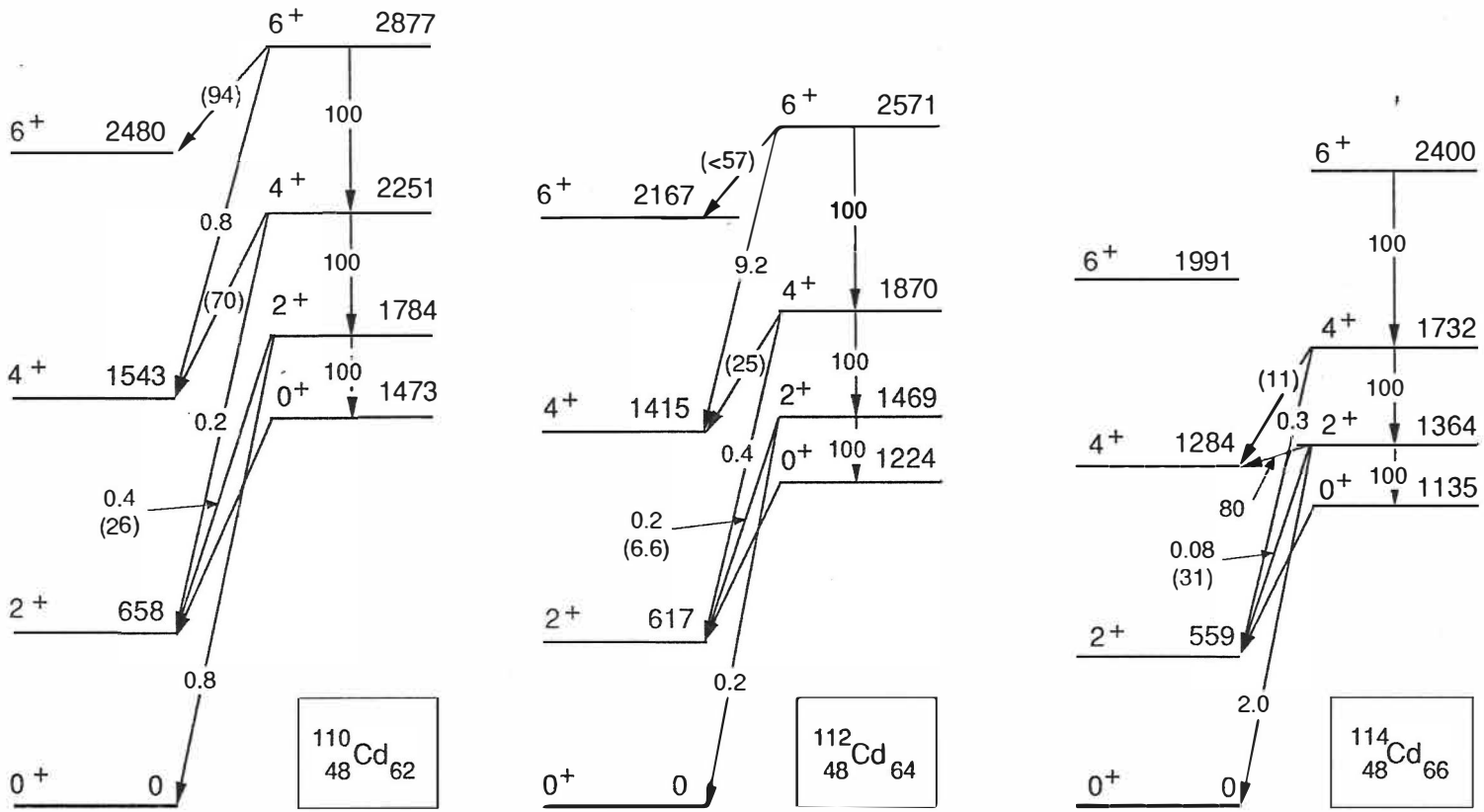

Fig. 5.4: The intruder band and the ground state band up to spin 6^+ in the even $^{110,112,114}Cd$. The relative B(E2) branching ratios between these bands are marked. In parenthesis is given the B(E2) value when the E2/M1 mixing ratio is not used.

As mentioned above, in ^{110}Cd, ^{112}Cd and ^{114}Cd there are candidates for higher spin members of the intruder band on top of the 0_2^+ state. The ground state band and the intruder band in these Cd isotopes are shown in Fig. 5.4. The relative B(E2) ratios between the ground state band and the intruder band are from the present work for ^{110,112}Cd and from Ref. [Fah88] for ^{114}Cd (see also Tables 4.1 and 4.3).

The intruder band is clearly rotational and to a good approximation it obeys the energy rule E = a I(I + 1) + b as illustrated in Fig. 5.5. The kinematical moment of inertia $\mathcal{J}^{(1)} = I/\omega = (2I\text{-}1)/E_\gamma$ derived for the intruder band e.g. in ^{110}Cd is about 10, 15 and 18 $\hbar^2$MeV^{-1} for the first three transitions, respectively. For same band, the dynamical moment of inertia $\mathcal{J}^{(2)} = dI/d\omega = 4/dE_\gamma$ is about 25 $\hbar^2$MeV^{-1}. The corresponding values for the first three transitions in the ground state band of ^{110}Cd are: $\mathcal{J}^{(1)}$ from about 5 to 12 $\hbar^2$MeV^{-1} and $\mathcal{J}^{(2)}$ about 18 and 77 $\hbar^2$MeV^{-1}.

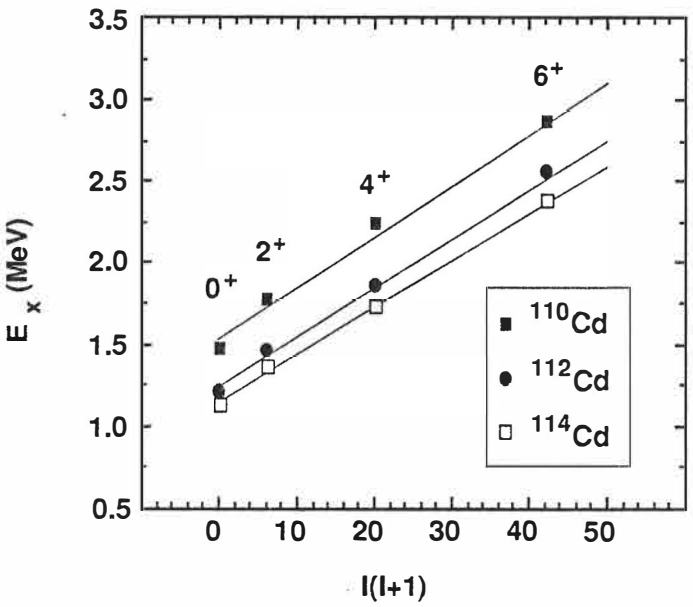

Fig. 5.5: The intruder level energy plotted as a function of I(I + 1) for ^{110,112,114}Cd. The solid line is a straight line E_x = a I (I + 1) + b fitted to the experimental values illustrated by symbols.

The B(E2) values for transitions inside the intruder bands are generally larger than those for the interband transitions. In some cases it is observed that the 2^+ member de-excites with strong E2 transitions also to the 4_1^+ and 2_2^+ states (Table 4.1). However, these transitions are generally unobserved and thus only upper limits of the B(E2) values are given. Furthermore, the E2/M1 mixing ratio of the 2_3^+ - 2_2^+ transition is unknown. The enhancement of the intraband transitions may become more pronounced for the higher spin states of the intruder band, as it is the case for the intruder bands in the even $^{112\text{-}118}$Sn isotopes [Bro79]. Experimentally the high-spin states of the intruder band are difficult to observe as they are expected to be strongly non-yrast.

The level energies of the intruder band resemble the ground state band of the corresponding Ru or Ba isotones (Fig. 5.3). At present comparison of the absolute B(E2) for the 2^+ member is not conclusive. In the ^{108,110,112}Ru isotopes (isotones of ^{112,114,116}Cd, respectively) B(E2;2_1^+ - 0_1^+) is about 70 W.u. [Ram87]. The data for the light Ba isotopes are not available, but for ^{126}Ba B(E2;2_1^+ - 0_1^+) is about 100 W.u. [Ram87]. From the life-time of the 2_3^+ state in ^{112}Cd [DeF89], the value for B(E2;2_3^+ - 0_2^+) can be deduced. By using our branching ratios the value is B(E2;2_3^+ - 0_2^+) < 140 W.u.; when using the branching ratio of Ref. [DeF89] the value is about 50 W.u. In ^{114}Cd the B(E2;2_3^+ - 0_2^+) is 16 W.u. according to Coulomb excitation [Fah88] and 67 W.u. when the branching ratios of Ref. [Mhe84] are used, as pointed out also by Fahlander et al. [Fah88]. The preliminary life-time of the 2_3^+ state in ^{116}Cd reveals the value 4 < B(E2;2_3^+ - 0_2^+) < 33 W.u. [MacPC]. Evidently, these values must be clarified before any definitive conclusions about the B(E2) values can be drawn.

In Ref. [Apr84], using a schematic mixing model, Aprahamian et al. associate the intruder 0^+ state with the 0^+ state having a large R-value, which in our notation is the 0_B^+ state. This interpretation is clearly different from ours as summarized next.

In summary, the main arguments supporting our interpretation of the 0_A^+ state as the intruder state are as follows:

(i) Strong population in the ^{110,112}Cd(^{3}He,n) reaction [Fie77] provides an evidence for a strong 2p component in the wave function of the 0_A^+ state.

(ii) The 2_3^+ levels are closely related to the intruder candidates; those levels could represent the beginning of rotational intruder bands in even $^{106\text{-}120}$Cd. The data from the (α,2n) reactions seem to support such a picture and even higher spin members are observed in ^{110,112,114}Cd.

(iii) The band built on the 0_A^+ state resembles the ground state band in the Ru and Ba isotones supporting the intruder 2p-4h configuration for protons.

(iv) In the general systematic behaviour of the energies of the 0_A^+ state, the minimum is reached exactly at the mid-shell point, i.e., N = 66.

5.4. The role of mixing

The similarities in Fig. 4.1 (c) indicate that the 2_3^+ - 0_A^+ energy differences in the Cd isotopes are not seriously affected by the mixing with the other states. In the (^{3}He,n) reaction [Fie77] only one excited 0^+ state in ^{110}Cd is strongly populated, which may indicate that the mixing between the excited 0^+ states is not large. In Ref. [ODo88] the authors conclude that some mixing between the two excited 0^+ states and the ground state is needed to reproduce the experimental (t,p) transfer strengths. However, they deduced a rather small mixing, which allowed them to identify different kinds of 0^+ states.

The fact that only weak E0 transitions are observed between the 0_A^+ and 0_B^+ states in ^{112,114}Cd [Jul80] can be taken as evidence for weak mixing of the two levels, so that one indeed can identify two essentially different sets of 0^+ states.

Although empirical evidence does not support strong mixing between the 0_A^+ and 0_B^+ states, yet strong mixing seems necessary in the theoretical calculations. In order to reproduce the E2 and E0 decay properties of the low-lying states in ^{112}Cd and ^{114}Cd, Heyde et al. [Hey82] assumed a strong mixing of the intruder and vibrational states. Actually, they used two models, but only with the one allowing a sizeable mixture of

the ground state into the excited 0^+ states was it possible to reproduce the fast $E0(0_2^+ \rightarrow 0_1^+)$ transitions in ^{112}Cd and ^{114}Cd [Jul80].

Mixing calculations for ^{110}Cd have been carried out by Kusnezov et al. [Kus87]. These calculations have reproduced many of the E2 properties by introducing a strong mixing of the intruder and the phonon states, e.g. the wave functions for the 0_2^+ and 0_3^+ states are composed of almost equal amplitudes of the two-phonon vibration-like 0^+ and the first rotation-like 0^+ configurations. This kind of mixing leads to a situation where the B(E2) values are modified to such an extend that the identities of the ground state band and the intruder band are lost [Kus87]. In the mixing scheme of Aprahamian et al. [Apr84], which is based on Ref. [Hey82], the mixing of intruder states with other states is increasing when approaching the neutron midshell reaching maximum mixing at N = 66.

Strong mixing of the excited 0^+ states at $N \approx 66$ used in the calculations of Heyde et al. [Hey82], Kusnezov et al. [Kus87] and Aprahamian et al. [Apr84] is not in agreement with the empirical facts discussed above. However, in Fig. 5.2, the $2_3^+ - 0_A^+$ energy difference is slightly increasing when moving away from the neutron midshell where it does not closely follow the trend of the energies of the 2^+ states in Ru or Ba isotones. Our result may indicate that the mixing with other states is increasing when moving away from the neutron midshell. Strong fragmentation of the (^{3}He,n) strength in ^{106,108}Cd [Fie77] may also support such a picture.

5.5. Conclusions

The general view is that the intruder states in the even Cd isotopes are "extra" states among the vibrational phonon states. This would mean that when we interpret the 0_A^+ state as the intruder, the 0_B^+ state should be the two-phonon 0^+ state. However, the de-excitation of the 0_B^+ state is very different from that of a typical two-phonon 0^+ state. In contrast, it is the 0_A^+ state which de-excites with a strong E2 transition to the

2_1^+ state, characteristic to a two-phonon state. The above considerations lead to a paradoxical conclusion; the intruder-like behaving 0_A^+ state is the state which in the phonon picture plays the role of the two-phonon 0^+ state. In the same way, in a simple vibrator picture, the 2_3^+ state which belongs to the proposed intruder band would represent a three-phonon state.

Our studies on Te isotopes [Kum86, Kum87] may indicate a similar situation. At least in ^{118}Te the 0_2^+ state is regarded as an intruder state [Sha85, Rik89], while it also has a strong B(E2) to the 2_1^+ state [Kum87]. In ^{108,110}Pd the rotational band has been observed on top of the 0_2^+ state [Sve89, Kot89], which has long been considered as a two-phonon state with large B(E2;0_2^+ - 2_1^+). In the lighter nuclei, such as in ^{58,60}Ni (Z = 28) the 0^+ state strongly populated in the (^{3}He,n) and (^{6}Li,d) reactions and weakly in the (p,t) and (t,p) reactions is the one having an enhanced E2 to the 2_1^+ state [Pas81], thus historically representing the two-phonon 0^+ state.

New experiments and theoretical calculations are called for to clarify the situation, and it should be carefully studied if this kind of behaviour of low-lying 0^+ state is more widespread phenomenon. In our view the concepts of intruder and phonon states represent different approaches which may not fit into the same framework, at least in even-mass Cd nuclei.

6. Summary

Considerable amount of new data for the low-lying, low-spin collective states in ^{106}Cd, ^{108}Cd, ^{110}Cd and ^{112}Cd were obtained in this work by employing various methods of in-beam and off-beam γ-ray and conversion-electron spectroscopy. From the deduced level systematics for the even $^{106\text{-}120}$Cd isotopes it is inferred that the excited 0^+ states cross between ^{114}Cd and ^{116}Cd, i.e. the 0_2^+ and 0_3^+ states fully exchange their properties. No corresponding crossing in the neutron deficient isotopes was observed. We found that the 2_3^+ state is closely related to the 0_A^+ state which is the 0_2^+ state in $^{106\text{-}114}$Cd and the 0_3^+ state in $^{116\text{-}120}$Cd. In ^{110}Cd, ^{112}Cd and ^{114}Cd there were also found higher-spin members of the band built on top of the 0_A^+ state. We have shown that, in the Cd isotopes, the 0_A^+ state has properties of a two-phonon state and of an intruder state, as well. The concept of intruder and phonon states having separate identity finds no support in the present systematics of even-mass Cd nuclei.

References

And85 W. Andrejtscheff, L. K. Kostov, H. Rotter, H. Prade, F. Stary, M. Senba, N. Tsoupas, Z. Z. Ding, and P. Raghavan, Nucl. Phys. **A437**, 167 (1985).

Apr84 A. Aprahamian, D. S. Brenner, R. F. Casten, R. L. Gill, A. Piotrowski, and K. Heyde, Phys. Lett. **140B**, 22 (1984).

Apr85 A. Aprahamian, Ph.D. thesis, Clark University, 1985, unpublished.

Apr87 A. Aprahamian, D. S. Brenner, R. F. Casten, R. L. Gill, and A. Piotrowski, Phys. Rev. Lett. **59**, 535 (1987).

Aub72 R. L. Auble, D. J. Horen, F. E. Bertrand, and J. B. Ball, Phys Rev. C**6**, 2223 (1972).

Bäc81 A. Bäcklin, N. G. Jonsson, R. Julin, J. Kantele, M. Luontama, A. Passoja, and T. Poikolainen, Nucl. Phys. **A351**, 490 (1981).

Bar67 P. D. Barnes, J. R. Comfort, and C. K. Bockelman, Phys. Rev. **155**, 1319 (1967).

Bel70 D. A. Bell, C. E. Aveledo, M. G. Davidson, and J. P. Davidson, Can. J. Phys. **48**, 2542 (1970).

Ber73 L. von Bernus, U. Schneider, and W. Greiner, Lett. Nuovo Cimento **6**, 527 (1973).

Bla81 J. Blachot, J. P. Husson, J. Oms, G. Marguier, and F. Haas, Nucl. Data Sheets **32**, 287 (1981).

Boe65 J. de Boer, J. Stockstad, R.G. Symons, and A. Winther, Phys. Rev. Lett. **14**, 564 (1965).

Boh75 A. Bohr, B. R. Mottelson, Nuclear Structure, Vol. 2 (W. A. Benjamin Inc., Reading, Mass., 1975).

Bri65 D. M. Brink, A. F. R. De Toledo Piza, and A. K. Kerman, Phys. Lett. **19**, 413 (1965).

Bro79 J. Bron, W. H. A. Hesselink, A. Van Poelgeest, J. J. A. Zalmstra, M. J. Uitzinger, H. Verheul, K. Heyde, M. Waroquier, H. Vincx, and P. Van Isacker, Nucl. Phys. **A318**, 335 (1979).

Brü82 W. Brüchle, and G. Herrman, Radiochimica Acta **30**, 1 (1982).

Cas88 R. F. Casten, and D. D. Warner, Rev. Mod. Phys. **60**, 389 (1988).

Cli86 D. Cline, Ann. Rev. Nucl. Part. Sci. **36**, 683 (1986).

Dan77 J. Daniere, R. Beraud, M. Meyer, R. Rougny, J. Genevey-Rivier, and J. Treherne, Z. Phys. **A280**, 363 (1977).

DeF88 D. De Frenne, E. Jacobs, M. Verboven, and G. De Smet, Nucl. Data Sheets **53**, 73 (1988).

DeF89 D. De Frenne, E. Jacobs, and M. Verboven, Nucl. Data Sheets **57**, 443 (1989).

DeG83 P. De Gelder, E. Jacobs, and D. De Frenne, Nucl. Data Sheets **38**, 545 (1983).

DeL89 R. De Leo, N. Blasi, S. Micheletti, M. Pignanelli, W. T. A. Borghols, J. M. Schippers, S. Y. van der Werf, G. Maino, and M. N. Harakeh, Nucl. Phys. **A504**, 109 (1989).

Dem76 A. M. Demidov, L. I. Govor, O. K. Zhuravlev, M. M. Komkov, and I. B. Shukalov, Bull. Acad. Sci. USSR, Phys. Ser. **40**, no. 1, 132 (1976).

Dem76a A. M. Demidov, L. I. Govor, O. K. Zhuravlev, M. M. Komkov, and I. B. Shchukalov, Bull. Acad. Sci. USSR, Phys. Ser. **40**, no. 6, 119 (1976).

Dem78 A. M. Demidov, L. I. Govor, Yu. K. Cherepantsev, M. R. Ahmed, S. Al-Najjar, M. A. Al-Amili, N. Al-Assafi, and N. Rammo, ATLAS of gamma-ray spectra from the inelastic scattering of reactor fast neutrons, Moscow Atomizdat, (1978).

Dey72 J. A. Deye, R. L. Robinson, and J. L. C. Ford, Jr., Nucl. Phys. **A180**, 499 (1972).

Dey73 J. A. Deye, R. L. Robinson, and J. L. C. Ford, Jr., Nucl. Phys. **A204**, 307 (1973).

Die75 W. Dietrich, A. Bäcklin, C. O. Lannergård, and I. Ragnarsson, Nucl. Phys. **A253**, 429 (1975).

Eji89 H. Ejiri, and M. J. A. de Voigt, Gamma-Ray and Electron Spectroscopy in Nuclear Physics, (Clarendon Press, Oxford, 1989).

Esa76 M. T. Esat, D. C. Kean, R. H. Spear, and A. M. Baxter, Nucl. Phys. **A274**, 237 (1976).

Fah88 C. Fahlander, A. Bäcklin, L. Hasselgren, A. Kavka, V. Mittal, L. E. Svensson, B. Varnestig, D. Cline, B. Kotlinski, H. Grein, E. Grosse, R. Kulessa, C. Michel, W. Spreng, H. J. Wollersheim, and J. Stachel, Nucl. Phys. **A485**, 327 (1988).

Fie77 H. W. Fielding, R. E. Anderson, C. D. Zafiratos, D. A. Lind, F. E. Cecil, H. H. Wieman, and W. P. Alford, Nucl. Phys. **A281**, 389 (1977).

Fla75 S. Flanagan, R. Chapman, G. D. Dracoulis, J. L. Durell, W. Gelletly, and J. N. Mo, J. Phys. **G1**, 77 (1975).

Fla76 S. Flanagan, R. Chapman, J. L. Durell, W. Gelletly, and J. N. Mo, J. Phys. **G2**, 589 (1976).

Gei74 R. Geiger, P. von Brentano, H. G. Friederichs, B. Heits, W. Schuh, K. O. Zell, H. Weigmann, and A. Berinde, Z. Phys. **271**, 129 (1974).

Gia89 A. Giannatiempo, A. Nannini, A. Perego, and P. Sona, preprint DFF110/10/89, to be published in Phys. Rev. C.

Gne71 G. Gneuss, and W. Greiner, Nucl. Phys. **A171**, 447 (1971).

Gul90 J. Gulyas, Zs. Dombradi, T. Fenyes, J. Timar, A. Passoja, J. Kumpulainen, and R. Julin, Nucl. Phys. **A506**, 196 (1990).

Hae82 R. L. Haese, F. E. Bertrand, B. Harmatz, and M. J. Martin, Nucl. Data Sheets **37**, 289 (1982).

Har88 H. Harada, T. Murakami, K. Yoshida, J. Kasagi, T. Inamura, and T. Kubo, Phys. Lett. **B207**, 17 (1988).

Har89 H. Harada, M. Sugawara, H. Kusakari, H. Shinohara, Y. Ono, K. Furono, T. Hosoda, M. Adachi, S. Matsuki, and N. Kawamura, Phys. Rev. **C39**, 132 (1989).

Hey82 K. Heyde, P. Van Isacker, M. Waroquier, G. Wenes, and M. Sambataro, Phys. Rev. C **25**, 3160 (1982).

Hey83 K. Heyde, P. Van Isacker, M. Waroquier, J. L. Wood, and R. A. Meyer, Phys. Rep. **102**, 291 (1983).

Hey87 K. Heyde, J. Jolie, J. Moreau, J. Ryckebush, M. Waroquier, P. Van Duppen, M. Huyse, and J. L. Wood, Nucl. Phys. **A466**, 189 (1987).

Hua78 H. Huang, B. P. Pathak, and J. K. P. Lee, Can. J. Phys. **56**, 936 (1978).

Jac77 S. V. Jackson, and R. A. Meyer, Phys. Rev. **C15**, 1806 (1977).

Jän79 J. Jänecke, F. D. Becchetti, and C. E. Thorn, Nucl. Phys. **A325**, 337 (1979).

Jul80 R. Julin, J. Kantele, M. Luontama, A. Passoja, T. Poikolainen, A. Bäcklin, and N.-G. Jonsson, Z. Phys. **A296**, 315 (1980).

Jul87 R. Julin, J. Kantele, J. Kumpulainen, M. Luontama, A. Passoja, W. Trzaska, E. Verho, and J. Blomqvist, Phys. Rev. **C36**, 1129 (1987).

Jul88 R.Julin, J. Kantele, J. Kumpulainen, M. Luontama, V. Nieminen, A. Passoja, W. Trzaska, and E. Verho, Nucl. Instr. Meth. **A270**, 74 (1988).

JulPC R. Julin, private communication.

Juu89 S. Juutinen, R. Julin, P. Ahonen, C. Fahlander, J. Hattula, J. Kumpulainen, A. Lampinen, T. Lönnroth, D. Müller, J. Nyberg, A. Pakkanen, M. Piiparinen, I. Thorslund, S. Törmänen, and A. Virtanen, JYFL Annual Report 1989, 5.7., and to be published.

Kan79 J. Kantele, R. Julin, M. Luontama, A. Passoja, T. Poikolainen, A. Bäcklin, and N.-G. Jonsson, Z. Phys. **A289**, 157 (1979).

Kan84 J. Kantele, in "Heavy Ions and Nuclear Structure", Proceedings of the XIV Summer School, Mikolajki 1984, edited by B. Sikora and Z. Wilhelmi (Harwood, Academic, New York , 1984).

Kaw72 Y. Kawase, K. Okano, S. Uehara, and T. Hayashii, Nucl. Phys. **A193**, 204 (1972).

Ker90 J. Kern, A. Bruder, S. Drissi, V. A. Ionescu, and D. Kusnezov, preprint, to be published in Nucl. Phys.

Kim66 Y. S. Kim, and B. L. Cohen, Phys. Rev. **142**, 788 (1966).

Kot89 B. Kotlinski, D. Cline, A. Bäcklin, and D. Clark, Nucl. Phys. **A503**, 575 (1989).

Kra72 K. S. Krane, Nucl. Instr. and Meth. **98**, 205 (1972).

Kra89a A. Krasznahorkay, Zs. Dombradi, J. Timar, T. Fenyes, J. Gulyas, J. Kumpulainen, and E. Verho, Nucl. Phys. **A499**, 453 (1989).

Kra89b A. Krasznahorkay, Zs. Dombradi, J. Timar, Z. Gacsi, T. Kibedi, A. Passoja, R. Julin, J. Kumpulainen, S. Brant, and V. Paar, Nucl. Phys. **A503**, 113 (1989).

Kum75 K. Kumar, in "The Electromagnetic Interaction in Nuclear Spectroscopy", edited by W. D. Hamilton (North-Holland Publ. Co., Oxford, 1975), Chap. 3.

Kum86 J. Kumpulainen, R. Julin, J. Kantele, A. Passoja, and E. Verho, JYFL Annual Report 1986, 5.9., unpublished.

Kum87 J. Kumpulainen, R. Julin, J. Kantele, A. Passoja, and E. Verho, JYFL Annual Report 1987, 5.9., unpublished.

Kum90 J. Kumpulainen, R. Julin, J. Kantele, A. Passoja, W. H. Trzaska, E. Verho, and J. Väärämäki, Z. Phys. **A335**, 109 (1990).

Kus87 D. Kusnezov, A. Bruder, V. Ionescu, J. Kern, M. Rast, K. Heyde, P. Van Isacker, J. Moreau, M. Waroquier, and R. A. Meyer, Helv. Phys. Act. **60**, 456 (1987).

Lan82 J. Lange, K. Kumar, and J. H. Hamilton, Rev. Mod. Phys. **54**, 119 (1982).

Lip84 P. O. Lipas, in "Int. Review of Nuclear Physics", Vol. 2, edited by T. Engeland, J. Rekstad and J. S. Vaagen (World Scientific, Singapore 1984), Chap. 2.

Lip86 P. O. Lipas and S. Niittynen, JYFL Annual Report 1986, 4.2.; and S. Niittynen, Pro Gradu, JYFL 1986, unpublished.

Lum74 A. H. Lumpkin, A. W. Sunyar, K. A. Hardy, and Y. K. Lee, Phys. Rev. **C9**, 258 (1974).

Lut69 H. F. Lutz, W. Bartolini, and T. H. Curtis, Phys. Rev. **178**, 1911 (1969).

Mac89 H. Mach, M. Moszynski, R. F. Casten, R. L. Gill, D. S. Brenner, J. A. Winger, W. Krips, C. Wesselborg, M. Büscher, F. K. Wohn, A. Aprahamian, D. Alburger, A. Gelberg, and A. Piotrowski, Phys. Rev. Lett. **63**, 143 (1989).

MacPC H. Mach, private communication.

Mal81 G. Mallet, J. Phys. Soc. Japan **50**, 384 (1981); G. Mallet et al., J. Phys. **G7**, 1259 (1981).

Mat74 E. der Mateosian, and A. W. Sunyar, At. Data and Nucl. Data Tables **13**, 407 (1974).

McG65 F. K. McGowan, R. L. Robinson, P. H. Stelson, and J. L. C. Ford Jr, Nucl. Phys. **66**, 97 (1965).

Med87 L. R. Medsker, H. T. Fortune, J. D. Zumbro, C. P. Browne, and J. F. Mateja, Phys. Rev. **C36**, 1785 (1987).

Mey76 R. A. Meyer, R. D. Griffioen, J. Graber Lefler, and W. B. Walters, Phys. Rev. **C14**, 2024 (1976).

Mey77 R. A. Meyer, and L. Peker, Z. Phys. **A283**, 379 (1977).

MeyPC R. A. Meyer, and J. R. Van Hise, private communication in Nucl. Data Sheets **38**, 545 (1983).

Mhe84 A. Mheemeed, K. Schreckenbach, G. Barreau, H. R. Faust, H. G. Börner, R. Brissot, P. Hungerford, H. H. Schmidt, H. J. Scheerer, T. von Egidy, K. Heyde, J. L. Wood, P. Van Isacker, M. Waroquier, G. Wenes, and M. L. Stelts, Nucl. Phys. **A412**, 113 (1984).

Mil69 W. T. Milner, F. K. McGovan, P. H. Stelson, R. L. Robinson, and R. O. Sayer, Nucl. Phys. **A129**, 687 (1969).

Mor71 R. Moreh, and A. Nof, Phys. Rev. **C4**, 2265 (1971).

Mos89 M. Moszynski, J. H. Bjerregard, J. J. Gaardhøje, B. Herskind, P. Knudsen, and G. Sletten, Nucl. Instr. and Meth. **A280**, 73 (1989).

Mum85 A. I. Muminov, A. Akbarov, B. Ibragimov, D. I. Kochetov, I. K. Kuldzhanov, and R. Razhabbaev, Bull. Acad. Sci. USSR, Phys. Ser. **49**, No. 5, 60 (1985).

New80 T. M. Newton, J. M. Davidson, W. K. Dawson, P. W. Green, H. R. Hooper, W. J. McDonald, G. C. Neilson, and D. M. Sheppard, Can. J. Phys. **58**, 8 (1980).

ODo88 J. M. O'Donnell, A. Kotwal, and H. T. Fortune, Phys. Rev. **C38**, 2047 (1988).

Paa79 V. Paar, and R. A. Meyer, J. Phys. **G5**, L75 (1979).

Pas81 A. Passoja, R. Julin, J. Kantele, and M. Luontama, Nucl. Phys. **A363**, 399 (1981).

Pig84 M. Pignanelli, S. Micheletti, E. Cereda, M. N. Harakeh, S. Y. van der Werf, and R. De Leo, Phys. Rev. **C29**, 434 (1984).

Ram87 S. Raman, C. H. Malarkey, W. T. Milner, C. W. Nestor, JR., and P. H. Stelson, At. Data Nucl. Data Tables **36**, 1 (1987).

Rik89 J. Rikovska, N. J. Stone, P. M. Walker, and W. B. Walters, Nucl. Phys. **A505**, 145 (1989).

Rot84 G. Rotbard, M. Vergnes, J. Vernotte, G. Berrier-Ronsin, S. Gales, and G. M. Crawley, Bull. Am. Phys. Soc. **29**, 1041 (1984).

Rou81 B. Roussiere, P. Kilcher, J. Sauvage-Letessier, R. Beraud, R. Duffait, M. Meyer, J. Genevey-Rivier, and J. Treherne, "4th International Conference on Nuclei Far From Stability" Proceedings, CERN 81-09, p. 465.

Rou84 B. Roussiere, P. Kilcher, J. Sauvage-Letessier, C. Bourgeois, R. Beraud, R. Duffait, M. Meyer, J. Genevey-Rivier, and J. Treherne, Nucl. Phys. **A419**, 61 (1984).

Rös78 F. Rösel, H. M. Fries, K. Alder, and H. C. Pauli, At. Data Nucl. Data Tables **21**, 91 (1978).

Sak81 M. Sakai, INS-J-161 (Aug. 1981).

Sak84 M. Sakai, At. Data Nucl. Data Tables **31**, 399 (1984).

Sam78 L. E. Samuelson, F. A. Rickey, J. A. Grau, S. I. Popik, and P. C. Simms, Nucl. Phys. **A301**, 159 (1978).

Sam79 L. E. Samuelson, J. A. Grau, S. I. Popik, F. A. Rickey, and P. C. Simms, Phys. Rev. **C19**, 73 (1979).

Sam82 M. Sambataro, Nucl. Phys. **A380**, 365 (1982).

Sar69 D. G. Sarantites, Nucl. Phys. **A142**, 649 (1969).

Shr79 R. E. Shroy, A. K. Gaigalas, G. Schatz, and D. B. Fossan, Phys. Rev. C **19**, 1324 (1979).

Sch82 K. Schreckenbach, A. Mheemeed, G. Barreau, T. von Egidy, H. R. Faust, H. G. Börner, R. Brissot, M. L. Stelts, K. Heyde, P. van Isacker, M. Waroquier, and G. Wenes, Phys. Lett. **110B**, 364 (1982)

Sha85 T. L. Shaw, V. R. Green, N. J. Stone, J. Rikovska, P. M. Walker, S. Collins, S. A. Hamada, W. D. Hamilton, and I. S. Grant, Phys. Lett. **153B**, 221 (1985).

Spe77 R. H. Spear, J. P. Warner, A. M. Baxter, M. T. Esat, M. P. Fewell, S. Hinds, A. M. R. Joye, and D. C. Kean, Aust. J. Phys. **30**, 133 (1977).

Sve89 L. E. Svensson, Ph.D. thesis, Uppsala University, 1989, unpublished.

Ver79 H. R. Verma, A. K. Sharma, R. Kaur, K. K. Suri, and P. N. Trehan, J. Phys. Soc. Japan **47**, 16 (1979).

Wal72 G. Wallace, G. J. McCallum, and N. G. Chapman, Nucl. Phys. **A182**, 417 (1972).

Wal85 W. B. Walters, "Int. Symp. on Nuclear Orientation and Nuclei Far From Stability" Proceedings, Hyp. Int. **22**, 317 (1985).

Wat87 D. L. Watson, J. M. O'Donnell, and H. T. Fortune, J. Phys. **G13**, 1443 (1987).

Wis80 I. N. Wischnewski, H. V. Klapdor, P. Herges, H. Fromm, and W. A. Zheldonozhski, Z. Phys. **A298**, 21 (1980).

WooPC J. L. Wood, private compilation.

Yam67 T. Yamazaki, Nuclear Data **A3**, 1 (1967).

Yat88 S. W. Yates, R. Julin, J. Kumpulainen, and E. Verho, Phys. Rev. **C37**, 2877 (1988).

Zam89 N. V. Zamfir, R. F. Casten, and P. von Brentano, Phys. Lett. **B226**, 11 (1989).